**EXTRA BUDGETARY PROJECT
ON
SEISMIC SAFETY OF EXISTING NUCLEAR POWER PLANTS**

**KAshiwazaki-Kariwa Research Initiative for Seismic Margin Assessment
KARISMA BENCHMARK**

Part 1 - STRUCTURE

Final Report

ITER-Consult

October 2012

**INTERNATIONAL SEISMIC SAFETY CENTRE (ISSC)
DIVISION OF NUCLEAR INSTALLATION SAFETY (NSNI)
DEPARTMENT OF NUCLEAR SAFETY AND SECURITY (NS)**

Date of issue 31.10.2012
Doc. N. ITC TD IAEA-KK 04 R1

IAEA – ISSC – EBP
KARISMA BENCHMARK : PART 1 - STRUCTURE

EXECUTIVE SUMMARY

After the Niigataken-chuetsu-oki earthquake (NCOE), on 16 July 2007 that affected the Tokyo Electric Power Company (TEPCO) Kashiwazaki-Kariwa Nuclear Power Station (NPS) with a magnitude of 6.6, a benchmark on the seismic behaviour of NPP has been organized by IAEA, in the framework of the Working Area 2 (WA2) of the International Atomic Energy Agency – Extra Budgetary Programme (IAEA-EBO) on Seismic Safety of Existing Nuclear Power Plants.

The report contains the contribution of ITER-Consult to the benchmark, with specific reference to the activities requested in Task 1- *Structural benchmark.*

Analyses have been developed to study the soil response, using ground motion records provided by Tokyo Electric Power Company (TEPCO). Response spectra have been evaluated at free surface and at specific depths using aftershock and main shock data. Maximum spectral accelerations of about 4.8 g have been calculated during the main shock.

A 3D finite element model has been developed and used to evaluate the displacements and forces at specific points of the reactor building (RB) structure.
Stick models derived from the data in the Guidance Document have been also developed to check the 3D model.
Preliminary analyses have been performed applying vertical and horizontal acceleration as requested for the benchmark. A modal analysis has been also performed on the FE models.

In Subtask 1.2 of the benchmark, the main shock response of the structure has been evaluated, with the two hypotheses of fixed base and with soil structure interaction, taking into account the nonlinear behaviour of the structure. The obtained results have been compared to the recorded data during the NCOE earthquake.
The soil structure interaction phenomena have been inserted in the model by means of spring and dashpots applied underneath the basemat.

Last subtask of the benchmark was devoted to margin assessment. The objectives of this assessment and main problems encountered are discussed in the last paragraphs of the report.
The structural behaviour has been studied applying increasing acceleration time-histories, defined by IAEA Secretariat.
The response has been evaluated taking into account the nonlinear behaviour of the structure. With respect of the SSI approach used in the first subtasks of the benchmark, margin assessment has been conducted using an improved SSI model.

As general consideration, the general objective of a Margin Assessment, as referred to the RB seismic response, can be seen from two perspectives:

A. Assess margin with respect to ultimate status of RB structure. That is the increase in the seismic demand causing the ultimate status of the RB structure, either collapse or extensive cracking with loss of containment.

B. Assess margin with respect to the loss of the ‘’NPP capacity to bring and maintain the NPP (reactor core and spent fuel) in a safe status". This loss is logically linked with the systems and equipment needed to ensure the three main safety functions caused by interaction of the RB structure with systems and equipment. In fact even if the structural limit state of the RB is not attained, the displacements and/or accelerations can cause the loss of capacity of systems and components needed to ‘’bring and maintain the NPP in safe status’’. This second aspect (perspective) is linked with activity of Task 2 of the Benchmark.
   We think that margins have to be evaluated according this last approach (B).

To do that, it is necessary to develop (and investigate) the needed assessment about the interfaces between structures and systems/equipment to identify the margins with respect to loss of NPP system capacity to ‘’ bring and maintain the NPP in a safe status’’.

However, in this study, the focus was maintained on the structural behaviour of the Reactor Building.
In this framework, the assessment of margins required the identification of the “ultimate” earthquake that the structure can sustain, to be compared with the NCOE earthquake that effectively strikes the NPP.

Main lessons learned from the benchmark can be summarized as follows:

- The soil structure interaction is a key problem in the assessment of margins characterizing the seismic response of the structure, at least in cases with soil properties comparable to those at KK site.
- Collapse of soil-foundation system, in the sense of excessive displacements, seems to anticipate extensive structural damage.
- Activities are deemed necessary in defining standards for the evaluation of NPP structures under beyond design basis seismic motion.
- While suitable procedures have been included in codes and standard for ordinary buildings and bridges (in beyond design scenarios), there is the need to extend these approaches to NPP structures, that are unique for stiffness, strength, behaviour and required performance.

IAEA – ISSC – EBP
KARISMA BENCHMARK : PART 1 - STRUCTURE

ITER-Consult Final Report

Authors:

V. Lucarelli
G. Orsini,
R. Romeo (up to middle 2012)

with the cooperation of:

D. Casertano
A. Madonna
G. Maresca
D. Mazzini
G. Pino
A. Pugliese
T. Sanò

Quality Management:

The work performed by ITER -Consult in the frame of KARISMA Benchmark, and here reported, has been conducted in agreement with a Specific Quality Plan described in the internal Doc. ITC TD IAEA-KK 2 R0.

iter consult

Piazza San Pietro, 36
I - 00029 Vicovaro (Roma)
Ph: +39 06 77072888
Fax: +39 06 23328132
Email: iter@iter-consult.it
www.iter-consult.it

KARISMA BENCHMARK : PART 1 - STRUCTURE

CONTENTS

1. INTRODUCTION....10

2. DESCRIPTION OF NUMERICAL MODELS....12
2.1 Objective and main assumptions....12
2.2 Numerical modelling: Structure, Soil, Soil-Structure....14
2.2.1 Development of Reactor Pressure Vessel (RPV) local model....14
2.2.2 Stick model of the global building....17
2.2.3 Global Finite Elements Model of the Reactor Building....24
2.2.4 Simplified Finite Elements Model of Dynamic Analysis of Reactor Building....27
2.3 Material properties....29
2.4 Soil description....30
2.4.1 Soil column analyses....30
2.4.2 Finite Elements Model for Soil Structure Interaction....31
2.5 Boundary conditions....36
2.6 Computer codes and methods used....36

3. MAIN RESULTS OF PERFORMED ANALYSES....37
3.1 Task 1.1 Construction and validation of the soil and structure models....37
3.1.1 Task 1.1.1 Static and model analysis of the fixed base model....37
3.1.2 Task 1.1.2 Soil column analyses....47
3.1.3 Task 1.1.3 Analysis of the complete model....50
3.2 Task 1.2 NCOE Response....57
3.2.1 Reference Analysis of the Soil-Structure Model....57
3.2.2 Best estimate analysis of the soil-structure model....59
3.3 Task 1.3 Margin Assessment....62
3.3.1 Pushover Analysis and ATC 40 approach....65
NCOE 1 – Dir. x – Fixed base....67
NCOE 1 – Dir. Y – Fixed basE....67
NCOE 1 – Dir. x – Def. base....67
NCOE 1 – Dir. Y – dEF. basE....67
NCOE 2 – Dir. x – Fixed base....68
NCOE 2 – Dir. Y – Fixed basE....68
NCOE 2 – Dir. x – Def. base....68
NCOE 2 – Dir. Y – dEF. basE....68
NCOE 4 – Dir. x – Fixed base....69
NCOE 4 – Dir. Y – Fixed basE....69
NCOE 4 – Dir. x – Def. base....69
NCOE 4 – Dir. Y – dEF. basE....69
NCOE 6 – Dir. x – Fixed base....70
NCOE 6 – Dir. Y – Fixed basE....70
NCOE 6 – Dir. x – Def. base....70
NCOE 6 – Dir. Y – dEF. basE....70
3.3.2 Dynamic Response Analysis....71

4. DISCUSSIONS 78

5. CONCLUDING REMARKS ON THE BENCHMARK 79
5.1 Main difficulties encountered and their resolution 79
5.2 Main lessons learned from the benchmark 80
5.3 Suggestion on improving future benchmarks 80

REFERENCES 81

APPENDIX A - LIST OF TEAM MEMBERS 82

List of Figures

Figure 2.1 – Cross Section XZ (Ref. [1]) 12
Figure 2.2 – Cross Section YZ (Ref. [1])) 13
Figure 2.3 – Floor plan: 1st Floor (Ref. [1])) 13
Figure 2.4 – Stick model of the vessel 15
Figure 2.5 – Cross section of the 3D model of the vessel 15
Figure 2.6 – Stick model of the R/B in YZ plane 18
Figure 2.7 – Stick model: Modal shapes of the R/B in YZ direction 19
Figure 2.8 – Stick model of the R/B in XZ plane 21
Figure 2.9 – Stick model: Modal shapes of the R/B in XZ direction 22
Figure 2.10 – General view of the F.E.model 24
Figure 2.11 – Cross section XZ of the F.E.model (without the vessel) 25
Figure 2.12 – Cross section YZ of the F.E.model (without the vessel) 26
Figure 2.13 – Cross section YZ of the F.E.model (with the rough model of the vessel) 26
Figure 2.14 – Particular of the roof model 27
Figure 2.15 – Simplified Model for Non linear TH Analyses 28
Figure 2.16 – Soil Vs profile 31
Figure 2.17 – Soil Structure Interaction Model 32
Figure 2.18 – Comparison 1D model Vs IAEA ground motion: Basemat 34
Figure 2.19 – Comparison 1D model Vs IAEAground motion: free surface 34
Figure 2.20 – 3D model 35
Figure 3.1 – Vertical loads – deformed shape 37
Figure 3.2 – Vertical loads – Principal minimum stress of the walls at the top of the basemat 38
Figure 3.3 – Vertical loads – Principal minimum stress al el. 12.3 m 38
Figure 3.4 – Horizontal acceleration X – Deformed shape 39
Figure 3.5 – Horizontal acceleration X – Primcipal minimum stresses (KN/m2) 40
Figure 3.6 – Horizontal acceleration X – Principal minimum stresses (KN/m2) – External wall 40
Figure 3.7 – Horizontal acceleration Y – Deformed shape 41
Figure 3.8 – Horizontal acceleration Y – Principal minimum stress (KN/m2) 42
Figure 3.9 – Horizontal acceleration Y – Principal minimum stress (KN/m2) – External wall 42
Figure 3.10 – Cumulative distribution of participating modal mass 45
Figure 3.11 – Modal analysis- First mode (4.48 Hz) 46
Figure 3.12 – Modal analysis- Second mode (4.77 Hz) 46
Figure 3.13 – Aftershock I: response spectrum X direction 47
Figure 3.14 – Aftershock I: response spectrum Y direction 48
Figure 3.15 – Aftershock II: response spectrum X direction 48
Figure 3.16 – Aftershock II: response spectrum Y direction 49
Figure 3.17 – Main shock: response spectrum X direction 49
Figure 3.18 – Main shock: response spectrum Y direction 50
Figure 3.19 – Foundation stiffness evaluation 51
Figure 3.20 – Evaluation of the equivalent shear modulus (Ref. [5]) 52
Figure 3.21 – Modal analysis with SSI- First mode (1.91 Hz) 56
Figure 3.22 – Modal analysis with SSI - Second mode (1.96 Hz) 56
Figure 3.23 – Modal analysis with SSI- First mode (2.098 Hz) 58
Figure 3.24 – Modal analysis with SSI - Second mode (2.153 Hz) 59
Figure 3.25 – Results at 3rd Basemat Level 60
Figure 3.26 – Results at 3rd Floor Level 60
Figure 3.27 – Push Over Analyses results: Fixed base model 66
Figure 3.28 – Push Over Analyses results: deformed base model 66
Figure 3.29 – Response Spectrum and the Capacity Spetrum (ADRS): NCOE 1 67

Figure 3.30 – Response Spectrum and the Capacity Spetrum (ADRS): NCOE 2 68
Figure 3.31 – Response Spectrum and the Capacity Spetrum (ADRS): NCOE 4 69
Figure 3.32 – Response Spectrum and the Capacity Spetrum (ADRS): NCOE 6 70
Figure 3.33 – Push Over Analyses results: deformed base model (Best Estimated Analyses)..... 71
Figure 3.34 – Reference Analyses: BP1 Results 72
Figure 3.35 – Reference Analyses: FP2 Results 72
Figure 3.36 – Best Estimated Analyses: BP1 Results 72
Figure 3.37 – Best Estimated Analyses: FP2 Results 73
Figure 3.38 – Comparison Reference - Best Estimated Analyses: BP1 Results 73
Figure 3.39 – Comparison Reference - Best Estimated Analyses: FP2 Results 73
Figure 3.40 – Comparison Best Estimated Analyses and Recorded signal: FP2 Results 74
Figure 3.41 – Response spectra at the bottom of the basemat 74
Figure 3.42 – Residual vertical displacement Vs CAV (Reference Analyses) 77

List of Tables

Table 1.1 – Karisma benchmark project 11
Table 2.2 – RPV stick model 16
Table 2.3 – Vessel 3D model 16
Table 2.4 – Stick model in YZ plane 18
Table 2.5 – Stick model YZ plane: results 19
Table 2.6 – Stick model in YZ plane: Modal Participation Factors and Modal Masses 20
Table 2.7 – Stick model in YZ plane: Modal Participating Mass Ratios 20
Table 2.8 – Stick model in XZ plane 21
Table 2.9 – Stick model XZ plane: results 21
Table 2.10 – Stick model in XZ direction: Modal Participation Factors and Modal Masses 23
Table 2.11 – Stick model in XZ direction: Modal Participating Mass Ratios 23
Table 3.1 – Modal frequencies 43
Table 3.2 – Modal masses 44
Table 3.3 – Soil shear modulus profile 53
Table 3.4 – Equivalent Soil shear moduli for the different dof's 53
Table 3.5 – Modal analysis result fo SSI model 58
Table 3.6 – Performance points: NCOE 1 68
Table 3.7 – Performance points: NCOE 2 69
Table 3.8 – Performance points: NCOE 4 70
Table 3.9 – Performance points: NCOE 6 71
Table 3.10 – Performance factors increasing earthquake severity 76
Table 3.11 – Performance factors increasing earthquake severity (Best Estimated Analyses) ... 78

IAEA – ISSC – EBP
KARISMA BENCHMARK : PART 1 - STRUCTURE

1. INTRODUCTION

After the Niigataken-Chuetsu-Oki Earthquake (NCOE), on 16 July 2007 that affected the Tokyo Electric Power Company (TEPCO) Kashiwazaki-Kariwa Nuclear Power Station (NPS) with a magnitude of 6.6, a benchmark on the seismic behaviour of NPP has been organized by IAEA, in the framework of the Working Area 2 (WA2) of the International Atomic Energy Agency – Extra Budgetary Programme (IAEA-EBP) on Seismic Safety of Existing Nuclear Power Plants.
The large amount of observations and data collected on site and the significant instrumentation which measured acceleration at different locations in soil and in structures (both inputs and outputs), raised the idea of organizing a benchmark on seismic behavior in the framework of the WA2 of the IAEA-EBP.

The benchmark, was defined at the beginning of 2008; an expert meeting, held in May 2008, elaborated the main characteristics of the IAEA-EBP KAshiwazaki-Kariwa Research Initiative for Seismic Margin Assessment (KARISMA).

The first Organizing Committee (OC) meeting of the KARISMA Benchmark was held in Vienna on January 19-20, 2009 in order to confirm the objective of the benchmark and review availability and completeness of data package (drawings and input signals) provided by TEPCO.

Although it appears that the earthquake of 16 July 2007 significantly exceeded the level of the seismic input taken into account in the design of the plant, the installation behaved in a safe manner, during and after the earthquake.

In particular, the automatic shutdown of the reactors of Units 3, 4 and 7, which were at full power, and of the reactor of Unit 2, which was in the start up state, were performed successfully. According to review findings from IAEA, this is probably due to the conservatisms introduced at different stages of the design process, the so-called "design safety margins". The combined effects of these conservatisms were apparently sufficient to compensate the severity of the occurred earthquake with respect to the design SSE.

The major objectives of the benchmark are:

1. To understand what happened to soil and structures during the July 2007 earthquake;
2. Understanding of margins: quantifying what happens both in soil and in structure when the input is increased;
3. Calibration of different simulation methodologies for soil, structures and soil-structure interaction;
4. Identification of main parameters influencing the response;

5. Consideration of the effect of differential movements beneath buildings;
6. Understanding of equipment behaviour for some selected equipment and approaches to margin evaluation

The general project concerns both structure benchmark and equipment benchmark. In particular, the following tasks and sub-tasks have been planned:

Table 1.1 – KARISMA benchmark structure

<table>
<tr><th>TASK</th><th>SUBTASK</th><th colspan="2">SUB-SUBTAKS</th></tr>
<tr><td rowspan="6">TASK 1
Structural Benchmark</td><td rowspan="3">Subtask1.1
Construction and validation of the soil and structures models</td><td colspan="2">Subtask 1.1.1
Static and modal analysis of the fixed base model under vertical and horizontal forces</td></tr>
<tr><td colspan="2">Subtask 1.1.2
Soil Column analyses</td></tr>
<tr><td colspan="2">Subtask 1.1.3
Analysis of the complete model</td></tr>
<tr><td rowspan="3">Subtask 1.2
Main shock response</td><td rowspan="2">Subtask 1.2.1
Transfer of spectra analysis</td><td>Conventional basic design study</td></tr>
<tr><td>Best estimate study</td></tr>
<tr><td colspan="2">Subtask 1.2.2
Analysis of the main shock</td></tr>
<tr><td></td><td colspan="3">Subtask 1.3
Margins assessment</td></tr>
<tr><td rowspan="3">TASK 2
Equipment Benchmark</td><td colspan="3">Subtask 2.1
Piping System</td></tr>
<tr><td colspan="3">Subtask 2.2
Sloshing of the fuel pool</td></tr>
<tr><td colspan="3">Subtask 2.3
Atmospheric tanks buckling</td></tr>
</table>

2. DESCRIPTION OF NUMERICAL MODELS

2.1 Objective and main assumptions

The Reactor Building of Unit 7 is a very complex and large structure. The overall building dimensions in plan are 59.6 m by 56.6 m. The height of the building, from the bottom of the base mat to the top of the roof, is 63.4 m.
The structure is typically made by reinforced concrete walls and slabs. In the interior part of the structure some reinforced concrete columns are present, connected by reinforced concrete beams. The floor slabs are supported by the walls and the column-beam system.

Some steel beams are also present in the structure, typically at the higher levels. The roof composite structure is made of steel trusses with a connected reinforced concrete plate.

All detailed information have been collected in the Guidance Document (Ref. [1]).

In Figure 2.1 and Figure 2.2 the cross sections of the building along XZ and YZ are shown.

A generic floor plan is reported in Figure 2.3.

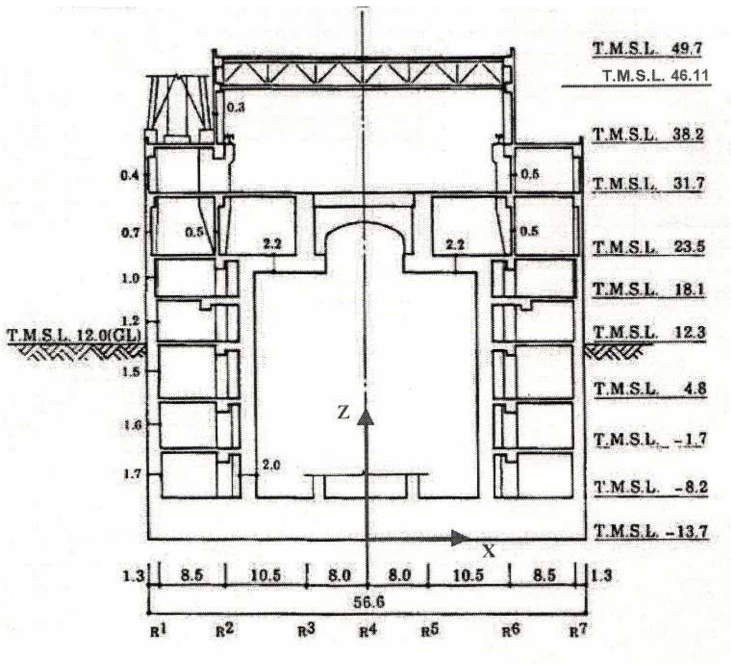

Figure 2.1 – Cross Section XZ (Ref. [1])

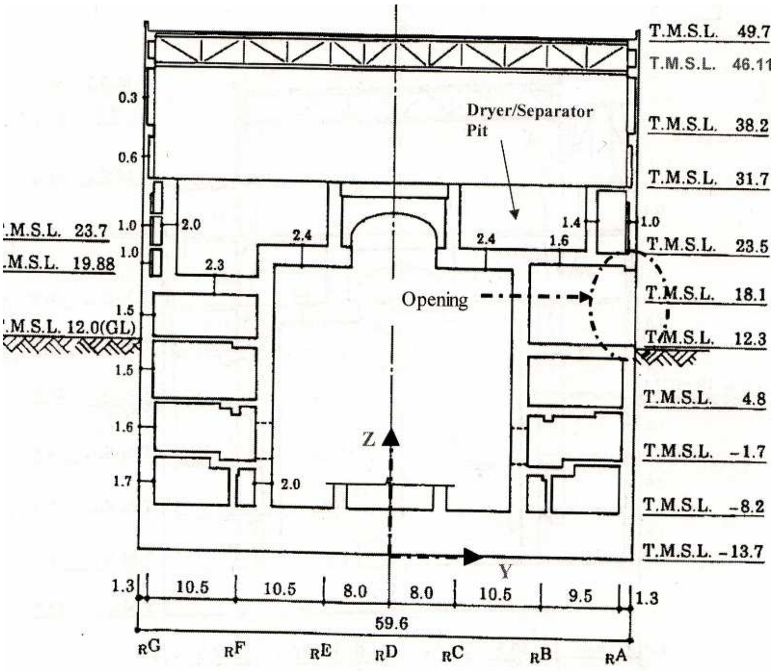

Figure 2.2 – Cross Section YZ (Ref. [1]))

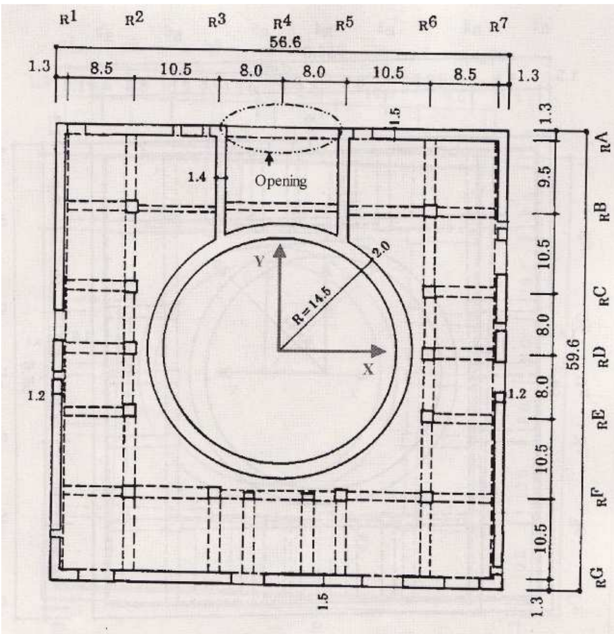

Figure 2.3 – Floor plan: 1st Floor (Ref. [1]))

The general objective of the benchmark is the evaluation of the seismic response of the structure during the NCOE Earthquake, taking into account soil structure interaction. The final aim is to evaluate effective safety margins of such structures in case of a seismic input higher than the design basis earthquake.

This kind of analyses requires an evaluation of the behaviour of the structure beyond the elastic limit. Then, for the subsequent phases of the study, a non linear analysis of the structure is planned, to evaluate the damage progression in the structure under increasing load.
In dynamic analyses this subject is still more complex and onerous.
In any case, the evaluation of the damage due to seismic loads, and the consequent residual safety level of the structure, requires a detailed model; at first onset of inelastic behaviour, the damage process usually affects specific and detailed parts of the structure that the analyst has to identify and control.

Due to this, a too coarse model of the structure is not adequate to evaluate the initial stage of the damage and its progression.
On the contrary, a detailed representation of the structure implies large Finite Element Models (FEM), with hundreds of thousand Degree Of Freedom (DOF).

For the KARISMA project, it was then decided to develop a detailed Finite Element Model. The reinforced concrete structures have been modelled using 3D brick elements. Truss and shell elements have been also used to model the roof structure. This model has been checked against the stick model described in the Guidance Document to validate its behaviour.

The non linear analyses performed to evaluate the response of the structure during the Main Shock and the margin assessment studies required additional models.
In particular, a non linear dynamic analysis on the global Finite Model described above is very time consuming; moreover, in margin assessment evaluations several acceleration time histories analyses shall be performed. Due to this, simplified models have been constructed to perform the non linear dynamic analyses, obtained performing at first push-over analyses on the global model and then identifying the characteristics of equivalent non-linear single degree of freedom model representing the elevation structure.

2.2 Numerical modelling: Structure, Soil, Soil-Structure

As anticipated in the introduction, specific studies have been conducted to support the construction of the global model. Main results of these studies are summarized in the following.

2.2.1 Development of Reactor Pressure Vessel (RPV) local model

The geometrical and mechanical parameters of the 3D mesh of the RPV, inserted in the global model, have been identified by comparative analyses conducted on a stick model of the RPV structure, as described in the guidance document. In Figure 2.4 the stick model is shown. The frequencies obtained from the stick model of the vessel have been used to backfit the parameters of the brick model, just reproducing the main vibration frequency and the total mass.

In the Figure 2.5 the section obtained in the Global z-x plane is shown. Each element is repeated 84 times in a circumference around the vertical axis z to create an axis-symmetric component. For the wall of the RPV a thickness of 17 cm has been used with an inner diameter of 6,8 m.

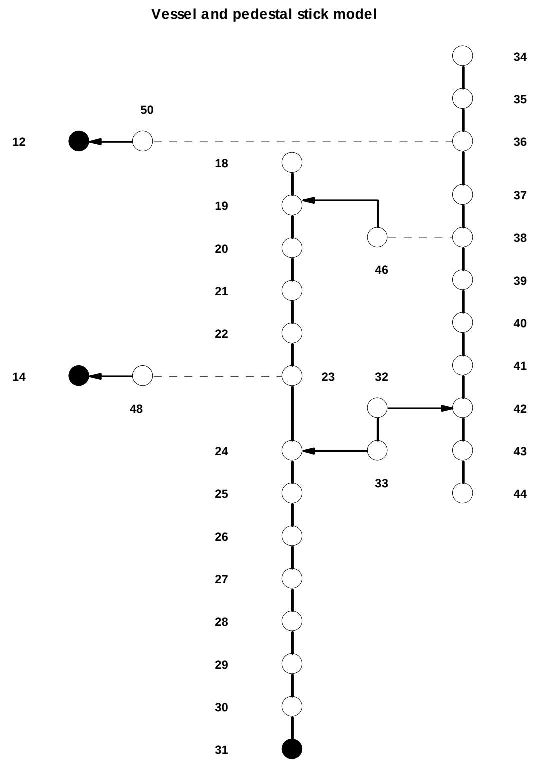

Figure 2.4 – Stick model of the vessel

Spring Constants

K1 = 3.23 E+04 t/m (50-36)   K2 = 6.29 E+05 t/m (46-38)   K3 = 1.72 E+07 t/m (48-23)

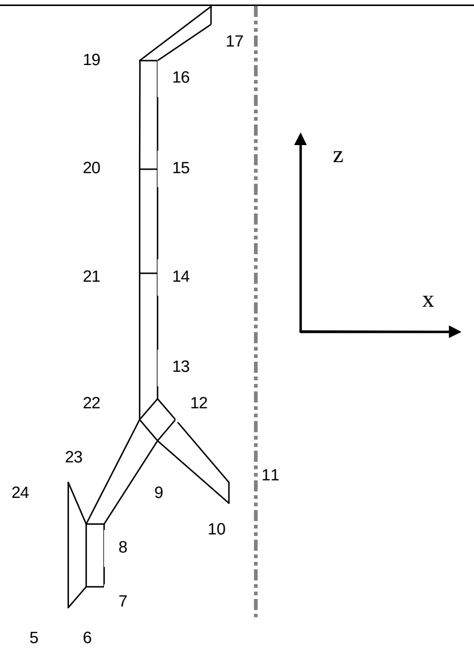

Figure 2.5 – Cross section of the 3D model of the vessel

The comparative analyses conducted on the stick model and on the isolated 3D brick model of the RPV are summarized in the following tables. The frequencies and modal participation factors calculated on the stick model are reported:

Table 2.2 – RPV stick model

Stick Model Geometry and Mass Properties

Direction	Mass (KNs^2/m)	Center of gravity Z (m)	Rotational Inertia (KNs^2/m^3)
X	2.024E+03	1.288E+01	4.0261E+05
Y	2.024E+03	1.288E+01	4.0261E+05
Z	2.024E+03	1.288E+01	

Frequencies

Mode Number	Circular Freq. (rad / sec)	Frequency (cycles / sec)	Period (sec)
1	0.8688E+02	0.1383E+02	0.7232E-01
2	0.8688E+02	0.1383E+02	0.7232E-01
3	0.2204E+03	0.3508E+02	0.2851E-01
4	0.2204E+03	0.3508E+02	0.2851E-01
5	0.2970E+03	0.4727E+02	0.2116E-01

Modal Participation Factors and Modal Masses

Mode Number	X direction	Y direction)	Z direction)	Mass X	Mass Y	Mass Z
1	0.2249E+02	-0.2249E+02	-0.8678E-16	505,8	505,8	
2	0.2249E+02	0.2249E+02	0.8737E-16	505,8	505,8	
3	0.1429E+02	0.2690E+02	0.1005E-14	204,2	723,6	
4	0.2690E+02	-0.1429E+02	-0.5278E-15	723,6	204,2	
5	0.8556E-11	0.1454E-11	-0.3862E+0			0,1492
Total				1939,4		

The frequencies and modal participation factors calculated on the 3D brick model are reported in the table below.

Table 2.3 – Vessel 3D model

Brick Model Geometry and Mass properties

Direction	Mass (KNs^2/m)	Center of gravity Z (m)	Rotational Inertia (KNs^2/m^3)
X	2.024E+03	1.288E+01	4.1339E+05
Y	2.024E+03	1.288E+01	4.1339E+05
Z	2.024E+03	1.288E+01	.9976E+04

Frequencies

Mode Number	Circular Freq. (rad / sec)	Frequency (cycles / sec)	Period (sec)
1	0.8401E+02	0.1337E+02	0.7479E-01
2	0.8401E+02	0.1337E+02	0.7479E-01
3	0.1709E+03	0.2720E+02	0.3676E-01
4	0.1709E+03	0.2720E+02	0.3676E-01
5	0.1906E+03	0.3033E+02	0.3297E-01
6	0.1938E+03	0.3085E+02	0.3242E-01
7	0.1938E+03	0.3085E+02	0.3242E-01
8	0.2130E+03	0.3389E+02	0.2950E-01
9	0.2130E+03	0.3389E+02	0.2950E-01
10	0.2902E+03	0.4619E+02	0.2165E-01
11	0.3027E+03	0.4817E+02	0.2076E-01
12	0.3027E+03	0.4817E+02	0.2076E-01
13	0.3085E+03	0.4910E+02	0.2037E-01
14	0.3085E+03	0.4910E+02	0.2037E-01

Modal Participation Factors and Modal Masses

Mode Number	Frequency (cycles / sec)	X direction $(KNs^2/m)^{1/2}$	Y direction $(KNs^2/m)^{1/2}$	Z direction $(KNs^2/m)^{1/2}$	Mass X (KNs^2/m)	Mass Y (KNs^2/m)	Mass Z (KNs^2/m)
1	13,37	0.2037E+01	0.2694E+02	-0.5027E-09	4,166	725,8	
2	13,37	0.2694E+02	-0.2037E+01	0.3304E-09	725,8	4,166	
3	27,20	-0.1072E-09	0.2722E-10	-0.3198E-10			
4	27,20	0.1278E-09	-0.5543E-11	-0.2233E-10			
5	30,33	0.2703E-06	0.2644E-06	0.5107E-08			
6	30,85	0.3486E-09	0.2724E-09	-0.1366E-09			
7	30,85	0.1217E-09	-0.2555E-10	-0.5097E-09			
8	33,89	-0.1216E-10	0.1017E-11	-0.9606E-11			
9	33,89	0.2370E-11	-0.4922E-11	0.1037E-11			
10	46,19	-0.1350E-07	0.9150E-08	0.3649E+02			
11	48,17	-0.3476E-08	-0.3539E-08	-0.2946E-10			1331
12	48,17	-0.3532E-08	-0.4121E-08	0.5139E-13			
13	49,10	0.1725E+02	0.1547E+02	0.1153E-06	297,6	239,3	
14	49,10	-0.1546E+02	0.1726E+02	0.4183E-05	239,0	297,9	
Total					1267	1267	1331

Using the 3D model, just the first frequency of the stick model can be reproduced with a quite good approximation (modes 1 and 2 at 13,37 Hz to be compared with 13,83 Hz of the stick model). In the brick model the second relevant contribution to the participating mass in fact comes from the modes 13 and 14 at 49,10 Hz.
This has been considered acceptable according to the role of the RPV model in the overall behaviour of the building. Anyway, the available information about vessel were not so detailed and not referred to operating conditions. .

2.2.2 Stick model of the global building

A stick model of the building has been studied at first, to estimate the global forces of the problem and to have a preliminary evaluation of the dynamic characteristics of the structure.

The model has been developed using the data in the Guidance Document [1].
In the following figures and tables are summarized the input data and the results obtained in terms of frequency, separately for the two model used in YZ and XZ directions.

Some comments about the results are common to both models, in view of the comparison with the complete 3D model of the reactor building.
In the range 0-20 Hz the stick models exhibit only 5 modes and the cumulated participating mass ratio is about 85% . The greater part of this ratio is given by the first mode (73% in YZ dir., 75% in XZ). The 2nd mode gives another 6%, other modes are almost negligible.

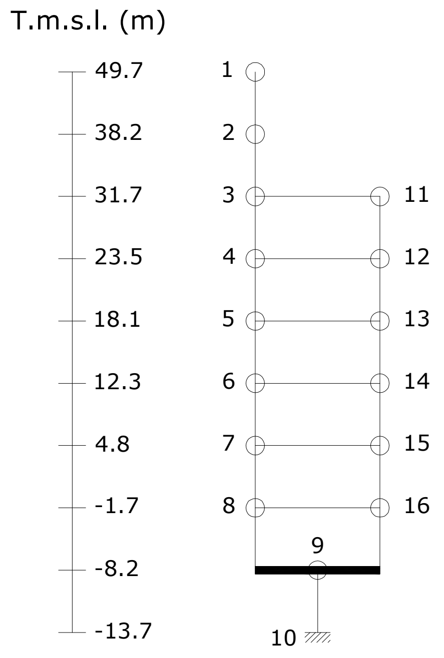

Figure 2.6 – Stick model of the R/B in YZ plane

Table 2.4 – Stick model in YZ plane

N°	Weight	Mass	Height	Rot Inertia weight Io	Rot Inertia mass Io
-	(kN)	(kNm/s2)	(m)	($x10^5$ kNm2)	(kNm3/s2)
1	39760	4053	49.7	71	723751
2	80820	8239	38.2	413	4209990
3	86110	8778	31.7	483	4923547
4	86400	8807	23.5	299	3047910
5	56460	5755	18.1	202	2059123
6	82650	8425	12.3	295	3007136
7	81700	8328	4.8	302	3078491
8	82900	8451	-1.7	304	3098879
9	349200	35596	-8.2	964	9826707
10	0	0	-13.7	0	0

N°sec	Shear cross-sectional area	Geom. Moment Inertia I
	(m^2)	(m^4)
9	41	13700
8	83	51100
7	188	70600
6	132.5	69000
5	149.4	84700
4	180.5	105000
3	183.2	112800
2	223.5	119000
1	3373.4	900600

Tot W	1771400
Tot M	180571
Tot Io	53465851

N°	Weight	Mass	Height	Rot Inertia weight Io	Rot Inertia mass Io
-	(kN)	(kNm/s2)	(m)	($x10^5$ kNm2)	(kNm3/s2)
11	93200	9501	31.7	33	336391
12	158100	16116	23.5	379	3863405
13	104900	10693	18.1	311	3170234
14	203200	20714	12.3	417	4250765
15	126500	12895	4.8	395	4026504
16	139500	14220	-1.7	377	3843017

N°sec	Shear cross-sectional area
	(m^2)
15	119.6
14	113
13	137.6
12	139.2
11	132.4
10	186.4

Material Properties have been assumed as:

Young’s modulus Ec = 3.13E+07 (kN/m2)
Shear modulus of elasticity G = 1.31E+07 (kN/m2)
Poisson’s ratio = 0.20

The main results are provided in the Table here below.

Table 2.5 – Stick model YZ plane: results

Model Control Data

Direction	Mass (KNs^2/m)	Center of gravity Z (m)	Rotational Inertia (KNs^2/m^3)
X	180571	-	-
Y	-	-	53465851
Z	0	11.68	-

Frequencies

Mode Number	Circular Freq. (rad / sec)	Frequency (cycles / sec)	Period (sec)
1	29.15	4.6393	0.2155
2	65.586	10.438	0.0958
3	72.955	11.611	0.0861
4	103.65	16.496	0.0606
5	119.09	18.954	0.0528
6	154.17	24.537	0.0408
7	166.07	26.431	0.0378
8	200.19	31.861	0.0314
9	206.27	32.828	0.0305
10	224.45	35.722	0.0280
11	242.79	38.641	0.0259
12	251.03	39.952	0.0250
13	293.89	46.774	0.0214
14	302.11	48.083	0.0208
15	312.37	49.716	0.0201
16	329.91	52.508	0.0190
17	338.42	53.861	0.0186
18	352.91	56.167	0.0178
19	423.62	67.422	0.0148
20	498.49	79.336	0.0126

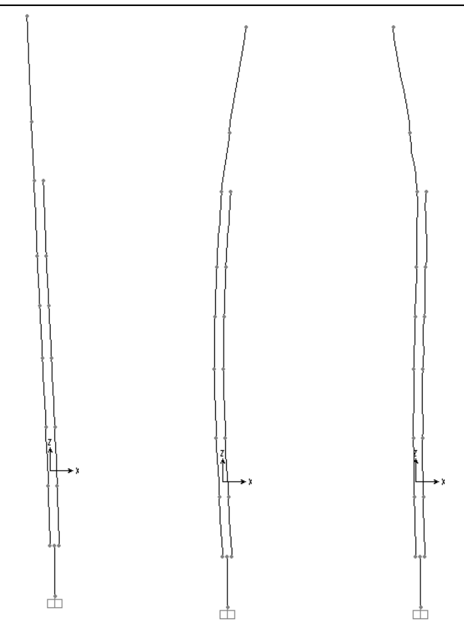

Figure 2.7 – Stick model: Modal shapes of the R/B in YZ direction

Table 2.6 – Stick model in YZ plane: Modal Participation Factors and Modal Masses

Mode Number	UX (KN-s2)	UY (KN-s2)	UZ (KN-s2)	RX (KN-m-s2)	RY (KN-m-s2)	RZ (KN-m-s2)	ModalMass (KN-m-s2)	ModalStiff (KN-m)
1	313.69	0	0	0	9509.56	0	1	850
2	170.64	0	0	0	-2737.92	0	1	4301
3	57.58	0	0	0	-759.99	0	1	5322
4	-22.90	0	0	0	-1818.56	0	1	10742
5	76.30	0	0	0	152.85	0	1	14183
6	69.24	0	0	0	-1442.90	0	1	23769
7	36.34	0	0	0	339.08	0	1	27580
8	63.61	0	0	0	-684.32	0	1	40076
9	19.68	0	0	0	1380.18	0	1	42546
10	44.49	0	0	0	-732.91	0	1	50377
11	9.94	0	0	0	435.06	0	1	58946
12	1.28	0	0	0	878.79	0	1	63015
13	-53.07	0	0	0	431.38	0	1	86372
14	1.29	0	0	0	566.74	0	1	91273
15	-22.17	0	0	0	381.70	0	1	97578
16	-7.62	0	0	0	-96.12	0	1	108844
17	0.40	0	0	0	844.28	0	1	114525
18	2.63	0	0	0	-71.13	0	1	124542
19	-1.88	0	0	0	-844.99	0	1	179456
20	-163.85	0	0	0	1174.63	0	1	248488

Table 2.7 – Stick model in YZ plane: Modal Participating Mass Ratios

Mode Number	UX (Unitless)	SumUX (Unitless)	RY (Unitless)	SumRY (Unitless)
1	0.544960	0.544960	0.751240	0.751240
2	0.161260	0.706220	0.062270	0.813520
3	0.018360	0.724580	0.004800	0.818320
4	0.002900	0.727490	0.027470	0.845790
5	0.032240	0.759730	0.000190	0.845980
6	0.026550	0.786280	0.017300	0.863280
7	0.007320	0.793600	0.000960	0.864230
8	0.022410	0.816000	0.003890	0.868120
9	0.002140	0.818150	0.015820	0.883950
10	0.010960	0.829110	0.004460	0.888410
11	0.000550	0.829660	0.001570	0.889980
12	0.000009	0.829670	0.006420	0.896400
13	0.015600	0.845260	0.001550	0.897950
14	0.000009	0.845270	0.002670	0.900610
15	0.002720	0.848000	0.001210	0.901820
16	0.000320	0.848320	0.000077	0.901900
17	0.000001	0.848320	0.005920	0.907820
18	0.000038	0.848360	0.000042	0.907860
19	0.000020	0.848380	0.005930	0.913800
20	0.148680	0.997050	0.011460	0.925260

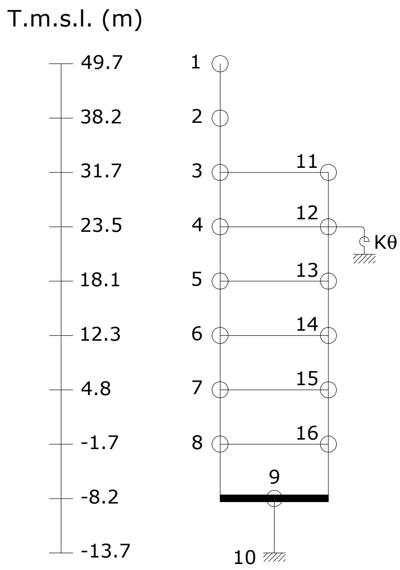

Figure 2.8 – Stick model of the R/B in XZ plane

Table 2.8 – Stick model in XZ plane

N°	Weight	Mass	Rot Inertia weight Io	Rot Inertia mass Io	N°sec	Shear cross-sectional area	Geom. Moment Inertia I
-	(kN)	(kNm/s2)	($x10^5$ kNm2)	(kNm3/s2)		(m^2)	(m^4)
1	39760	4053	148	1508665			
2	80820	8239	301	3068298	9	54.7	30000
3	91310	9308	305	3109072	8	122.9	62600
4	68600	6993	281	2864424	7	172.7	87900
5	51200	5219	215	2191641	6	131.8	81900
6	80110	8166	327	3333333	5	166.7	92800
7	78200	7971	323	3292559	4	179.3	114600
8	80800	8236	331	3374108	3	211.5	124000
9	349200	35596	1060	10805301	2	259.5	131000
10	0	0	0	0	1	3373.4	998600

N°	Weight	Mass	Rot Inertia weight Io	Rot Inertia mass Io	N°sec	Shear cross-sectional area	Geom. Moment Inertia I
-	(kN)	(kNm/s2)	($x10^5$ kNm2)	(kNm3/s2)		(m^2)	(m^4)
11	88000	8970	273	2782875			
12	175900	17931	484	4933741	15	219	6700
13	110160	11229	347	3537207	14	222.8	23300
14	205740	20972	462	4709480	13	207.4	23100
15	130000	13252	441	4495413	12	152.1	23400
16	141600	14434	418	4260958	11	180.1	21200
					10	164.4	23800

Tot P	**1771400**
Tot M	**180571**
Tot Io	**58267074**

Young's modulus Ec = 3.13E+07 (kN/m2)
Shear modulus of elasticity G = 1.31E+07 (kN/m2)
Poisson's ratio = 0.20
Rotational spring Kθ = 2.14E+10 (kNm/rad)

The main results obtained with the stick model in XZ plane are provided in the following Table.

Table 2.9 – Stick model XZ plane: results

Model Control Data

Direction	Mass (KNs^2/m)	Center of gravity Z (m)	Rotational Inertia (KNs^2/m^3)
X	-	-	58267074
Y	180571	-	-
Z	0	11.68	-

Frequencies

Mode Number	Circular Freq. (rad / sec)	Frequency (cycles / sec)	Period (sec)
1	31.37	4.993	0.200279
2	68.66	10.928	0.091506
3	79.90	12.716	0.078642
4	104.77	16.675	0.059971
5	119.79	19.065	0.052452
6	134.62	21.426	0.046672
7	157.47	25.062	0.039901
8	185.49	29.522	0.033873
9	209.27	33.307	0.030024
10	216.71	34.491	0.028993
11	224.09	35.665	0.028039
12	270.16	42.997	0.023258
13	279.87	44.542	0.022451
14	285.85	45.494	0.021981
15	319.96	50.924	0.019637
16	330.06	52.53	0.019037
17	378.17	60.188	0.016614
18	392.61	62.486	0.016004
19	499.14	79.441	0.012588
20	503.72	80.169	0.012474

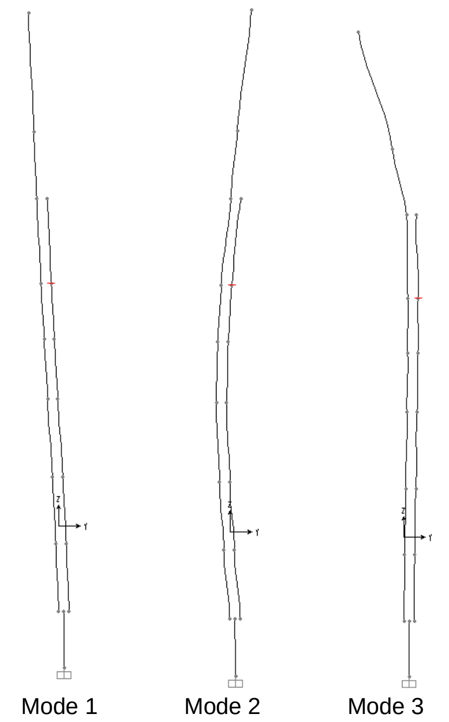

Figure 2.9 – Stick model: Modal shapes of the R/B in XZ direction

Table 2.10 – Stick model in XZ direction: Modal Participation Factors and Modal Masses

Mode Number	UX (KN-s2)	UY (KN-s2)	UZ (KN-s2)	RX (KN-m-s2)	RY (KN-m-s2)	RZ (KN-m-s2)	ModalMass (KN-m-s2)	ModalStiff (KN-m)
1	0	316.86	0	-9604.32	0	0	1	984
2	0	172.23	0	2925.58	0	0	1	4715
3	0	-11.83	0	-652.68	0	0	1	6383
4	0	51.54	0	1716.62	0	0	1	10977
5	0	40.36	0	-1631.44	0	0	1	14349
6	0	65.13	0	174.36	0	0	1	18124
7	0	64.63	0	1017.45	0	0	1	24797
8	0	-61.43	0	95.13	0	0	1	34408
9	0	18.38	0	1470.67	0	0	1	43795
10	0	-16.89	0	-980.00	0	0	1	46965
11	0	-53.67	0	-38.79	0	0	1	50216
12	0	-2.92	0	356.15	0	0	1	72984
13	0	-20.82	0	-704.79	0	0	1	78325
14	0	3.17	0	-908.80	0	0	1	81708
15	0	49.72	0	291.33	0	0	1	102377
16	0	-21.62	0	-211.76	0	0	1	108937
17	0	-4.62	0	-19.05	0	0	1	143016
18	0	0.66	0	-1015.15	0	0	1	154142
19	0	-138.87	0	-562.82	0	0	1	249144
20	0	85.91	0	1432.10	0	0	1	253731

Table 2.11 – Stick model in XZ direction: Modal Participating Mass Ratios

Mode Number	UY (Unitless)	SumUY (Unitless)	RX (Unitless)	SumRX (Unitless)
1	0.556010	0.556010	0.736900	0.7369
2	0.164280	0.720290	0.068380	0.8053
3	0.000770	0.721070	0.003400	0.8087
4	0.014710	0.735780	0.023540	0.8322
5	0.009020	0.744800	0.021260	0.8535
6	0.023490	0.768290	0.000240	0.8537
7	0.023140	0.791420	0.008270	0.862
8	0.020900	0.812320	0.000072	0.8621
9	0.001870	0.814190	0.017280	0.8793
10	0.001580	0.815770	0.007670	0.887
11	0.015950	0.831720	0.000012	0.887
12	0.000047	0.831770	0.001010	0.888
13	0.002400	0.834170	0.003970	0.892
14	0.000056	0.834230	0.006600	0.8986
15	0.013690	0.847920	0.000680	0.8993
16	0.002590	0.850510	0.000360	0.8996
17	0.000120	0.850630	0.000003	0.8997
18	0.000002	0.850630	0.008230	0.9079
19	0.106800	0.957430	0.002530	0.9104
20	0.040870	0.998300	0.016380	0.9268

2.2.3 Global Finite Elements Model of the Reactor Building

A general view of the used Finite Element Model is shown in Figure 2.10, Figure 2.11 and Figure 2.12.
The model has been constructed using 8-noded 3D solid elements for reinforced concrete structures and 3D truss elements have been adopted to model the steel roof .
A total number of 57316 finite elements have been used, with a number of nodes equal to 74780, for a total number of Degree OF Freedom (DOF) equal to 216168.

In detail 55594 Solid 3D elements, 978 QUAD elements, 669 Truss 3D elements and 75 Mass 1D elements have been used.
The thickness of the wall and columns and beams dimensions have been defined according to the information provided in the Guidance Document.
Reinforced concrete walls have been modelled using 3-4 elements through the thickness and 3 elements along the height. Reinforced concrete column have 4 elements in the cross sections and 3 elements along the height.

As previously described, the global Finite Element model include a rough representation of the vessel, using also in this case 3D brick elements, with the aim to reproduce the influence of this structure on the global behaviour of the building (Figure 2.13).

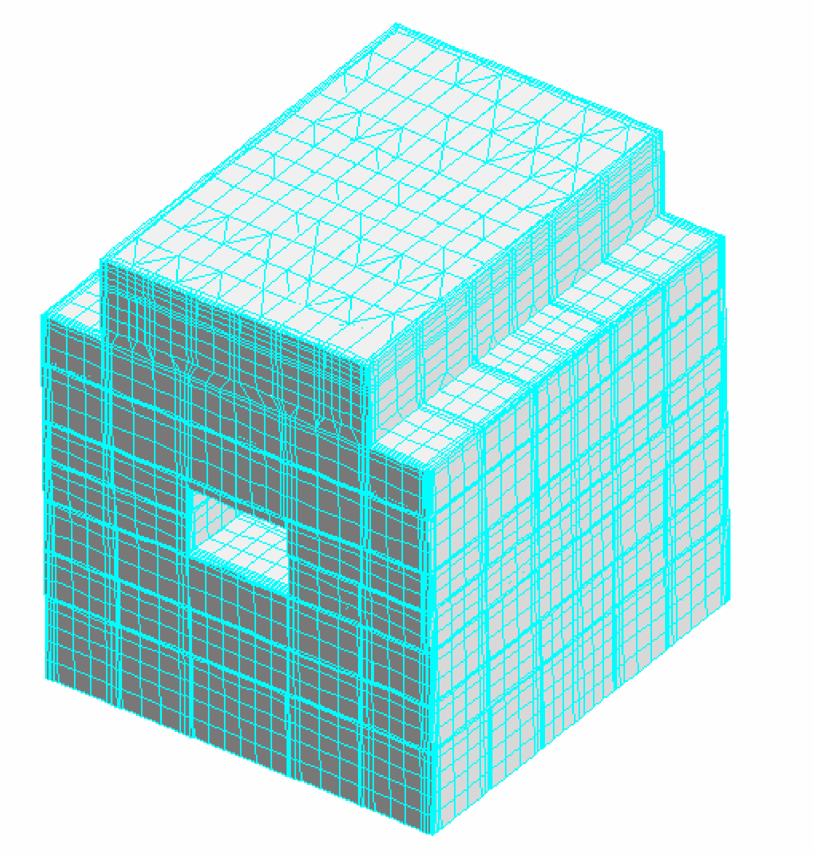

Figure 2.10 – General view of the F.E.model

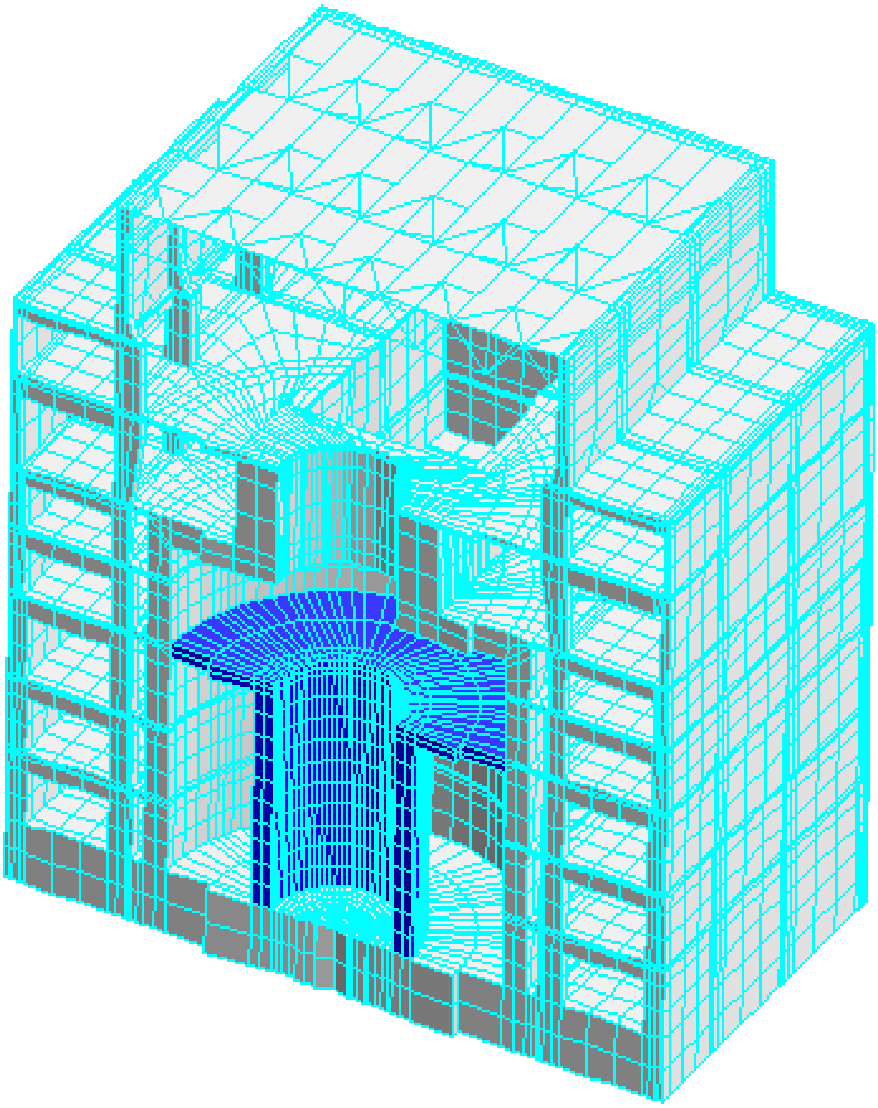

Figure 2.11 – Cross section XZ of the F.E.model (without the vessel)

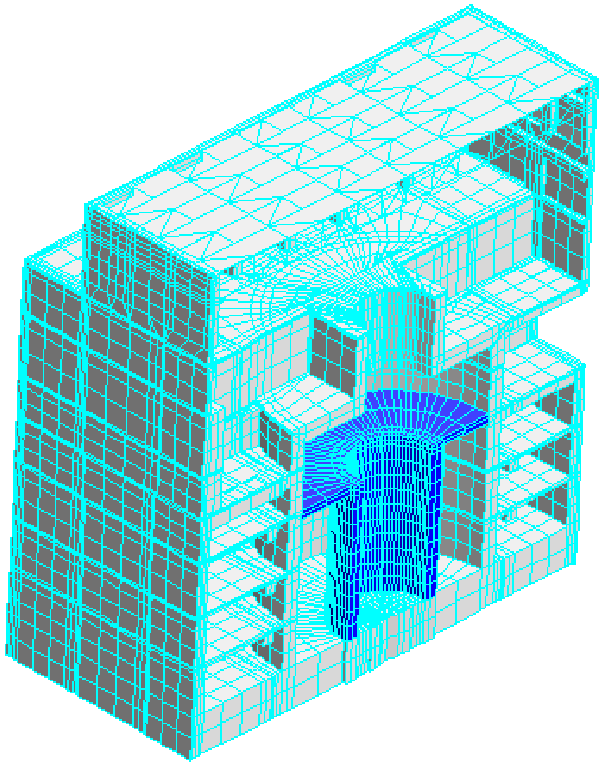

Figure 2.12 – Cross section YZ of the F.E.model (without the vessel)

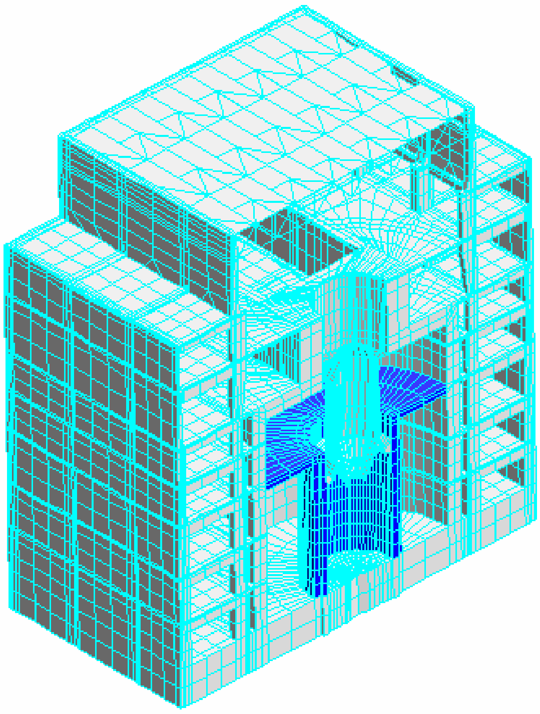

Figure 2.13 – Cross section YZ of the F.E.model (with the rough model of the vessel)

A detailed modelling of the roof has been implemented in the global Finite Element model of the building.
The steel truss beams, in both X and Y directions, have been represented using 3D truss elements, connected to an upper concrete slab simulated with membrane elements. A particular of the roof structure is shown in Figure 2.14.

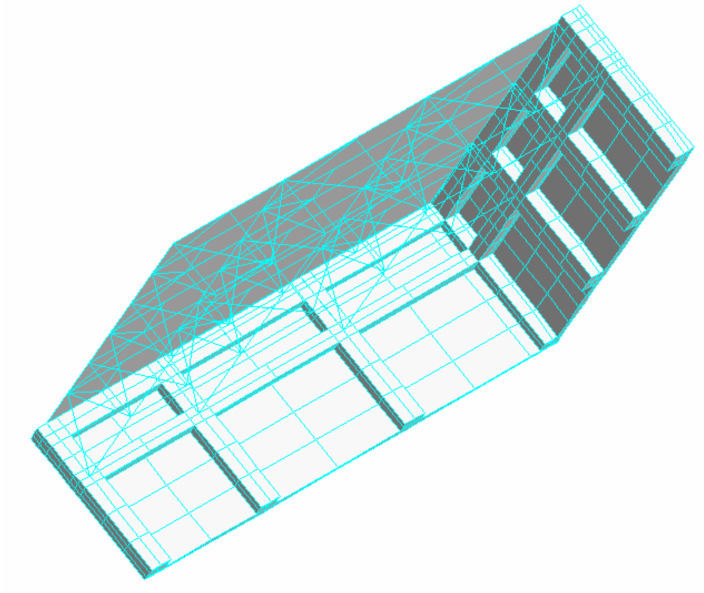

Figure 2.14 – Particular of the roof model

Additional masses have been included by means of 1D MASS elements. In some cases, 2D QUAD elements, with no bending and membrane stiffness, have been used to take into account live, pipe and equipments loads as described in paragraph 2.3.

2.2.4 *Simplified Finite Elements Model of the Dynamic Analysis of Reactor Building*

During Phase II of the Benchmark, time history analyses in non linear field are requested, to evaluate the acceleration and displacement time histories at selected points of the structure during the main shock as indicated in Ref 1.
To perform these analyses a simplified approach have been identified, based on ref. [9] and [10]
At first a non linear pushover analysis has been conducted on the global non linear model, applying the first and second modal shapes, in order to select the characteristics of a Non-linear Single Degree Of Freedom representing the structure above the foundation basemat.

This model have been used to identify a FEM representing the structure, taking into account the Soil Structure Interaction.
Below the basemat, springs and dashpots with equivalent properties have been used.
The linear behaviour of the springs has been calibrated, using a methodology explained later, to reproduce the global impedance of the foundation as outlined in the previous paragraph.
The simplified model is shown in Figure 2.15 with also a general theoretical sketch of the model.

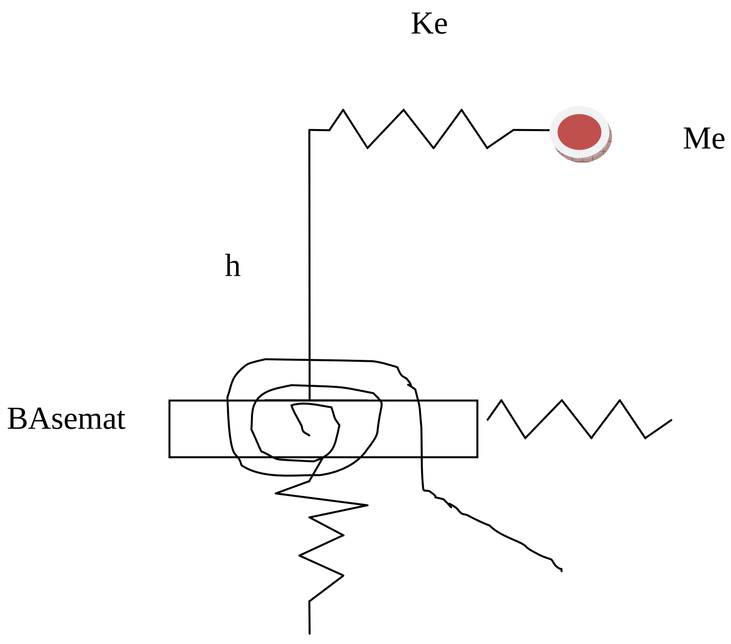

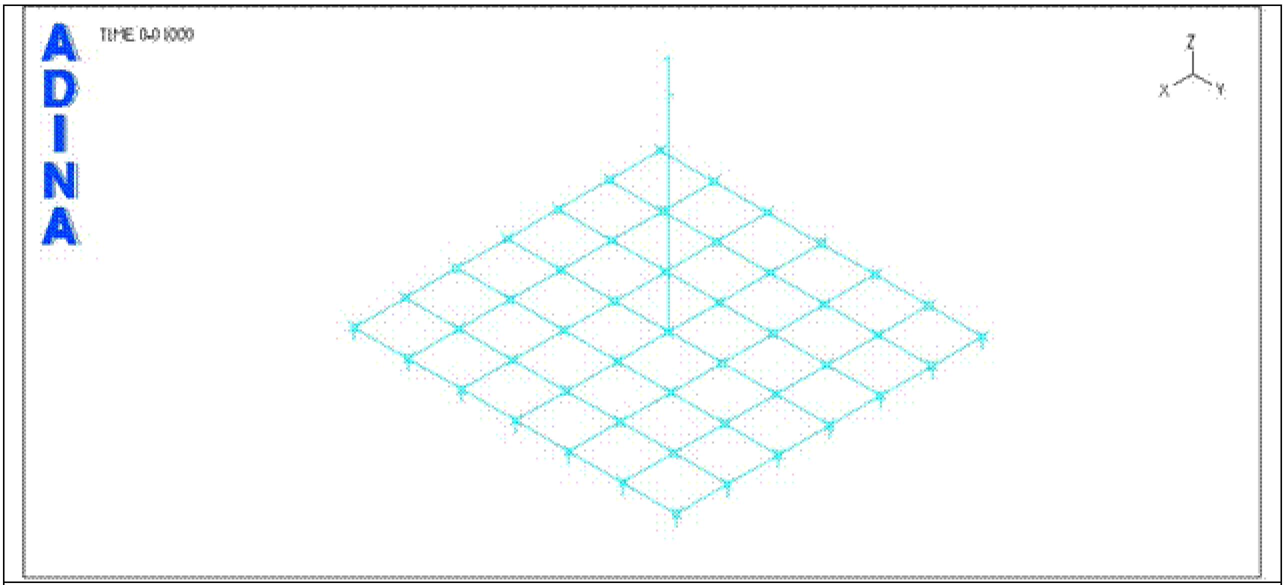

Figure 2.15 – Simplified Model for Non linear TH Analyses

The material characteristics Ke and Me have been evaluated using the results of push-over analyses conducted on the global FE Model, in particular using the force-displacement curves in X and Y directions obtained applying the X and Y eigenvectors respectively.

The equivalent stiffness of the spring can be evaluated by means of the following relationship:

$$K^* = \Gamma_n \sum_{i=1}^{numero\ \ nodi} s_n^* = \Gamma_n V_{base}$$

where:
s_n^* = vector of modal inertia force distribution, for the mode "n".
Γ_n = partecipating factor of mode "n"

V_{base} = shear force at the base of the structure, due to the summation of the modal inertia force distribution of the "n" mode.

Knowing K^* the equivalent mass can be evaluated by:

$$M^* = \frac{K^*}{\omega_n^2}$$

where ω_n circular frequency of model "n"

With pushover analyses the V_{base} value was calculated due to increasing displacement distribution, corresponding to the X and Y eigenvector. A maximum value (capacity value) has been selected and this value has been assumed as maximum force that the spring of the equivalent SDF element can sustain.

2.3 Material properties

Material properties were taken from the Guidance Document.

For the first phase of the benchmark, all structural materials have been assumed linearly elastic.

For concrete elements have been assumed the following values:
mass density = 2.4 t/m3;
Young Modulus = 31.300 MPa
Poisson's ratio = 0.2

For steel structures:
Mass density = 7.8 t/m3
Young Modulus = 205.000 MPa
Poisson's ratio = 0.3

The analyses requested in the Sub Task 1.1.1 consists in the application to the model of vertical and horizontal acceleration equal to 1 g.
Moreover, a modal analysis of the structure was requested.

In order to perform this kind of analyses, all live, pipes and equipments loads acting on the structure have to be inserted in the model in term of mass: this action has been simulated by the modification of the density of some floors structures.

Moreover, 1D mass elements have been used to model specific concentrated loads (masses).

With this approach, a further material identification was necessary to fit the global mass of the building provided in Guidance Document and used in the analyses separately conducted in the stick model of the building.
To improve the correspondence between the total mass of the 3D model and the stick model,
a 10% increase of reinforced concrete density has been adopted for walls, in order to take into account the presence of non structural elements in the building and reinforcing steel bars, not directly included in the model.

2.4 Soil description

2.4.1 Soil column analyses

In *Sub-task 1.1.2 – Soil column analyses,* 1-D equivalent-linear model of layered soils has been used to evaluate the earthquake site response. A layered soil column with plane-parallel strata characterized by a shear wave velocity profile up to 300 metres depth has been considered.

With specific reference to the Guidance Document, the Unit 5 vertical array displays a sequence of silty clays (Late Pleistocene Yasuda formation, about 30 metres thick), followed by a mudstone (Plio-Pleistocene Nishiyama formation) laying in turn above Mio-Pliocene Shiiya formation (geologic substratum as well as engineering bedrock with Vs>700 m/s). Each stratum, beyond shear wave velocity value, is characterized by unit weight, Poisson's ratio and shear modulus reduction curve along with damping curve as a function of shear strain.

The soil column has been finely discretized allowing the resolution of frequencies up to 50 Hz. The Vs profile has been checked both via the picking of the recorded signals and via the Fourier transfer functions between two successive in-hole seismometers.

Strain dependant soil characteristics have been also checked via a soil system identification procedure using earthquake records from aftershocks in the down hole array.
Strain dependant soil characteristics have been implemented according to the provided soil modulus and damping curves. Adjustments have been explored to both curves and initial damping in order to match at the best the recorded signals.

Almost all the site response is concentrated and governed by the first 30 metres (Yasuda stratum and the interface with the Nishiyama stratum).

In particular the first 10 metres (with an estimated shear wave velocity of 160 m/s) deserves to be better characterized since it influences the match of the signal coming up from the substratum with the target motion recorded at the free surface (control point 5-G1).

Preliminarily, the top-10m of the soil column seem to provide a better response when divided into a top-3m looser layer and a second-7m harder layer, in order to increase the seismic impedance ration and to make the computed motion on the free surface more consistent with the recorded one.

In sub-task 1.2 Main Shock response a linear time history analysis was required; two boundary conditions have to be considered:

1. **fixed base**
2. **with soil structure interaction**

For task 1.2, a spring-dashpots system has been used underneath the basemat. The procedures used to calibrate the finite elements characteristic are outlined in paragraph 3.1.3.

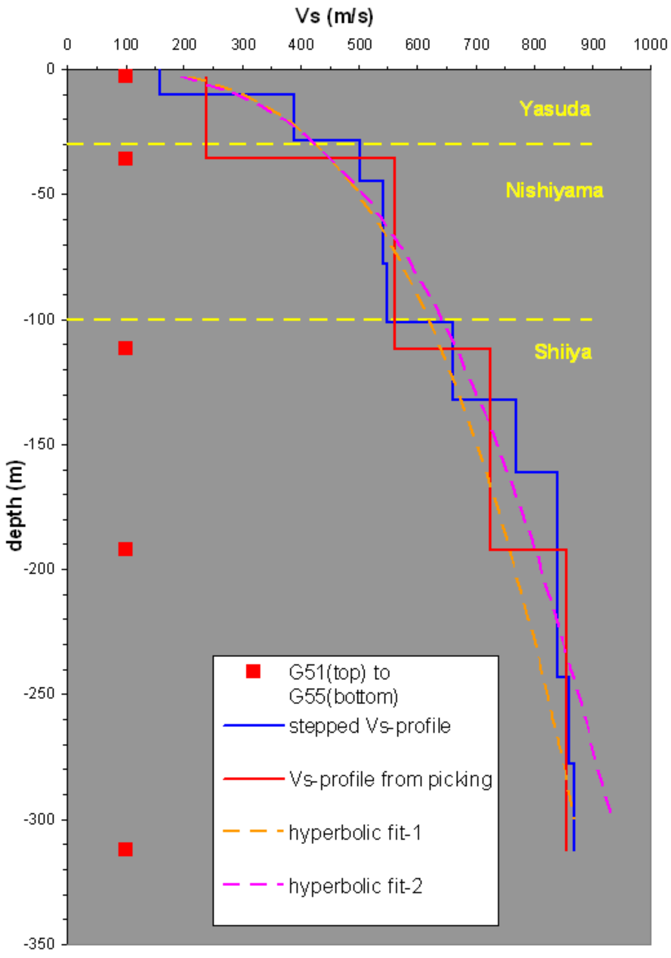

Figure 2.16 – Soil Vs profile

2.4.2 Finite Elements Model for Soil Structure Interaction

In Phase III of the Benchmark, an improvement of the Soil Structure Interaction approach has been taken into account.

The SSI analysis has been developed using a 3D time domain model of a soil island including the reactor building, studied with the ADINA finite element program.
The model size is 300x300 m in plan (about five times the size of the reactor building) and 167 m in depth, down to the assumed bedrock in the soil response analysis.

The soil island model is strictly linear. It has the main purpose of propagating the motion to the building foundation taking into account both kinematic and inertial interaction.
The first step of the analysis is the development and the calibration of a 3D model that yields approximately the same free field response of the 1D frequency domain analysis developed for the benchmark with an equivalent linear approach (SHAKE or EERA).

The size of the finite elements has been chosen having in mind the objective to keep the computational burden within a reasonable limit and to describe adequately the spectral content of the motion at the building foundation at the expected frequencies of the nonlinear stick models with base springs (about 1Hz). The element size along the vertical direction is not larger that $\lambda/8$, where λ is the wavelength corresponding to the maximum frequency f of interest ($\lambda = Vs/f$ where Vs shear waves velocity)

The smallest elements are required at the upper layer level, where the backfill shear wave velocity is lower.

The size of the element in plan is of about 3 m at the boundary of the building area and is increasing toward the boundary of the soil island. This choice allows a numerical attenuation of the waves due to the soil-structure interaction travelling outside from the building-soil interface..
The finite element model of the SSI system is shown in Figure 2.17.

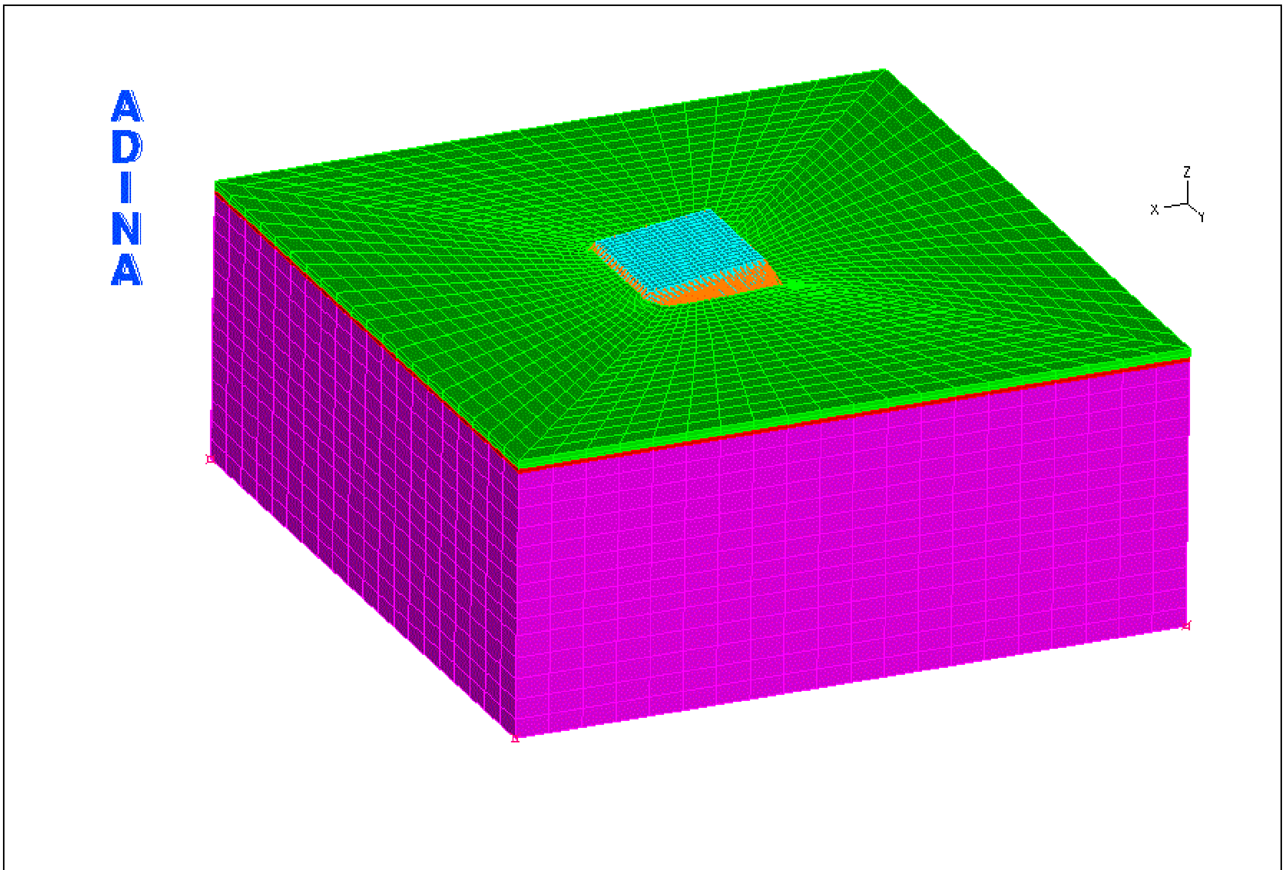

Figure 2.17 – Soil Structure Interaction Model

The soil properties used in the time domain model are those obtained by iteration in the 1D equivalent linear model. The damping model is different, because in the time domain analysis Rayleigh damping has to be used, while constant hysteretic damping is used in the equivalent linear model. The damping matrix C is assumed to be proportional to mass matrix M and stiffness matrix K according to the equation

$$C = \alpha M + \beta K$$

The Rayleigh damping coefficients have been evaluated to match the iterated damping values in the frequency range of interest, as shown in the figure below.

Time step, even for implicit integration schemes, is limited due to the fact that the smallest period of vibration needs to be represented by at least 10 points.
Hence the time step limitation can be formulated as follows (v is the highest volume wave velocity.)

$$Dt \le he / v$$

Where *he* is the element size.

Boundary condition of the 3D model
A Lysmer-Kuhlemeyer viscous boundary has been used at the base of the model. The nodes on the lateral surfaces of the model have been constrained to have equal horizontal displacements at same level and zero vertical displacements. This boundary condition is aimed to reproduce the free-field displacements and has been checked with a 1-D model as discussed in the following.

1D model
A 1D model has been developed to calibrate the soil parameters and check the validity of the ADINA time domain analysis against the 1D soil response analysis developed by IAEA consultants for the benchmark.

The discretization in the vertical direction of the 1D model is the same used in the 3D model to check the response in the relevant frequency range. The 1D model has only one brick element in plan with 1m x 1 m sides. Only the X displacement degree of freedom has been used in the analysis. The Lysmer-Kuhlemeyer viscous boundary has been included at the model base.

The time domain analysis has some limitations in the frequency range, mainly due to the size of the finite elements in the vertical direction and consequent minimum wavelength than can be described in the model. This kind of limitation does not exist in the equivalent linear frequency domain analysis, because an exact solution of the wave propagation equation is used.
The comparison of the response has been made at the surface level (+12) and at the base raft elevation (-13.7).

In the following Figure 2.18 the response spectra obtained by the 1D time domain analysis are compared with those obtained by IAEA consultants. The analysis have been developed with two approaches:

- use of a Lysmer-Kuhlemeyer viscous boundary and input given as boundary force at the viscous boundary (curve adina_force)
- use of a Lysmer-Kuhlemeyer viscous boundary and input given as inertia forces on the soil column (curve adina_inert)

As a comparison also the analysis without viscous boundary has been developed (curve adina_rig)

It can been seen that the spectral content in the range around 1 Hz is quite similar, with the obvious exception of the case without the viscous boundary. A good agreement is obtained up to 3-5 Hz.

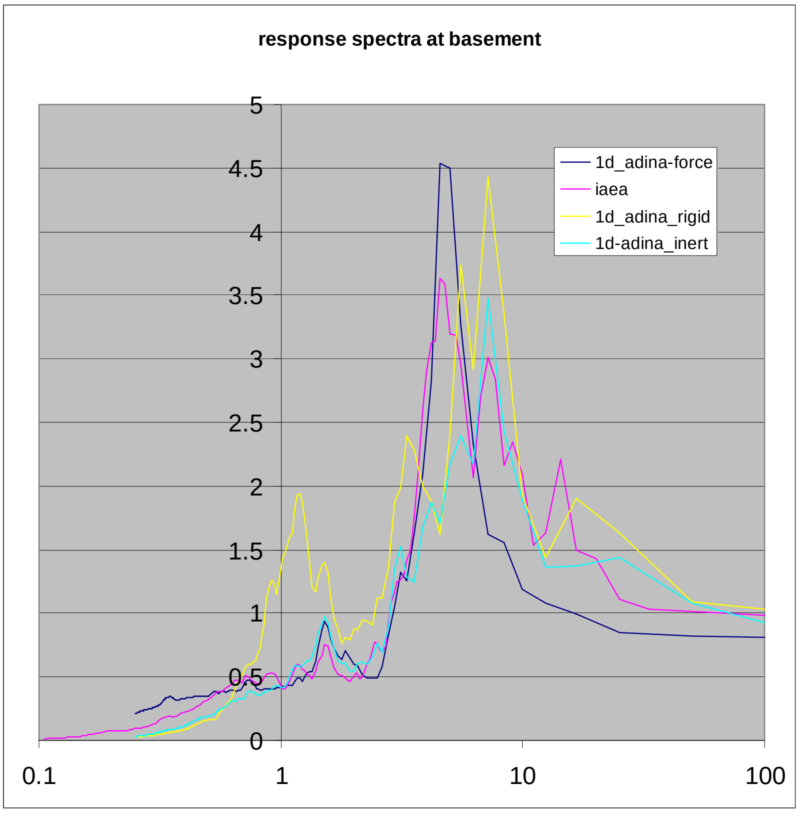

Figure 2.18 – Comparison 1D model Vs IAEA ground motion: Basemat

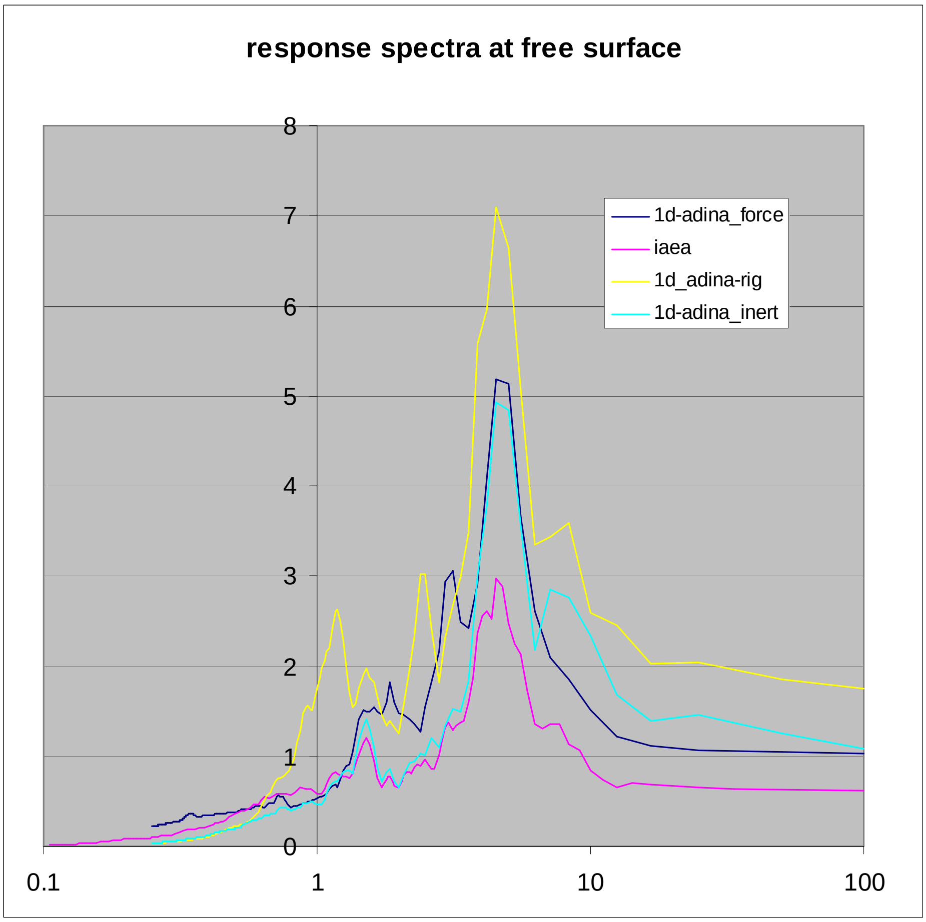

Figure 2.19 – Comparison 1D model Vs IAEA ground motion: free surface

3-D model

The soil volume around the building together with the appropriate boundary condition (periodic constraints on the lateral surface and Lysmer-Kuhlemeyer boundary at the bottom) represents the free field conditions for the seismic motion propagation and provides the elastic stiffness for the interaction motion. To capture the nonlinear behaviour at the interface between the building and the surrounding soil the contact has been modelled with elasto-plastic, compression only truss elements.

The main properties of the truss elements are:

- Side elements: compression only, yield limit corresponding to the horizontal passive pressure in the soil (depth dependent).
- Bottom elements: compression only, yield limit corresponding to a vertical pressure equal to 1600 KPa.

Both set of elements has a very high elastic stiffness, because the elastic deformation is provided by the surrounding soil.

Some views of the block representing the building and the interface are shown in the figures below.

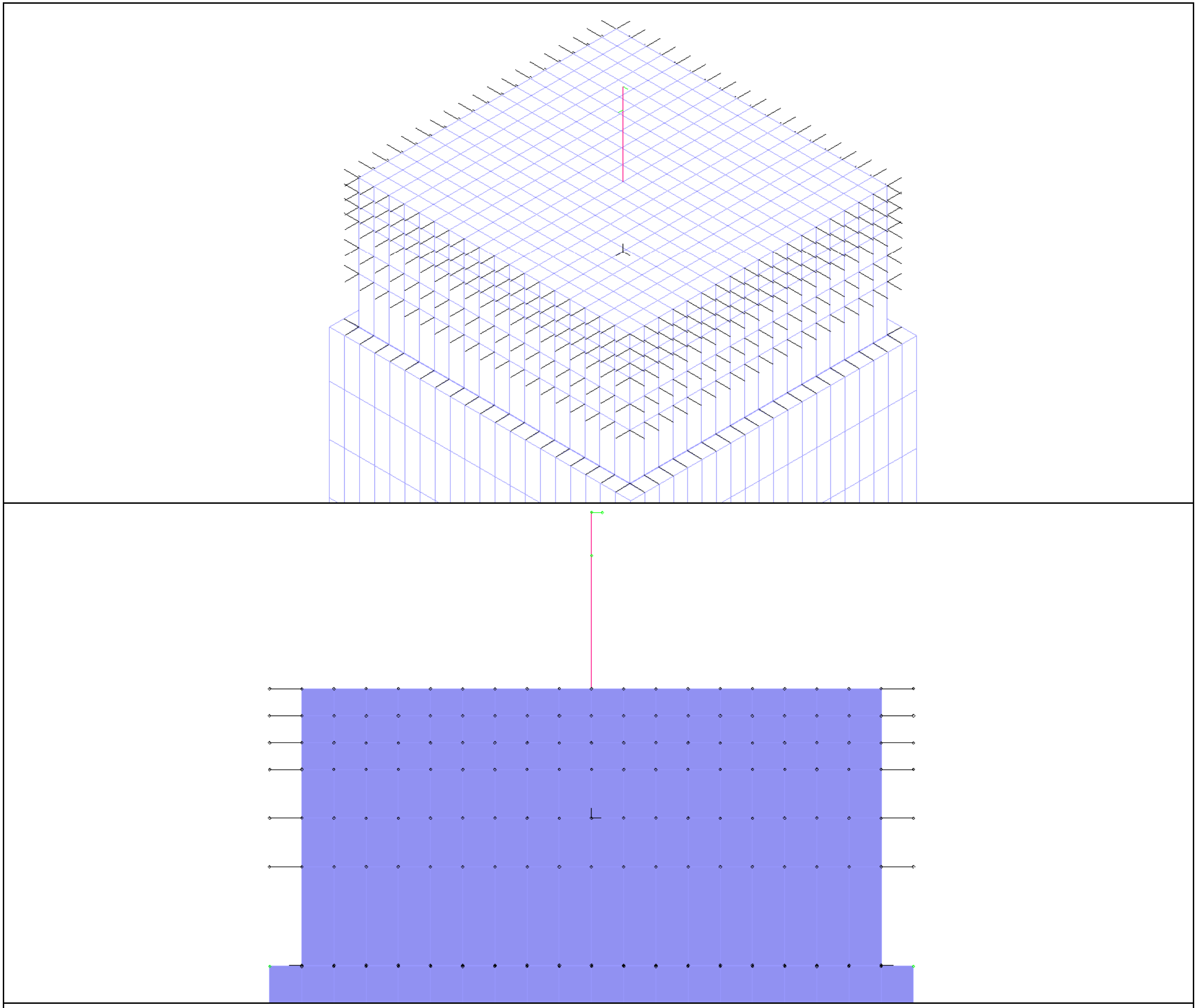

Figure 2.20 – 3D model

Key steps in the analysis:

The first step is a static analysis under gravity loads. This step is also necessary to give the initial compressive stress to the gaps.
It must be remembered that the dynamic model has only dampers as boundary condition and is free as a rigid body under static loads.

To avoid numerical problems the static reactions at the bottom of the model determined with a static, fixed base analysis have been applied in equilibrium with the gravity loads. Spring elements with a negligible stiffness (10000 kN/m) have been added in X,Y and Z direction at the four corners of the bottom surface of the model to provide a numerical constraint against rigid body modes.

2.5 Boundary conditions

In the first phase of the analyses the building has been fixed at the bottom of the basemat. All the model has been develop using elements with only displacements degrees of freedom. Shell elements have been used only with membrane behaviour. Some additional constraints have been used for the roof trusses where rod elements, with axial stiffness only, cannot develop global stiffness along the out of the truss-plane direction.

In the second and third phases of the benchmark, soil structure interaction effects have been taken into account. At first, a simplified model with springs and dashpots has been used. The final analyses have been conducted using a model with a direct representation of the soil.

2.6 Computer codes and methods used

The 3D model of the building has been developed using the COSMOS/M ver. 2.5 Finite element code. Stick model and the preliminary model of the vessel has been developed using SAP-IV Finite element code.

The soil column analyses have been performed using EERA computer program (release 2000) based on the core of Shake91.

The nonlinear analysis and the final time histories analyses have been conducted using the ADINA Code, ver.8.8.

3. MAIN RESULTS OF PERFORMED ANALYSES

3.1 Task 1.1 Construction and validation of the soil and structure models

3.1.1 Task 1.1.1 Static and model analysis of the fixed base model

The preliminary validation of the global structural model has been based on the check of the total weight of the structure.
Partial checks have been conducted during the development of the finite element model of the roof, due to its detail in the description of the individual truss members.

The deformed shape of the building due to the vertical load analysis performed on the fixed base model is shown Figure 3.21.
The maximum vertical displacement is recorded at the centre of the roof and is equal to about 17 mm.

In Figure 3.22 and Figure 3.23, the contour plot of the minimum principal stresses is reported at two different levels.
Higher values can be identified at the base of the internal columns, where the compressive strength reaches about 6. MPa. The maximum compressive strength at the base of the walls is about 3.1-3.2 MPa.

The global vertical reaction is equal to 1941 MN. With respect to the origin of the adopted coordinate system, positioned at the centre of the RCCV, a bending moment about the x axis has been estimated, equal to 1882, due to the fact that the origin of the coordinate system does not correspond to the centre of the basemat.

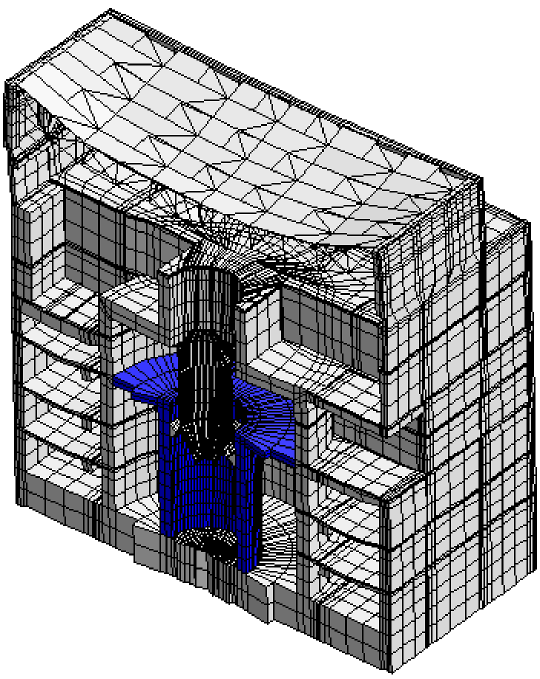

Figure 3.21 – Vertical loads – deformed shape

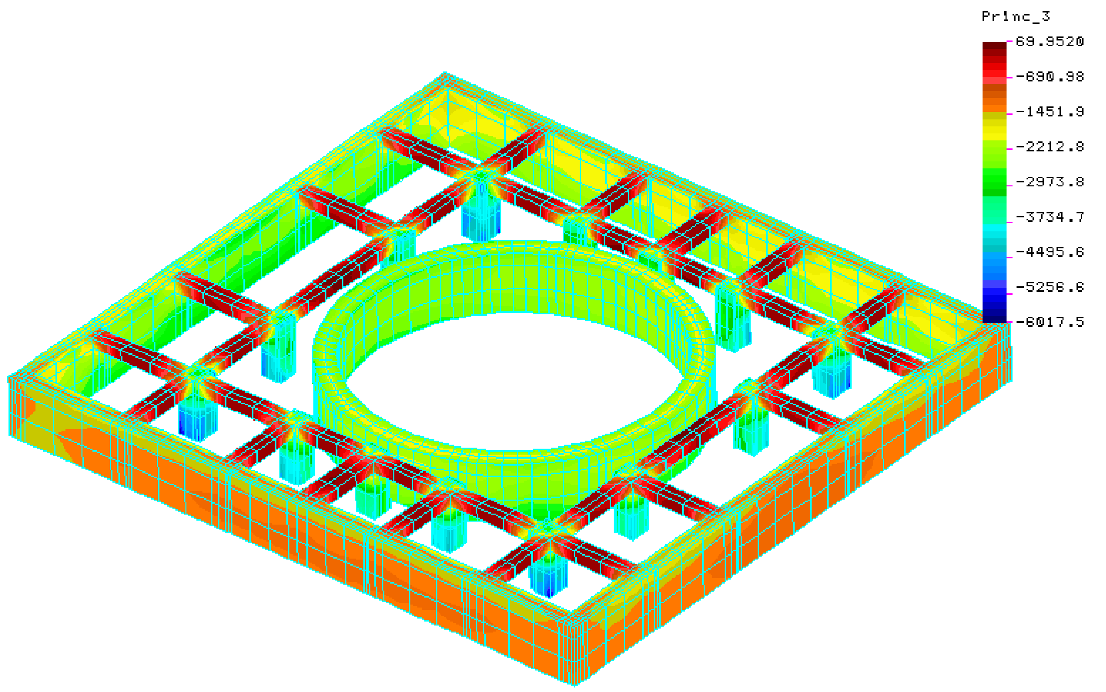

Figure 3.22 – Vertical loads – Principal minimum stress of the walls at the top of the basemat

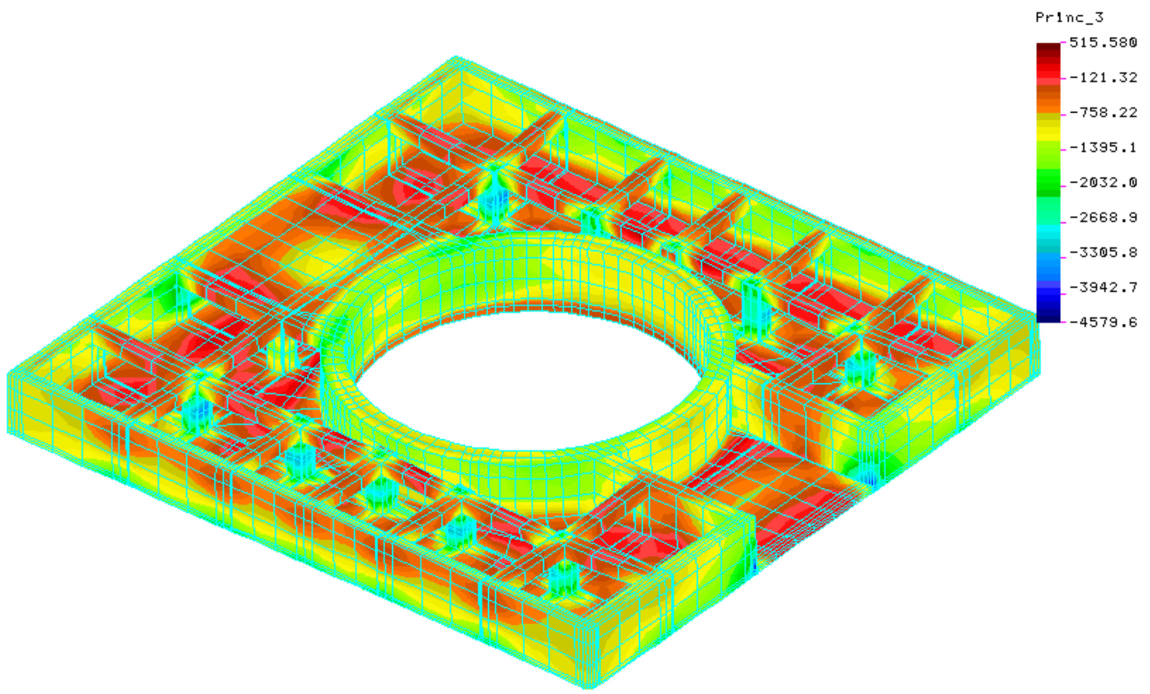

Figure 3.23 – Vertical loads – Principal minimum stress al el. 12.3 m

The results of the analyses performed under horizontal acceleration applied in X and Y directions are summarized in the following figures.

Figure 3.24 shows the deformed shape of the structure due to the 1 g horizontal acceleration in X direction. Figure 3.25 and Figure 3.26 give evidence of the stress state (minimum principal stress).

The maximum horizontal displacement is about 20 mm at roof level.

The horizontal reaction force in X direction is about 1942 MN and the bending moment about Y axis is 42860 MNm.

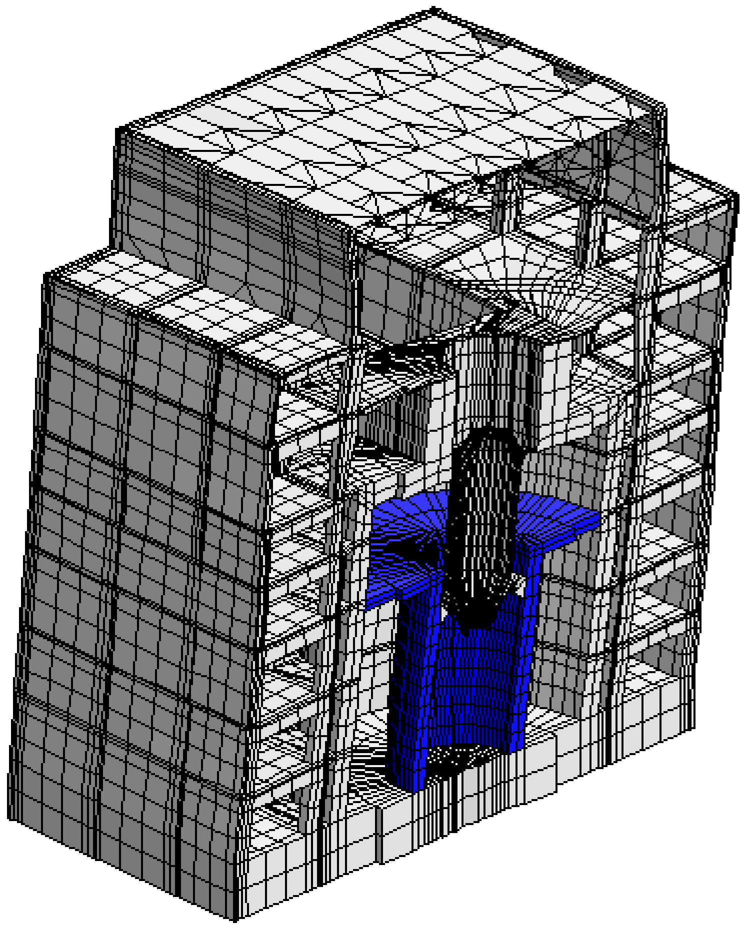

Figure 3.24 – Horizontal acceleration X – Deformed shape

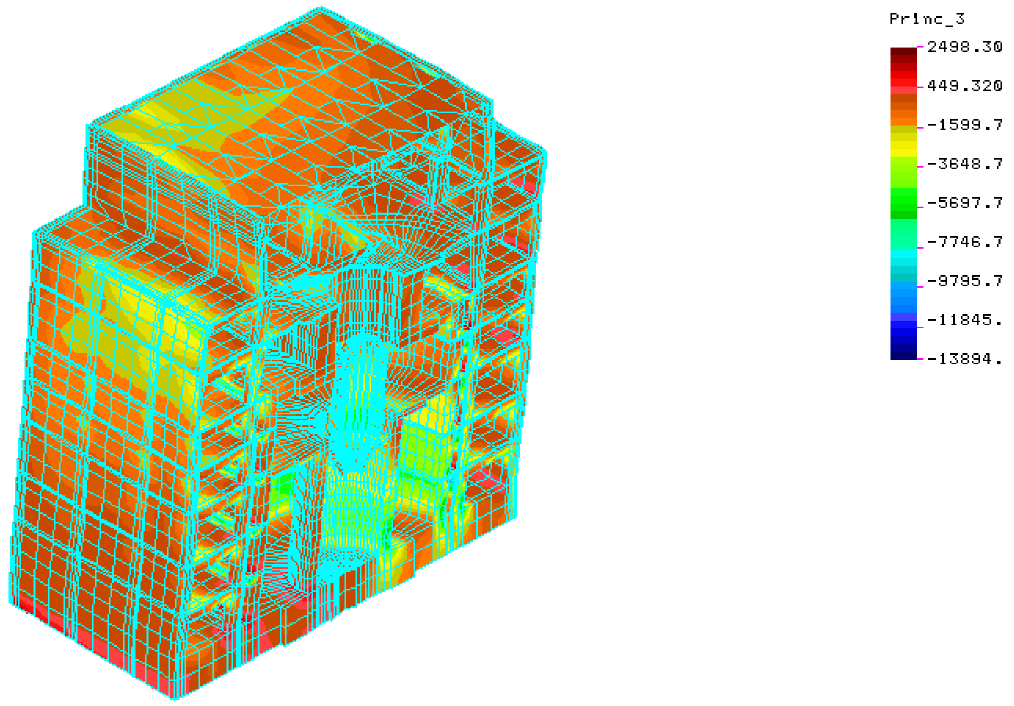

Figure 3.25 – Horizontal acceleration X – Principal minimum stresses (KN/m2)

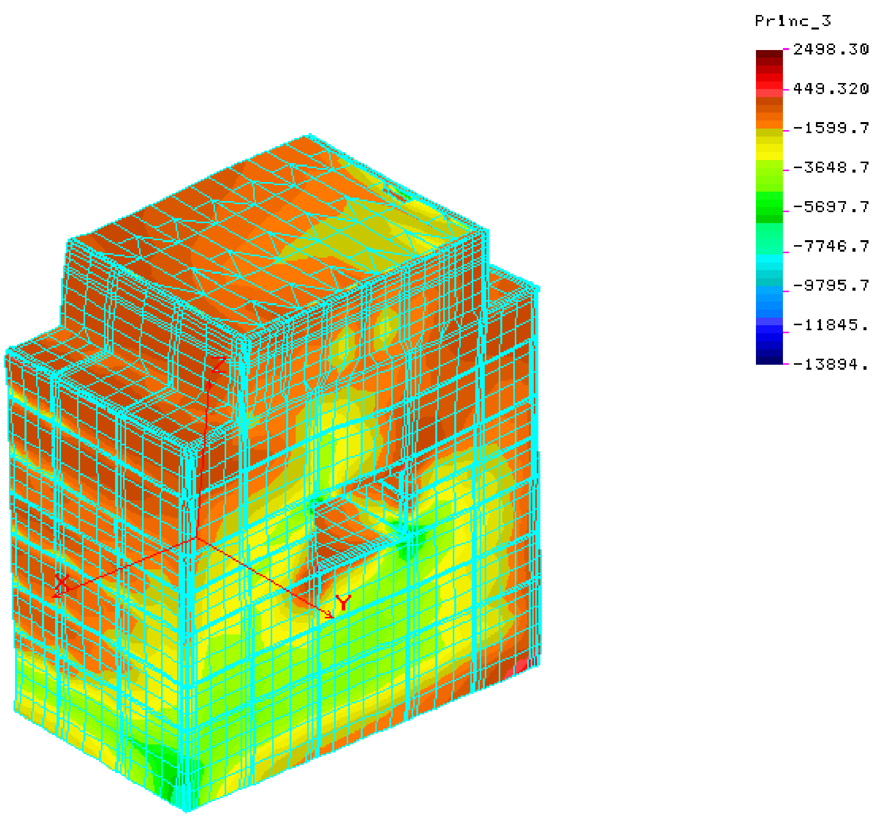

Figure 3.26 – Horizontal acceleration X – Principal minimum stresses (KN/m2) – External wall

The corresponding situation is shown in the subsequent figures for Y-direction acceleration..

The deformed shape is shown in Figure 3.27 and the stress state is illustrated in Figure 3.28 and Figure 3.29. The maximum horizontal displacement in y direction is equal to about 17 mm, also in this case at roof level.

The horizontal reaction force in Y direction is equal to 1942 MN and the bending moment about the X axis is equal to 42883 MNm.

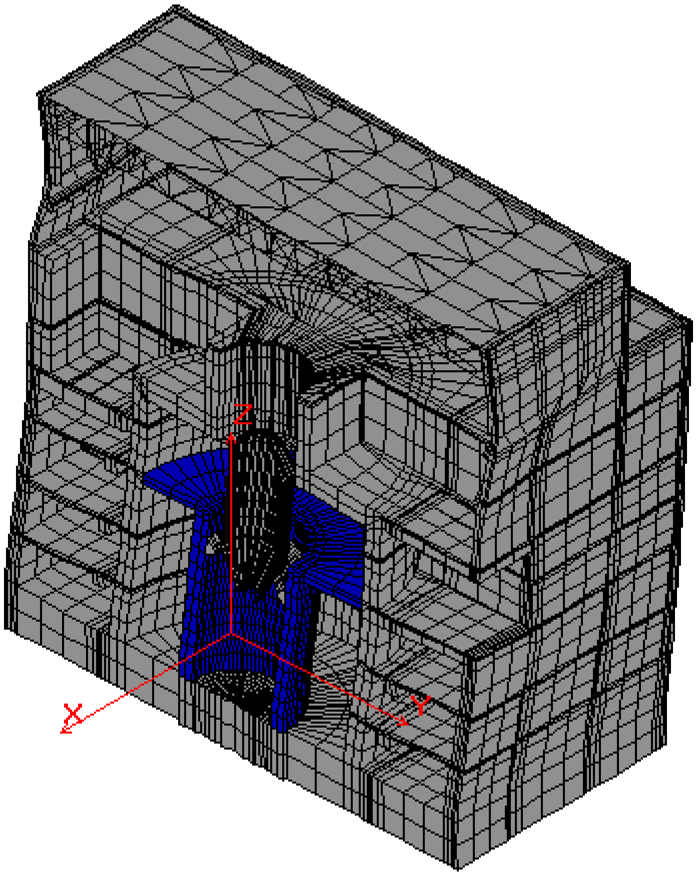

Figure 3.27 – Horizontal acceleration Y – Deformed shape

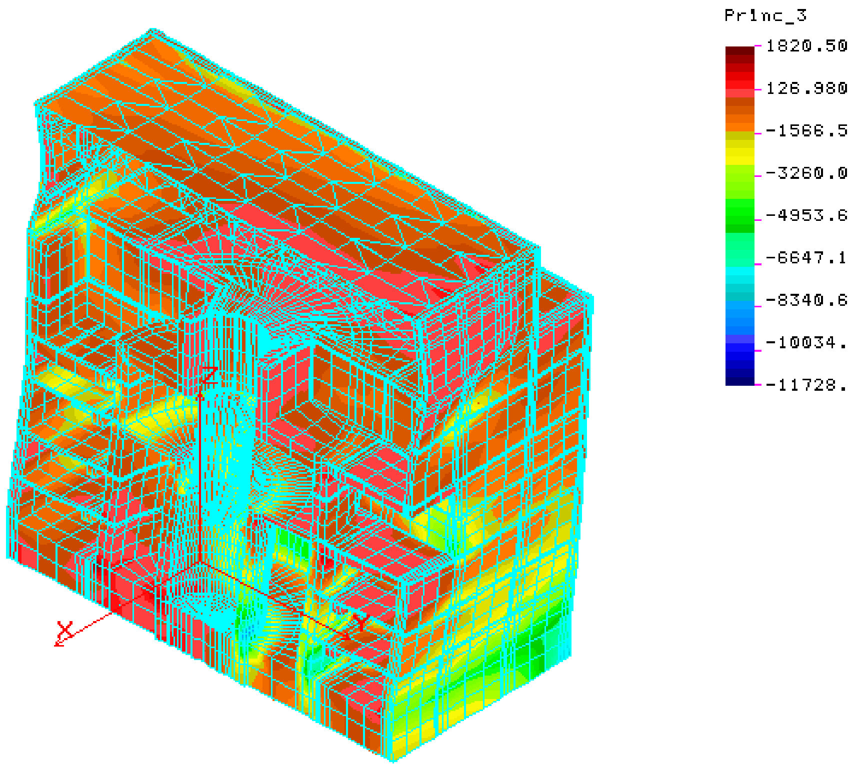

Figure 3.28 – Horizontal acceleration Y – Principal minimum stress (KN/m2)

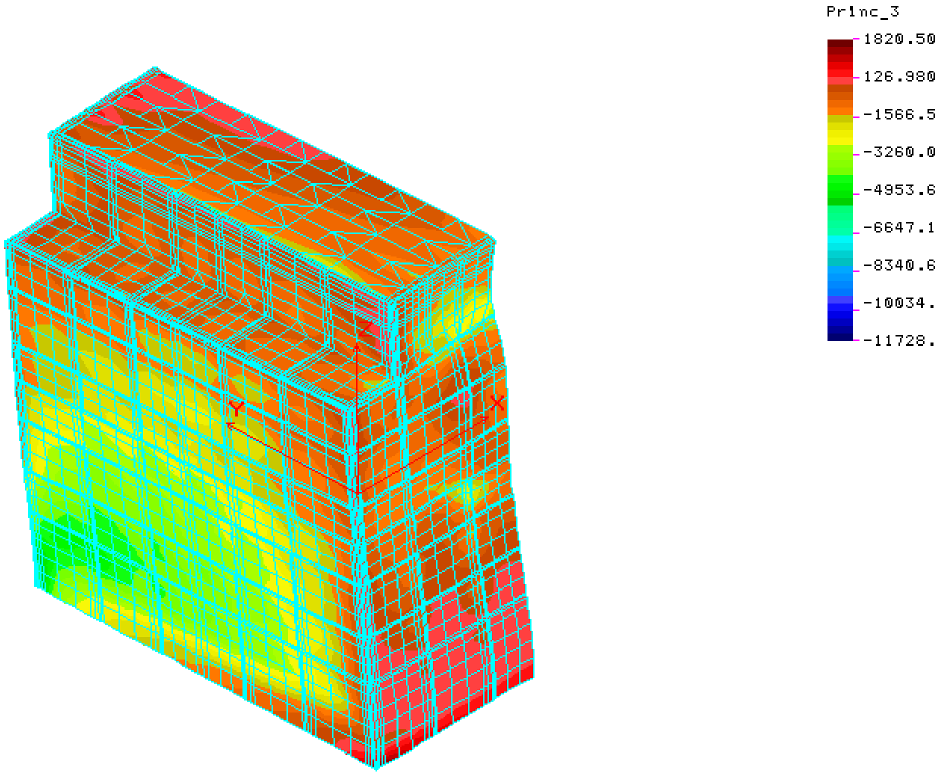

Figure 3.29 – Horizontal acceleration Y – Principal minimum stress (KN/m2) – External wall

With respect to modal analysis, it is worth noting that the 3D detailed model of the structure that has been developed with the aim to describe the nonlinear behaviour in the subsequent phases of the benchmark exhibits a large number of local modes with small participating mass.

The first modal analysis was run according the preliminary request of 30 frequencies in the template. Only about 60% of the total mass of the structure is included in the participating mass of these 30 frequencies and the maximum frequency included is only about 12 Hz.
The modal analysis was gradually extended up to 60 frequencies, but the cumulative participating mass increases only up to about 67%. The maximum frequency increased to 16 Hz.
A further analysis up to 100 modes, not reported for the sake of brevity, yielded a total participating mass ratio equal to 70% with a frequency up to about 19 Hz.
The model frequencies are reported in the Table 3.12. The participating mass results are shown in the Table 3.13 and in Figure 3.30.

Table 3.12 – Modal frequencies

FREQUENCY NUMBER	FREQUENCY (RAD/SEC)	FREQUENCY (CYCLES/SEC)	PERIOD (SECONDS)
1	0.2815663E+02	0.4481266E+01	0.2231512E+00
2	0.2997848E+02	0.4771223E+01	0.2095899E+00
3	0.3073151E+02	0.4891071E+01	0.2044542E+00
4	0.3846955E+02	0.6122618E+01	0.1633288E+00
5	0.4657942E+02	0.7413344E+01	0.1348919E+00
6	0.4700788E+02	0.7481536E+01	0.1336624E+00
7	0.4902949E+02	0.7803285E+01	0.1281512E+00
8	0.5107569E+02	0.8128948E+01	0.1230171E+00
9	0.5148829E+02	0.8194616E+01	0.1220313E+00
10	0.5373101E+02	0.8551555E+01	0.1169378E+00
11	0.5601818E+02	0.8915571E+01	0.1121633E+00
12	0.5643411E+02	0.8981767E+01	0.1113367E+00
13	0.5984792E+02	0.9525093E+01	0.1049859E+00
14	0.6017195E+02	0.9576663E+01	0.1044205E+00
15	0.6034984E+02	0.9604975E+01	0.1041127E+00
16	0.6267881E+02	0.9975641E+01	0.1002442E+00
17	0.6424532E+02	0.1022496E+02	0.9779990E-01
18	0.6650184E+02	0.1058410E+02	0.9448138E-01
19	0.6676174E+02	0.1062546E+02	0.9411357E-01
20	0.6825461E+02	0.1086306E+02	0.9205511E-01
21	0.6896601E+02	0.1097628E+02	0.9110554E-01
22	0.6906739E+02	0.1099242E+02	0.9097180E-01
23	0.7030675E+02	0.1118967E+02	0.8936817E-01
24	0.7285912E+02	0.1159589E+02	0.8623746E-01
25	0.7328338E+02	0.1166341E+02	0.8573821E-01
26	0.7361894E+02	0.1171682E+02	0.8534741E-01
27	0.7412959E+02	0.1179809E+02	0.8475948E-01
28	0.7457598E+02	0.1186914E+02	0.8425214E-01
29	0.7561910E+02	0.1203515E+02	0.8308993E-01
30	0.7642072E+02	0.1216273E+02	0.8221835E-01
31	0.7704593E+02	0.1226224E+02	0.8155117E-01
32	0.7883980E+02	0.1254774E+02	0.7969561E-01
33	0.8115174E+02	0.1291570E+02	0.7742515E-01
34	0.8156709E+02	0.1298180E+02	0.7703089E-01
35	0.8502360E+02	0.1353193E+02	0.7389931E-01
36	0.8647162E+02	0.1376239E+02	0.7266182E-01
37	0.8788635E+02	0.1398755E+02	0.7149217E-01
38	0.8803384E+02	0.1401102E+02	0.7137239E-01
39	0.8834454E+02	0.1406047E+02	0.7112138E-01
40	0.8904510E+02	0.1417197E+02	0.7056183E-01
41	0.8927718E+02	0.1420890E+02	0.7037841E-01

```
42         0.9120644E+02    0.1451596E+02  0.6888971E-01
43         0.9216180E+02    0.1466801E+02  0.6817560E-01
44         0.9286560E+02    0.1478002E+02  0.6765891E-01
45         0.9327841E+02    0.1484572E+02  0.6735948E-01
46         0.9357684E+02    0.1489322E+02  0.6714466E-01
47         0.9537332E+02    0.1517914E+02  0.6587991E-01
48         0.9681548E+02    0.1540866E+02  0.6489856E-01
49         0.9705919E+02    0.1544745E+02  0.6473561E-01
50         0.9764704E+02    0.1554101E+02  0.6434589E-01
51         0.9788600E+02    0.1557904E+02  0.6418881E-01
52         0.9815895E+02    0.1562248E+02  0.6401031E-01
53         0.9837438E+02    0.1565677E+02  0.6387014E-01
54         0.9854193E+02    0.1568344E+02  0.6376154E-01
55         0.1000186E+03    0.1591845E+02  0.6282019E-01
56         0.1005318E+03    0.1600014E+02  0.6249946E-01
57         0.1006203E+03    0.1601422E+02  0.6244452E-01
58         0.1008685E+03    0.1605372E+02  0.6229086E-01
59         0.1009395E+03    0.1606502E+02  0.6224705E-01
60         0.1016645E+03    0.1618041E+02  0.6180314E-01
```

Table 3.13 – Modal masses

MODE	Mx	My	Mz	Cum. Mx	Cum. My	Cum. Mz
1	0.538	2.19E-08	8.16E-07	0.538	2.19E-08	8.16E-07
2	1.00E-09	0.557	5.33E-05	0.538	0.557	5.41E-05
3	2.41E-04	3.63E-05	5.39E-03	0.539	0.557	5.44E-03
4	1.33E-06	2.94E-03	6.55E-06	0.539	0.56	5.45E-03
5	2.19E-03	2.76E-05	1.79E-05	0.541	0.56	5.46E-03
6	4.16E-06	1.82E-04	9.17E-04	0.541	0.56	6.38E-03
7	1.28E-11	3.19E-02	7.46E-05	0.541	0.592	6.46E-03
8	1.70E-02	2.83E-05	3.63E-03	0.558	0.592	1.01E-02
9	7.30E-03	1.24E-04	1.10E-05	0.565	0.592	1.01E-02
10	3.33E-04	8.42E-05	0.129	0.565	0.592	0.139
11	3.59E-07	2.64E-04	6.17E-05	0.565	0.593	0.139
12	2.15E-02	7.41E-07	6.69E-05	0.587	0.593	0.139
13	1.51E-03	8.02E-05	3.46E-03	0.588	0.593	0.143
14	2.08E-05	2.70E-03	7.95E-05	0.588	0.595	0.143
15	6.72E-06	3.53E-06	4.52E-05	0.588	0.595	0.143
16	1.30E-03	5.42E-06	1.20E-02	0.59	0.595	0.155
17	1.52E-04	7.53E-05	4.65E-04	0.59	0.595	0.155
18	1.02E-02	5.48E-03	5.57E-04	0.6	0.601	0.156
19	4.18E-03	1.49E-02	1.17E-04	0.604	0.616	0.156
20	2.48E-03	1.60E-04	2.01E-05	0.607	0.616	0.156
21	4.16E-05	8.48E-06	1.34E-02	0.607	0.616	0.17
22	1.58E-07	6.35E-08	7.98E-06	0.607	0.616	0.17
23	6.80E-07	2.25E-07	2.79E-04	0.607	0.616	0.17
24	2.51E-05	5.10E-04	0.303	0.607	0.617	0.473
25	2.49E-03	1.29E-05	4.03E-03	0.609	0.617	0.477
26	1.43E-04	1.58E-05	1.63E-03	0.61	0.617	0.479
27	7.22E-05	1.73E-03	6.97E-04	0.61	0.618	0.48
28	6.24E-05	6.65E-08	9.47E-06	0.61	0.618	0.48
29	8.54E-03	5.01E-05	3.94E-04	0.618	0.618	0.48
30	8.63E-05	5.07E-03	1.39E-03	0.618	0.623	0.481
31	1.65E-02	1.52E-04	2.68E-05	0.635	0.624	0.481
32	7.61E-05	1.91E-03	2.45E-03	0.635	0.625	0.484
33	4.08E-03	4.83E-06	2.47E-05	0.639	0.625	0.484
34	1.78E-04	5.89E-08	3.87E-09	0.639	0.625	0.484
35	2.24E-05	6.64E-04	3.80E-06	0.639	0.626	0.484
36	6.94E-04	1.48E-03	3.13E-03	0.64	0.628	0.487
37	1.01E-03	2.48E-06	5.69E-04	0.641	0.628	0.488
38	1.15E-03	4.46E-06	7.05E-03	0.642	0.628	0.495
39	2.38E-03	4.20E-04	3.50E-03	0.644	0.628	0.498
40	9.30E-03	2.88E-04	1.17E-03	0.654	0.628	0.499

41	8.43E-03	1.63E-04	4.23E-06	0.662	0.629	0.499
42	2.14E-04	1.34E-02	1.30E-03	0.662	0.642	0.501
43	4.28E-03	1.87E-04	1.33E-06	0.667	0.642	0.501
44	9.33E-05	1.73E-07	2.99E-03	0.667	0.642	0.504
45	4.01E-06	8.33E-03	1.11E-02	0.667	0.65	0.515
46	4.06E-07	1.56E-06	5.29E-06	0.667	0.65	0.515
47	1.02E-04	5.79E-06	7.85E-07	0.667	0.65	0.515
48	8.66E-06	1.37E-03	5.93E-04	0.667	0.652	0.515
49	4.64E-05	1.83E-06	2.75E-03	0.667	0.652	0.518
50	2.35E-05	4.99E-07	6.85E-04	0.667	0.652	0.519
51	7.61E-04	3.58E-05	2.82E-04	0.668	0.652	0.519
52	6.66E-07	4.50E-04	7.94E-03	0.668	0.652	0.527
53	9.66E-05	1.15E-05	3.65E-04	0.668	0.652	0.527
54	7.36E-08	2.20E-05	9.10E-04	0.668	0.652	0.528
55	2.40E-06	4.31E-03	1.29E-03	0.668	0.657	0.53
56	5.13E-08	2.54E-04	5.02E-05	0.668	0.657	0.53
57	8.81E-07	9.06E-03	2.01E-06	0.668	0.666	0.53
58	1.10E-04	1.04E-05	9.18E-05	0.668	0.666	0.53
59	4.89E-08	5.61E-04	1.79E-03	0.668	0.666	0.531
60	7.14E-06	1.41E-03	3.83E-04	0.668	0.668	0.532

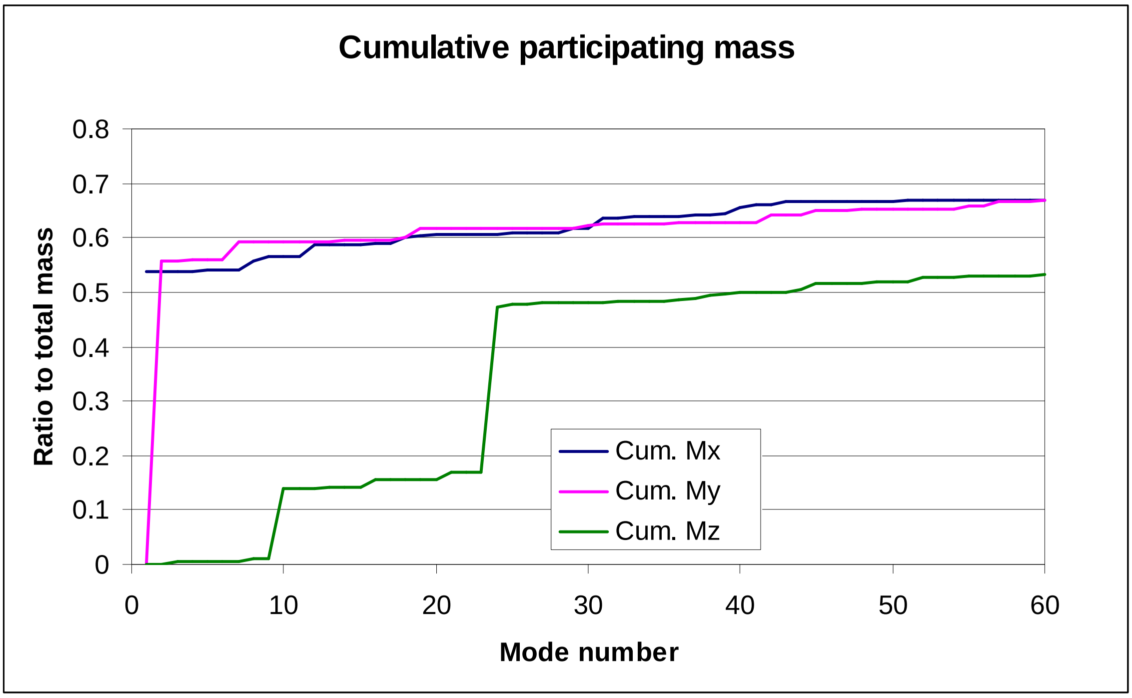

Figure 3.30 – Cumulative distribution of participating modal mass

As could be anticipated, the need of a detailed finite element model to study the nonlinear behaviour in the subsequent phases conflicts partially with that of capturing the high frequency response for the design of subsystems.

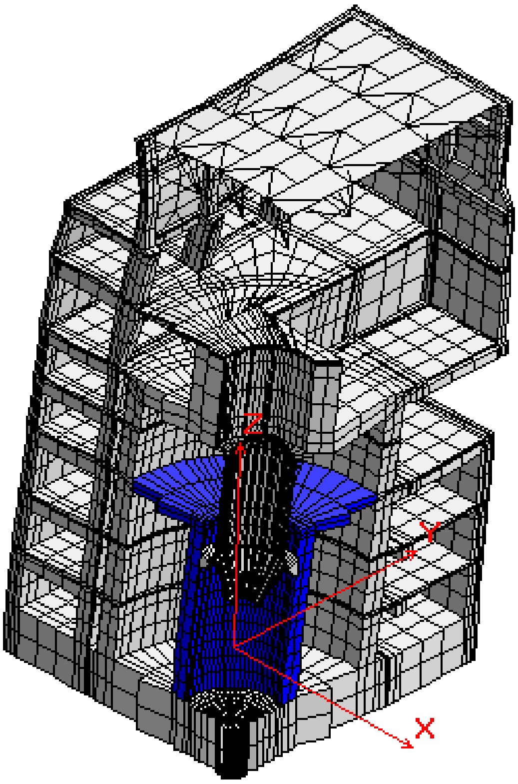

Figure 3.31 – Modal analysis- First mode (4.48 Hz)

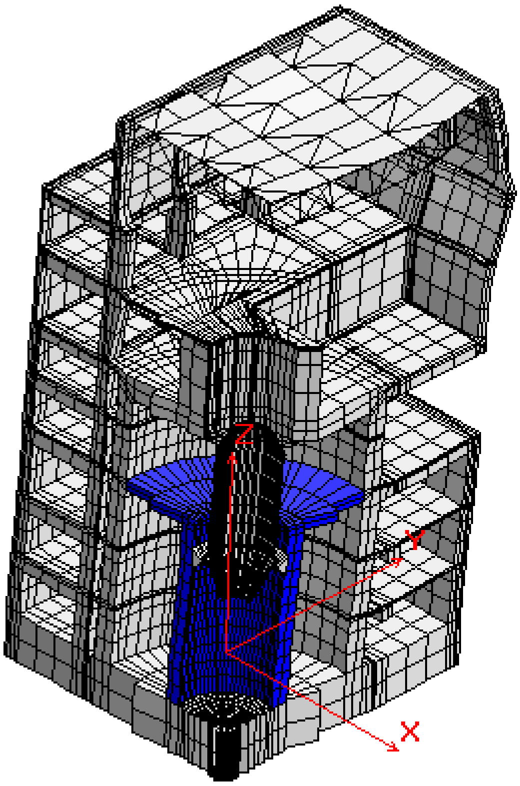

Figure 3.32 – Modal analysis- Second mode (4.77 Hz)

3.1.2 Task 1.1.2 Soil column analyses

The soil column analyses have been conducted for the aftershock I (16 july, 15:37), the aftershock II (16 july, 17:42) and for the main shock.

The response spectra evaluated at different depth in the soil are reported in the following figures

The main shock is characterized by a maximum acceleration equal to 1.13 g (Y direction), while the maximum acceleration values for the aftershocks are lower.

The spectral values evaluated for the main shock are very high, reaching approximately 3.1 g in X direction, for a frequency of about 4.5-5.0 Hz and a pick of 4.8 g in Y direction around a frequency of about 3.0 -4.0 Hz.

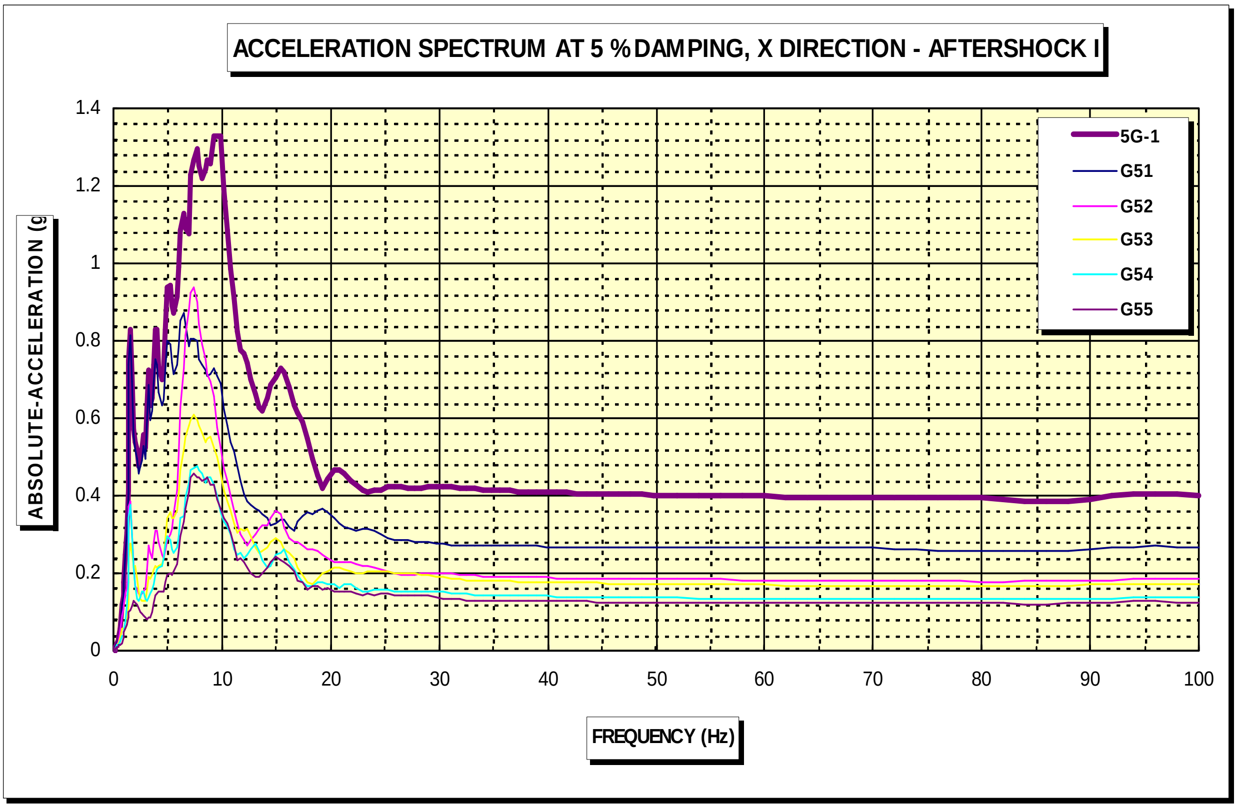

Figure 3.33 – Aftershock I: response spectrum X direction

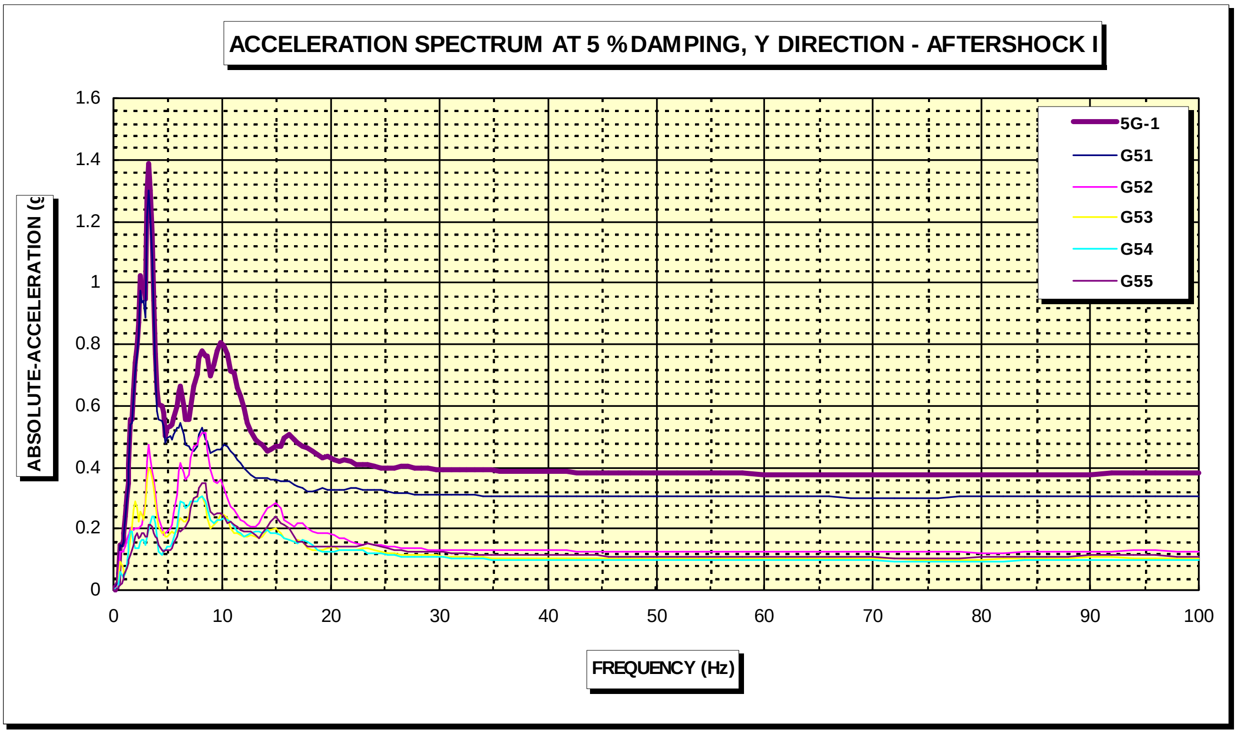

Figure 3.34 – Aftershock I: response spectrum Y direction

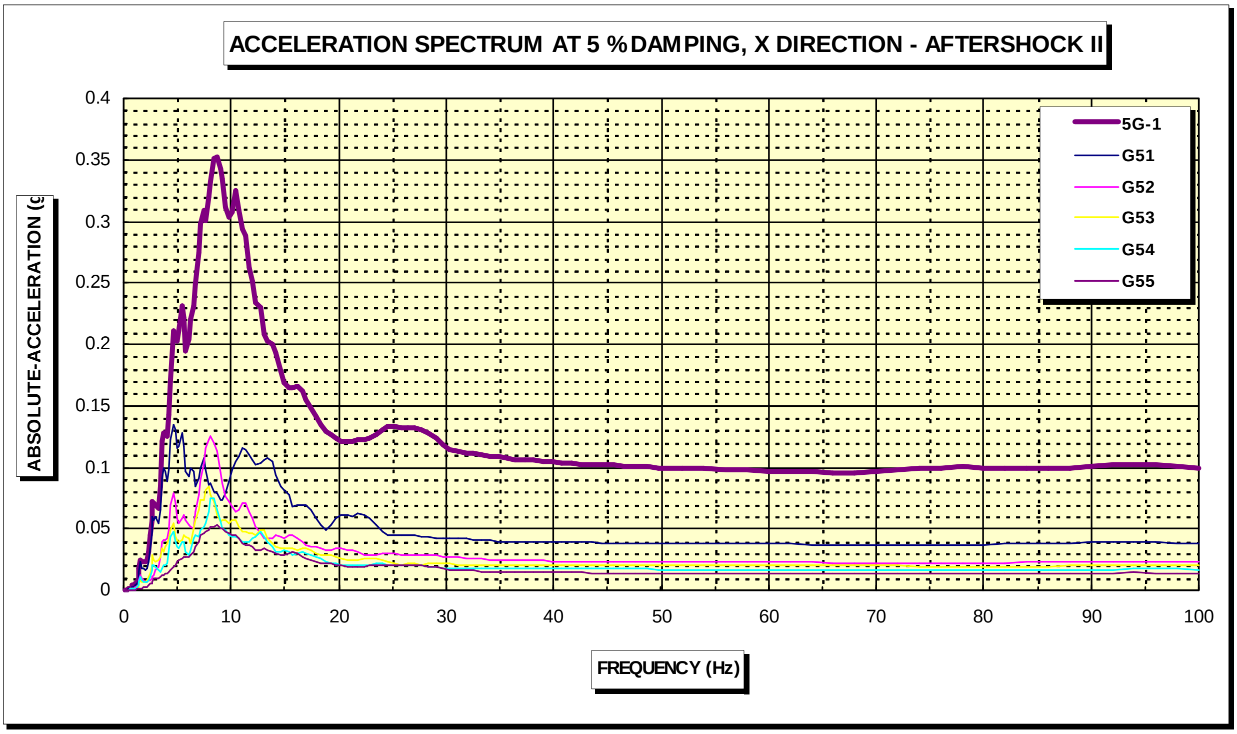

Figure 3.35 – Aftershock II: response spectrum X direction

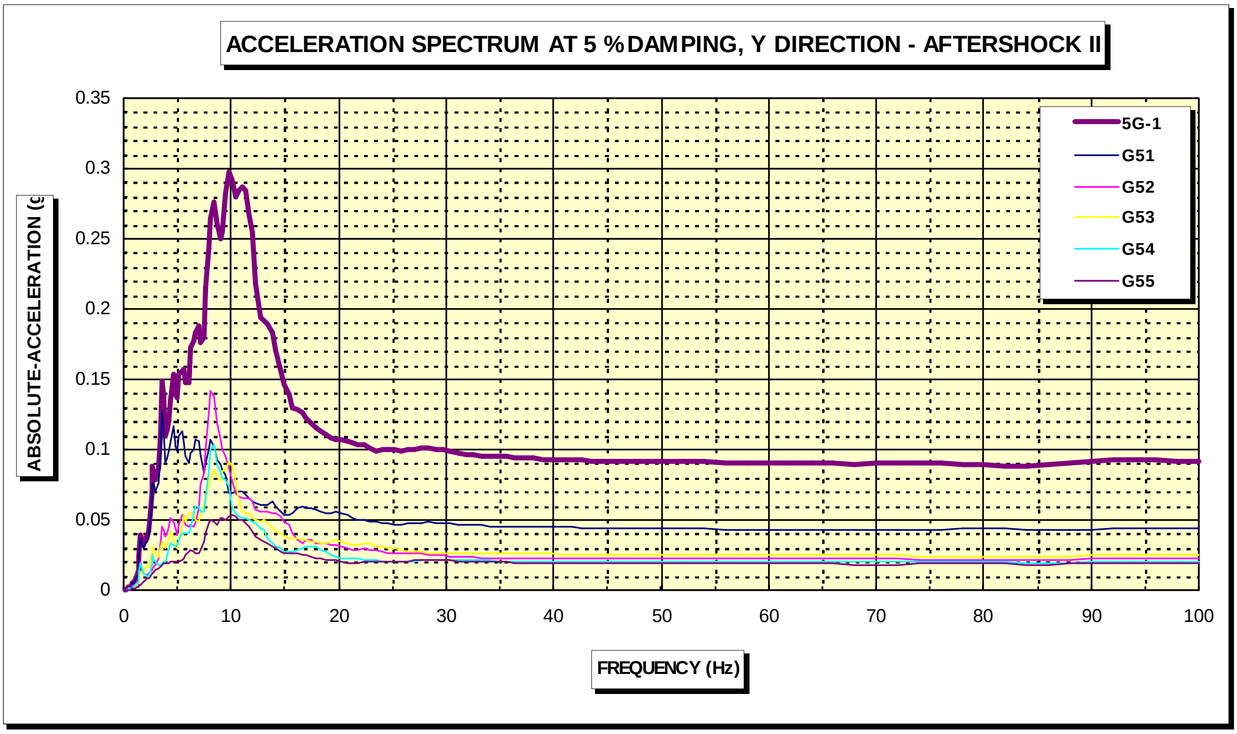

Figure 3.36 – Aftershock II: response spectrum Y direction

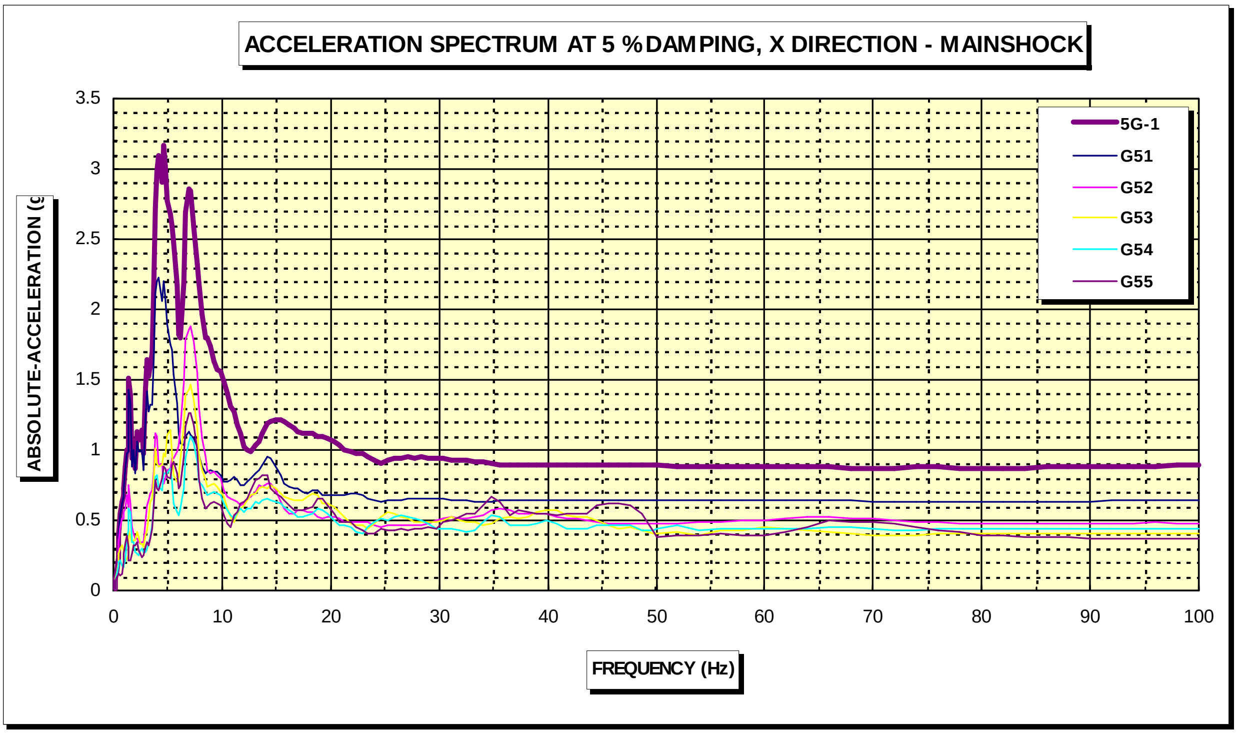

Figure 3.37 – Main shock: response spectrum X direction

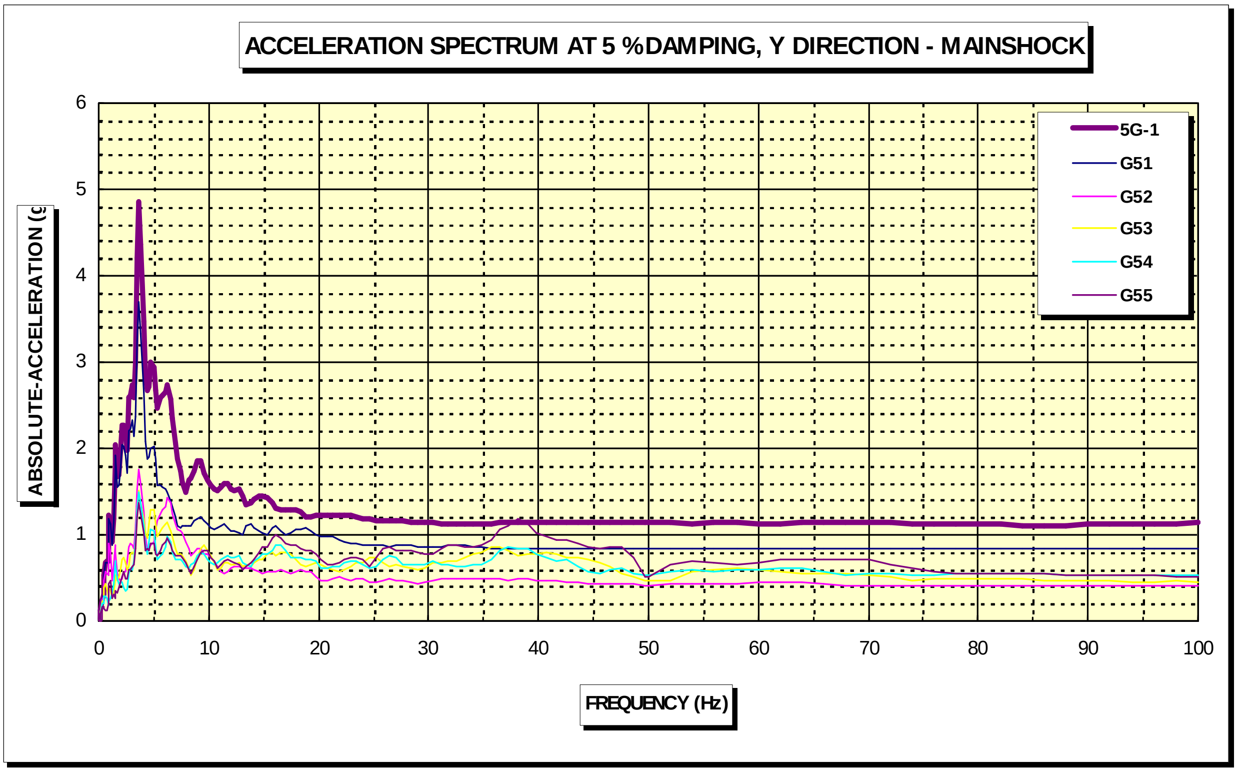

Figure 3.38 – Main shock: response spectrum Y direction

3.1.3 Task 1.1.3 Analysis of the complete model

General description of the soil-structure finite element model

The approach used for the soil structure interaction analysis was selected on the basis of the information provided in the Guidance document.
A key aspect is the consideration of the embedment, because the Guidance Document in chapter 3 states that "Due to the procedure used for construction, it can be considered that there is no backfill around the R/B."
Therefore, even if this is a rather strong assumption, the foundation was considered shallow.

The R/B basemat reaches the Nishiyama stratum. In this layer the shear wave velocity increases from 490 m/s at the top to about 600m/s at the bottom. A stiffer soil is then found with shear Wave velocity increasing up to 850 m/s at a depth of about 170m below the basemat.
The 5.5 m thick basemat can be considered as rigid, so the global stiffness can be evaluated using the formulas for rigid foundations as reported by Mylonakis et. al. 2003) [4], summarized in Figure 3.39

These formulas are valid for an homogeneous half space, while the soil profile at the site shows an increment in soil stiffness with depth. In the evaluation of the soil stiffness the possible reduction of the linear equivalent soil modulus has been considered checking the result of the

soil amplification analyses. It can be seen that the soil below the basemat (at a depth greater than 25 meters) behaves essentially linear even during the main shock.
So the shear moduli were assumed equal to the low strain values.

Table 2-I. Dynamic stiffness and dashpot coefficients for arbitrary shaped foundations on homogeneous halfspace surface.

Vibration Mode	Dynamic Stiffness $\mathcal{K} = K\,k(\omega)$ — Static Stiffness K — General Shape (foundation-soil contact surface area = A_b with equivalent rectangle 2Lx2B; L>B)†	Square $L = B$	Dynamic Stiffness Coefficient k (General Shape; $0 \le a_0 \le 2$)‡	Radiation Dashpot Coefficient C (General Shapes)
Vertical, z	$K_z = \frac{2GL}{1-\nu}(0.73 + 1.54\,\chi^{0.75})$ with $\chi = \frac{A_b}{4L^2}$	$K_z = \frac{4.54\,GB}{1-\nu}$	$k_z = k_z(\frac{L}{B}, \nu, a_0)$ plotted in Graph a	$C_z = (\rho\, V_{La}\, A_b)\,\bar{c}_z$ $\bar{c}_z = \bar{c}_z(\frac{L}{B}, a_0)$ plotted in Graph c
Horizontal, y (lateral direction)	$K_y = \frac{2GL}{2-\nu}(2 + 2.5\,\chi^{0.85})$	$K_y = \frac{9GB}{2-\nu}$	$k_y = k_y(\frac{L}{B}, a_0)$ plotted in Graph b	$C_y = (\rho\, V_s\, A_b)\,\bar{c}_y$ $\bar{c}_y = \bar{c}_y(\frac{L}{B}, a_0)$ plotted in Graph d
Horizontal, x (longitudinal direction)	$K_x = K_y - \frac{0.2}{0.75-\nu}\,GL(1 - \frac{B}{L})$	$K_x = K_y$	$k_x \simeq 1$	$C_x \simeq \rho\, V_s\, A_b$
Rocking, rx (around x axis)	$K_{rx} = \frac{G}{1-\nu}\, I_{bx}^{0.75}\,(\frac{L}{B})^{0.25}(2.4 + 0.5\,\frac{B}{L})$ with I_{bx} = area moment of inertia of foundation - - soil contact surface around x axis	$K_{rx} = \frac{0.45\,GB^3}{1-\nu}$	$k_{rx} = 1 - 0.20\,a_0$	$C_{rx} = (\rho\, V_{La}\, I_{bx})\,\bar{c}_{rx}$ $\bar{c}_{rx} = \bar{c}_{rx}(\frac{L}{B}, a_0)$ plotted in Graph e
Rocking, ry (around y axis)	$K_{ry} = \frac{G}{1-\nu}\, I_{by}^{0.75}\left[3(\frac{L}{B})^{0.15}\right]$ with I_{by} = area moment of inertia of foundation - - soil contact surface around y axis	$K_{ry} = K_{rx}$	$\nu < 0.45$: $k_{ry} \simeq 1 - 0.30\,a_0$; $\nu \simeq 0.5$: $k_{ry} \simeq 1 - 0.25\,a_0\,(\frac{L}{B})^{0.30}$	$C_{ry} = (\rho\, V_{La}\, I_{by})\,\bar{c}_{ry}$ $\bar{c}_{ry} = \bar{c}_{ry}(\frac{L}{B}, a_0)$ plotted in Graph f
Torsional	$K_t = G\,J_t^{0.75}\left[4 + 11(1 - \frac{B}{L})^{10}\right]$ with $J_t = I_{bx} + I_{by}$ = polar moment of inertia of foundation - soil contact surface	$K_t = 8.3\,GB^3$	$k_t \simeq 1 - 0.14\,a_0$	$C_t = (\rho\, V_s\, J_t)\,\bar{c}_t$ $\bar{c}_t = \bar{c}_t(\frac{L}{B}, a_0)$ plotted in Graph g

† Note that as $L/B \to \infty$ (strip footing) the theoretical values of K_z and $K_y \to 0$; values computed from the two given formulas correspond to footing of $L/B \approx 20$
‡ $a_0 = \omega B / V_s$

Figure 3.39 – Foundation stiffness evaluation

The variation of the shear modulus with depth was accounted for using the technique reported in Werkle 1986 [5].

The variation of the shear modulus with depth Z is given by

$$G(Z) = G_o\ (1 + \alpha \cdot Z/R)$$

Where Go is the shear modulus at the surface, R the foundation radius and α the gradient with depth.

The procedure for the evaluation of the equivalent shear modulus is shortly reviewed in Figure 3.40

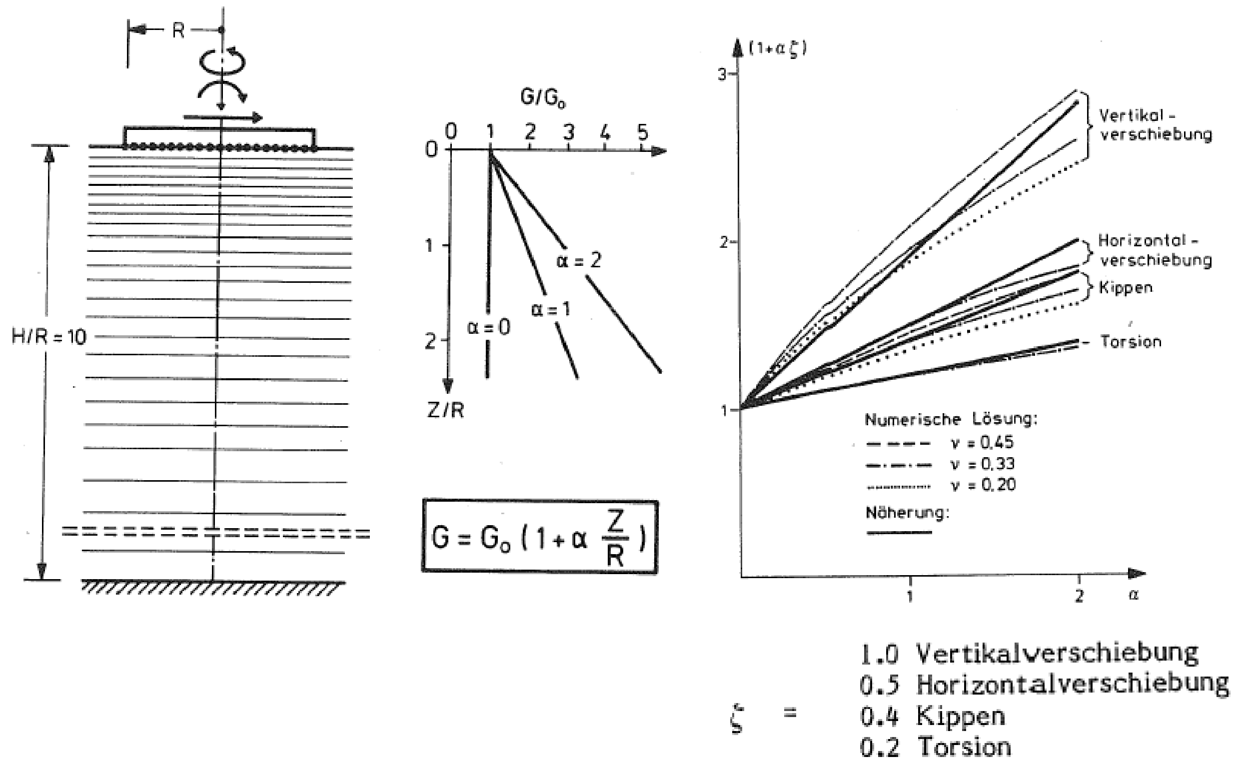

Figure 3.40 – Evaluation of the equivalent shear modulus (Ref. [5])

For each foundation degree of freedom an equivalent modulus given by the equation

$$\bar{G} = G_o(\ 1 + \alpha \cdot \zeta\ )$$

can be determined. The equivalent modulus is then the modulus evaluated at a representative depth $\bar{Z} = \zeta \cdot R$

Then with respect to the homogeneous halfspace the stiffness is increased by a factor $(1+\alpha\zeta)$.

The equivalent modulus is plotted versus the gradient α for different values of the Poisson coefficient in figure 2. The trends for the horizontal and torsional stiffness are not influenced by the Poisson coefficient.

With this approximation the increase in the equivalent modulus can be represented with a maximum error equal to 12%. In most cases the dynamic behaviour of the soil can be estimated only with some approximation so the simplification involved in this procedure is acceptable.

The variation of the shear modulus is detailed in the table below. The shear modulus profile shows a sharp increment in the gradient with the change in the geological formation. It was decided to make reference to the gradient in the first layer, that has the greatest influence in the results. In Table 3.14 below the following data are summarized:
Z : the depth below the basemat (m)
Z/r _ the relative depth, w/r to an equivalent half size equal to 29 m

Vs : the shear wave velocity (m/s)
G the shear modulus (kN/sqm)
G/Go the increment in modulus w/r to the surface
α : the gradient of the modulus in the layer

Table 3.14 – Soil shear modulus profile

Z	Z/r	vs	G	G/Go	α
0	0	490	4.322E+05	1	
70	2.410442	600	6.480E+05	1.499375	0.207172
140	4.820884	850	1.301E+06	3.009163	0.626353
average					0.416762

The equivalent modulus for each degree of freedom of the rigid foundation is reported in

Table 3.15 – Equivalent Soil shear moduli for the different dof's

	G(dof)	increment	adim. repr. Depth
Geq(uz)	5.217E+05	1.207	1
Geq(ux)	4.769E+05	1.104	0.5
Geq(rot)	4.680E+05	1.083	0.4
Geq(tors)	4.501E+05	1.041	0.2

Given these values for the equivalent modulus the global stiffnesses according to the above mentioned equations are:

Summary of stiffnesses

Kx	7.767E+07	kN/m
Ky	7.804E+07	kN/m
Kz	1.146E+08	kN/m
Krx	7.175E+10	kNm/rad
Kry	6.894E+10	kNm/rad
Krz	9.210E+10	kNm/rad

The foundation stiffness is accounted for in the 3-D finite element model using a set of lumped spring located under the basemat in 16 nodes, whose location has been selected to approximate the stiffness in all DOF's.
The spring elements used in the model are only translational. The values of the springs have been computed from the translational global stiffness in each direction. The rotational stiffnesses are reproduced by the eccentricity in the location of the translational springs. The resulting global rotational spring stiffnesses are evaluated below.

Vertical global stiffness	1.146E+08
no. of vertical springs	16
stiffness of each spring	7.163E+06
horizontal global stiffness in x	7.767E+07
no. of horizontal springs	16
stiffness of each spring	4.854E+06

horizontal global stiffness in y	7.804E+07
no. of vertical springs	16
no. of horizontal springs	4.878E+06

Rocking and torsion
coordinates of nodes

node	weight	x	y	Kx	Ky	Kz
228	1	26.6	27.6	5.456E+09	5.068E+09	7.149E+09
242	1	24.2333	27.6	5.456E+09	4.206E+09	6.562E+09
373	1	26.6	24.933	4.453E+09	5.068E+09	6.469E+09
394	1	24.2333	24.933	4.453E+09	4.206E+09	5.882E+09
32708	1	-26.6	27.6	5.456E+09	5.068E+09	7.149E+09
32722	1	-24.2333	27.6	5.456E+09	4.206E+09	6.562E+09
32847	1	-26.6	24.933	4.453E+09	5.068E+09	6.469E+09
32868	1	-24.2333	24.933	4.453E+09	4.206E+09	5.882E+09
1943	1	24.2333	-25.6	4.694E+09	4.206E+09	6.046E+09
1923	1	26.6	-28.6	5.859E+09	5.068E+09	7.422E+09
1922	1	26.6	-25.6	4.694E+09	5.068E+09	6.633E+09
1944	1	24.2333	-28.6	5.859E+09	4.206E+09	6.835E+09
34361	1	-26.6	-28.6	5.859E+09	5.068E+09	7.422E+09
34382	1	-24.2333	-28.6	5.859E+09	4.206E+09	6.835E+09
34360	1	-26.6	-25.6	4.694E+09	5.068E+09	6.633E+09
34381	1	-24.2333	-25.6	4.694E+09	4.206E+09	6.046E+09
total	16			8.185E+10	7.420E+10	1.060E+11
analytical				7.175E+10	6.894E+10	9.210E+10
error				1.407E-01	7.629E-02	1.508E-01

As can be seen the resulting rotational stiffnesses are between 7% and 15% greater than the analytical ones for a shallow foundation. This result can also reduce the strong approximation made in neglecting the contribution of the embedment to the stiffness.

The modal analysis of the structure including SSI yielded the following frequencies

FREQUENCY NUMBER	FREQUENCY (RAD/SEC)	FREQUENCY (CYCLES/SEC)	PERIOD (SECONDS)
1	0.1201935E+02	0.1912940E+01	0.5227557E+00
2	0.1234382E+02	0.1964580E+01	0.5090148E+00
3	0.1757045E+02	0.2796424E+01	0.3575996E+00
4	0.2373923E+02	0.3778216E+01	0.2646752E+00
5	0.2777596E+02	0.4420682E+01	0.2262094E+00
6	0.2780270E+02	0.4424937E+01	0.2259919E+00
7	0.3077883E+02	0.4898604E+01	0.2041398E+00
8	0.3851897E+02	0.6130484E+01	0.1631192E+00
9	0.4695536E+02	0.7473177E+01	0.1338119E+00
10	0.4880487E+02	0.7767535E+01	0.1287410E+00
11	0.4959531E+02	0.7893338E+01	0.1266891E+00
12	0.5114100E+02	0.8139343E+01	0.1228600E+00
13	0.5434287E+02	0.8648936E+01	0.1156212E+00
14	0.5600011E+02	0.8912695E+01	0.1121995E+00
15	0.5641753E+02	0.8979128E+01	0.1113694E+00
16	0.5750395E+02	0.9152038E+01	0.1092653E+00
17	0.5925056E+02	0.9430019E+01	0.1060443E+00
18	0.5929122E+02	0.9436490E+01	0.1059716E+00

19	0.6045189E+02	0.9621217E+01	0.1039370E+00
20	0.6110902E+02	0.9725802E+01	0.1028193E+00
21	0.6214705E+02	0.9891010E+01	0.1011019E+00
22	0.6336993E+02	0.1008564E+02	0.9915089E-01
23	0.6571962E+02	0.1045960E+02	0.9560593E-01
24	0.6678683E+02	0.1062945E+02	0.9407821E-01
25	0.6899025E+02	0.1098014E+02	0.9107353E-01
26	0.6900632E+02	0.1098270E+02	0.9105232E-01
27	0.6920729E+02	0.1101468E+02	0.9078791E-01
28	0.6975278E+02	0.1110150E+02	0.9007792E-01
29	0.7030991E+02	0.1119017E+02	0.8936416E-01
30	0.7168907E+02	0.1140967E+02	0.8764496E-01

As can be seen the fundamental frequencies in both X and Y directions are significantly lower than in the fixed base case. The first and second mode, shown in Figure 3.41 and Figure 3.42 are about 1.9 Hz versus the 4.5 Hz of the fixed base model.

Modal mass participation is summarized in the table below.

	INDIVIDUAL MODAL MASS / TOTAL MASS			CUMULATIVE EFFECTIVE MASS / TOTAL MASS		
MODE No.	Mx MASS	My MASS	Mz MASS	Cum. Mx MASS	Cum. My MASS	Cum. Mz MASS
1	0.790	0.123E-05	0.821E-07	0.790	0.123E-05	0.821E-07
2	0.141E-05	0.798	0.571E-03	0.790	0.798	0.572E-03
3	0.120E-06	0.737E-03	0.970	0.790	0.799	0.971
4	0.933E-04	0.703E-05	0.584E-08	0.790	0.799	0.971
5	0.260E-02	0.195	0.108E-03	0.793	0.993	0.971
6	0.203	0.248E-02	0.780E-06	0.996	0.996	0.971
7	0.781E-05	0.985E-06	0.785E-04	0.996	0.996	0.971
8	0.207E-07	0.308E-03	0.513E-06	0.996	0.996	0.971
9	0.164E-08	0.340E-06	0.302E-03	0.996	0.996	0.971
10	0.243E-09	0.168E-03	0.130E-04	0.996	0.996	0.971
11	0.634E-05	0.523E-06	0.118E-04	0.996	0.996	0.971
12	0.496E-07	0.333E-05	0.224E-02	0.996	0.996	0.973
13	0.539E-06	0.913E-04	0.217E-01	0.996	0.996	0.995
14	0.538E-06	0.759E-06	0.538E-06	0.996	0.996	0.995
15	0.961E-04	0.127E-07	0.662E-03	0.996	0.996	0.996
16	0.113E-02	0.182E-06	0.189E-08	0.997	0.996	0.996
17	0.209E-03	0.214E-06	0.172E-04	0.998	0.996	0.996
18	0.206E-05	0.206E-08	0.320E-05	0.998	0.996	0.996
19	0.770E-07	0.337E-03	0.147E-04	0.998	0.997	0.996
20	0.194E-04	0.865E-07	0.483E-07	0.998	0.997	0.996
21	0.106E-04	0.645E-06	0.156E-05	0.998	0.997	0.996
22	0.204E-04	0.553E-06	0.295E-04	0.998	0.997	0.996
23	0.180E-08	0.260E-06	0.107E-06	0.998	0.997	0.996
24	0.441E-10	0.180E-02	0.248E-03	0.998	0.999	0.996
25	0.192E-05	0.526E-04	0.182E-04	0.998	0.999	0.996
26	0.241E-04	0.466E-05	0.560E-05	0.998	0.999	0.996
27	0.220E-06	0.612E-06	0.722E-04	0.998	0.999	0.996
28	0.487E-04	0.552E-07	0.128E-05	0.998	0.999	0.996
29	0.245E-07	0.845E-07	0.983E-06	0.998	0.999	0.996
30	0.180E-03	0.659E-09	0.225E-05	0.998	0.999	0.996

In the first 6 modes almost the total mass of the structure is captured in the x and y direction and 97% of the total in z direction.

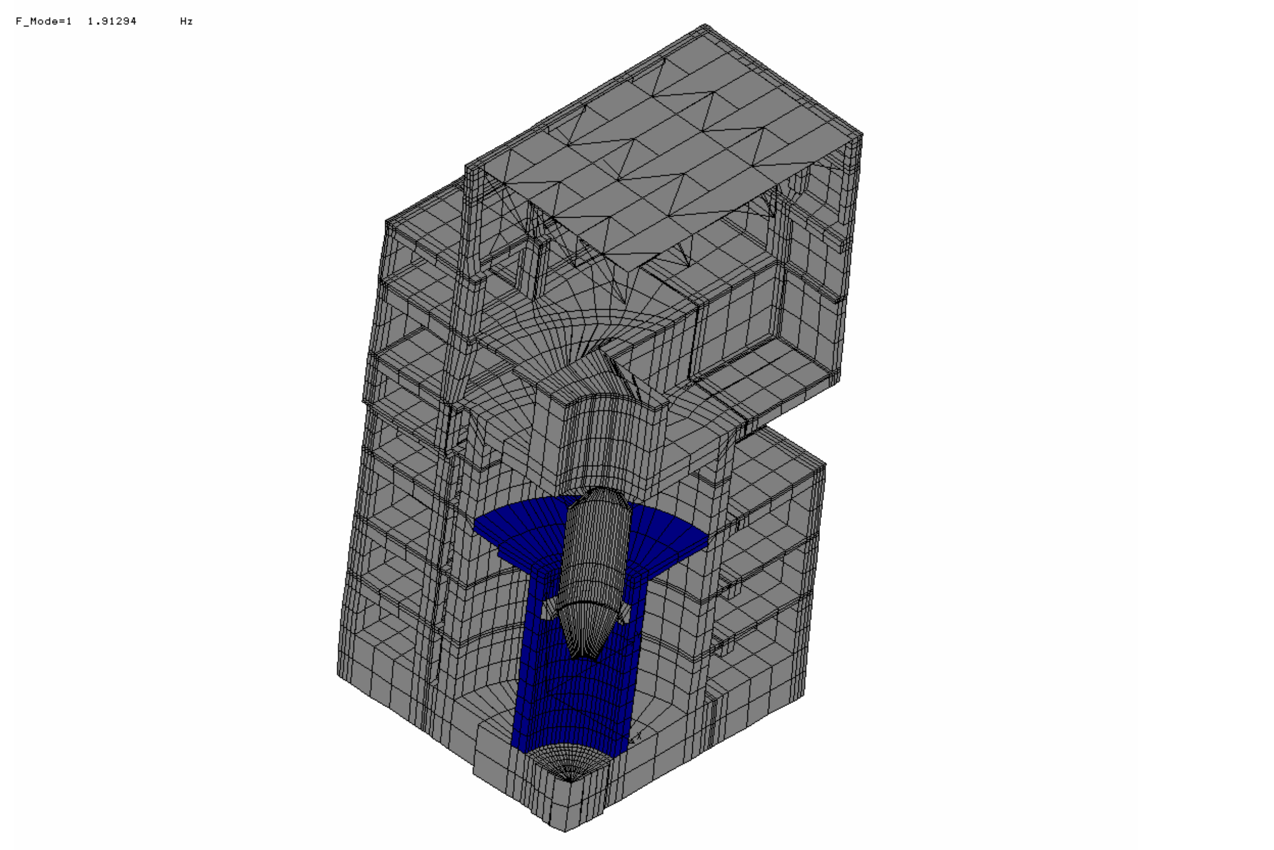

Figure 3.41 – Modal analysis with SSI- First mode (1.91 Hz)

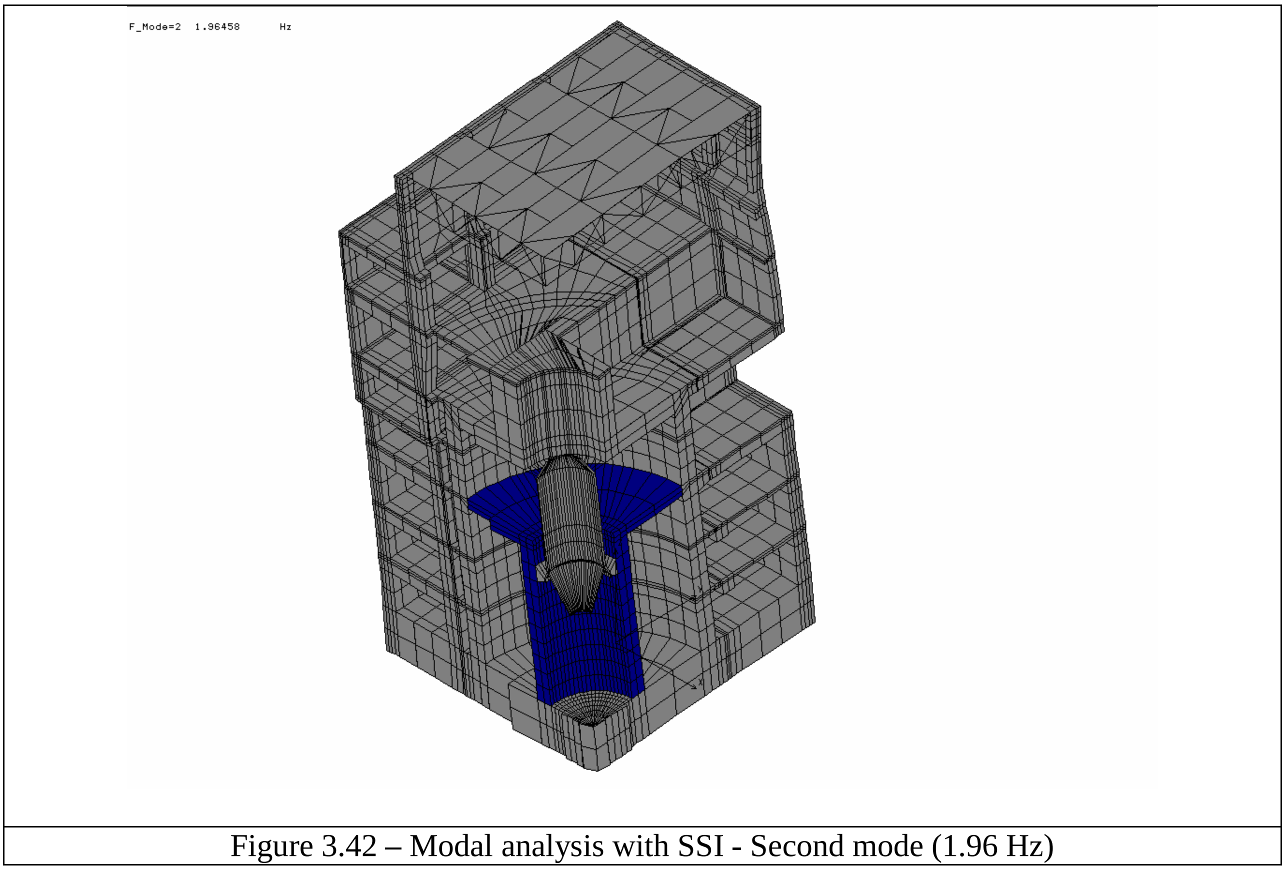

Figure 3.42 – Modal analysis with SSI - Second mode (1.96 Hz)

3.2 Task 1.2 NCOE Response

3.2.1 Reference Analysis of the Soil-Structure Model

3.2.1.1. Modal analysis of the soil-structure model

In task 1.2 the evaluation of the Response of the structure during NCOE earthquake has to be evaluated.
At first, a modal analysis taking into account the SSI effects have been performed.
The Soil Structure Interaction has been considered by means of a series of springs and dashpots applied underneath the foundation. The methodology used to evaluate the springs and dashpots characteristics has been previously outlined.
Updated values have been calculated for the springs below the foundation slab.
Kinematic interaction effects are treated by frequency-dependent ratios of the Fourier amplitudes (transfer functions) of foundation input motion (FIM) to free-field motion. The formulation in Stewart, Comartin and Moehle "Implementation of Soil-Structure Interaction Models in Performance Based Design Procedures" (Proceedings of Third UJNR Workshop on Soil-Structure Interaction, 2004) has been used both for the embedment effect and the ground motion incoherency.
The embedment effect has been considered as the reference approach. Only the averaging effect on the translation component has been considered. The base rotation effect has been neglected because the high frequency content of the input motion is quite low and this effect is important only in the high frequency range.

Base slab averaging effects have been subsequently included and the corresponding results have been considered as Best estimate results and reported in next paragraph.

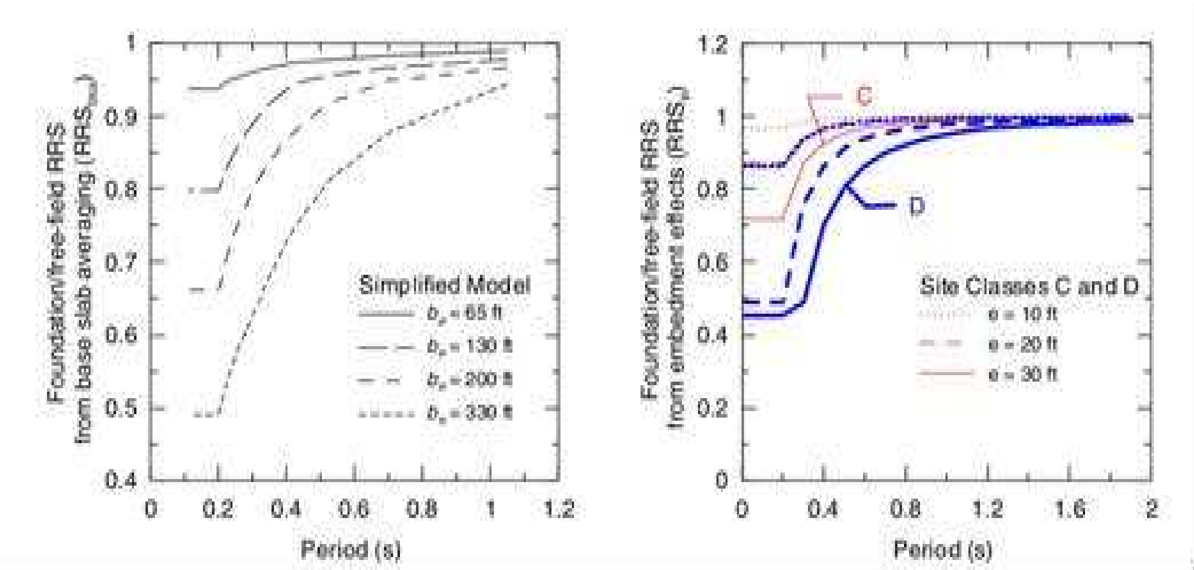

$$RRS_{bsa} = 1 - \frac{1}{14100}\left(\frac{b_e}{\tilde{T}_{eq}}\right)^{1.2}$$

$$RRS_e = \cos\left(\frac{2\pi\, e}{\tilde{T}_{eq} V_{s,r}}\right) \leq \cos\left(\frac{10\pi\, e}{V_{s,r}}\right) \geq 0.454$$

In the following Table 3.16 the results obtained in the first modes vibrations have been reported.

Table 3.16 – Modal analysis result fo SSI model

A1 Frequency, modal masses, participation factors								
Mode	Frequency (Hz)	Damping Ratio %	Modal participating mass ratios (%)			Modal participating mass ratios (%)		
			UX	UY	UZ	SumUX	SumUY	SumUZ
1	2.10		80.06	0.00	0.00	80.06	0.00	0.00
2	2.15		0.00	80.53	0.05	80.06	80.53	0.05
3	3.52		0.00	0.12	98.92	80.06	80.65	98.97
4	4.16		0.01	0.00	0.00	80.07	80.65	98.97
5	5.09		0.00	18.73	0.08	80.07	99.38	99.05
6	5.13		19.36	0.00	0.00	99.43	99.38	99.05
7	5.30		0.02	0.03	0.20	99.44	99.41	99.25
8	7.05		0.00	0.05	0.00	99.44	99.47	99.25
9	7.52		0.15	0.00	0.01	99.60	99.47	99.26
10	7.75		0.00	0.00	0.43	99.60	99.47	99.69

Some pictures of the mode shapes are reported in the following figures.

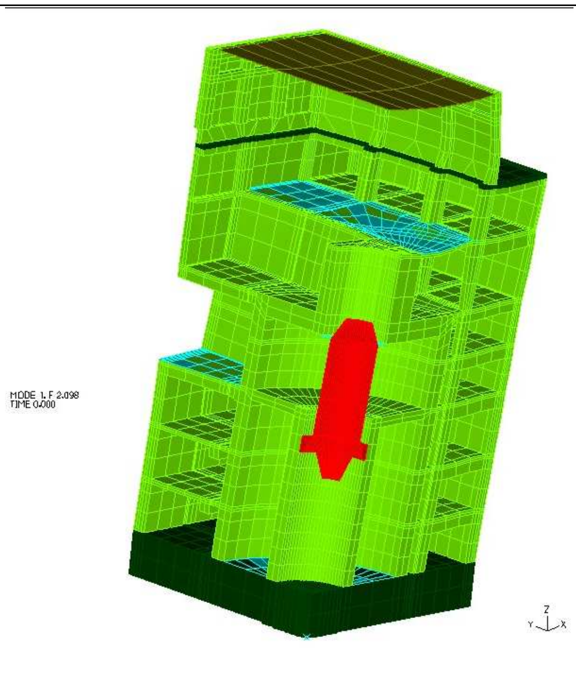

Figure 3.43 – Modal analysis with SSI- First mode (2.098 Hz)

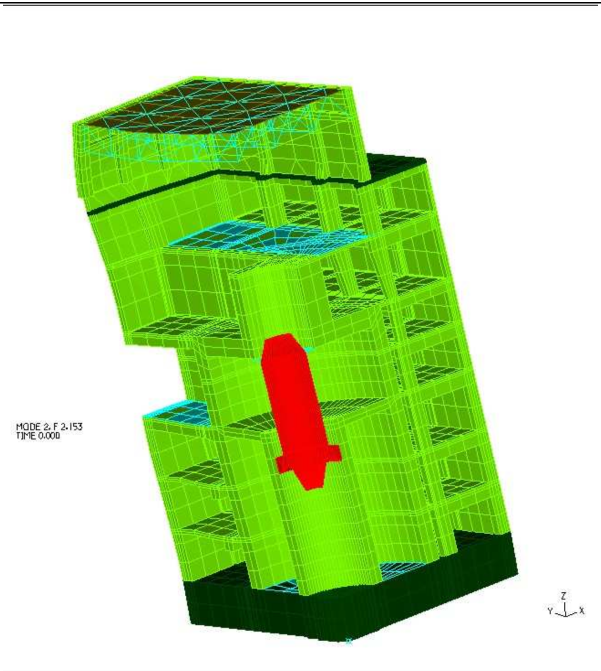

Figure 3.44 – Modal analysis with SSI - Second mode (2.153 Hz)

3.2.1.2. Frequency domain/Time domain analysis of the soil-structure model

Using the global finite model described in the previous paragraph, a direct time history analysis has been conducted applying the NCOE main shock records.

The acceleration time-histories at engineering bedrock outcrop level (- 155 m TMSL) of the NCOE mainshock, have been convolved through the soil column beneath the RB/7 changing iteratively the soil properties which resulted to behave, at the basemat level, as elastic, with a restrained soil stiffness reduction (G/Go > 0.9) and damping (in the order of 3-5%).

The acceleration and displacement time histories have been evaluated in several points of the structures, in particular the response has been evaluated in points at 3rd Basemat level (FP2_3B) and at 3rd Floor Level (FP2_3F) where records collected during the NCOE event are available.

The comparison between calculated and recorded time histories shows some differences in high frequency range (>2 Hz) that are discusses in next paragraph.

3.2.2 Best estimate analysis of the soil-structure model

Due to the differences among recorded and calculated time histories previously mentioned, an improvement of the soil structure interaction model has been attempted. In particular the base averaging effects have been included in evaluating the spring stiffness.

The results have been reported in Figure 3.45 and Figure 3.46 below.

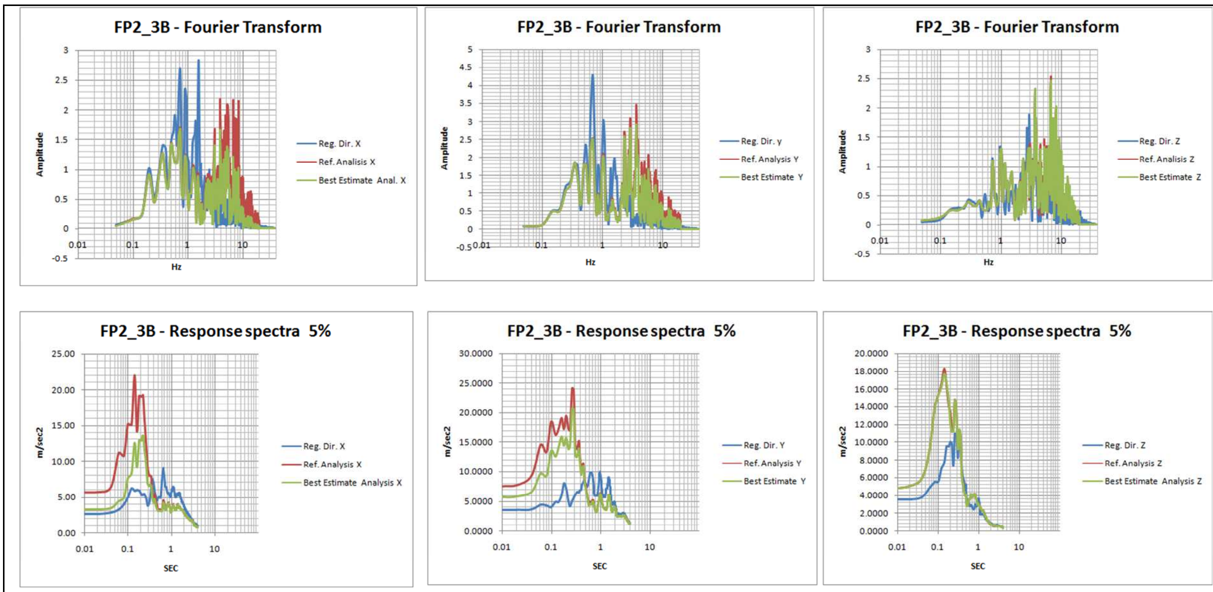

Dir X **Dir Y** **Dir Z**

Figure 3.45 – Results at 3rd Basemat Level

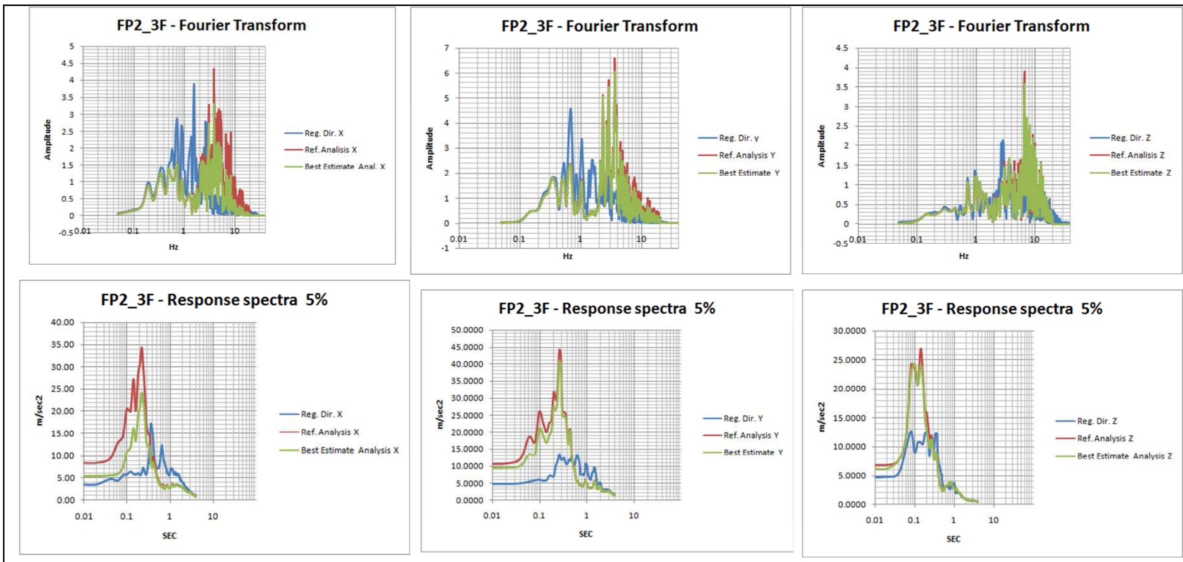

Dir X **Dir Y** **Dir Z**

Figure 3.46 – Results at 3rd Floor Level

The comparison among the recorded data and the analytical results evidenced that the analyses overestimates the response for frequencies higher than 3-5 Hz. In the best estimate analysis the response seams closer to the records; anyway, the difference is still evident.

The reasons of these results are not easily identifiable. Looking to the Fourier Transform of the input motion applied to the models, it seems that an high frequency content is in the input motion itself as evidenced in the following graph, so the analytical response seems to be directly correlated to the input strong motion.

In any case, the recorded data are not characterized by the mentioned high frequency content.

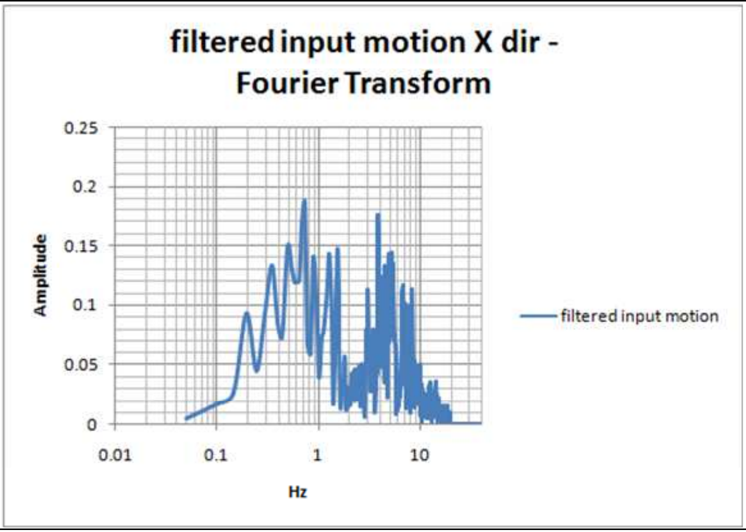

3.3 Task 1.3 Margin Assessment

The outcome of the Subtask 1.3 is to assess margins. This general objective, as referred to the RB seismic response, can be seen from two perspectives:

C. Assess margin with respect to ultimate status of RB structure. That is the increase in the seismic demand causing the ultimate status of the RB structure, either collapse or extensive cracking with loss of containment.

D. Assess margin with respect to the loss of the ‘’NPP capacity to bring and maintain the NPP (reactor core and spent fuel) in a safe status". This loss is logically linked with the systems and equipment needed to ensure the three main safety functions caused by interaction of the RB structure with systems and equipment. In fact even if the structural limit state of the RB is not attained, the displacements and/or accelerations can cause the loss of capacity of systems and components needed to ‘’bring and maintain the NPP in safe status’’. This second aspect (perspective) is linked with activity of Task 2 of the Benchmark.
   We think that margins have to be evaluated according this last approach (B).

To do that, it is necessary to develop (and investigate) the needed assessment about the interfaces between structures and systems/equipment to identify the margins with respect to loss of NPP system capacity to ‘’ bring and maintain the NPP in a safe status’’.

Criticalities of interfaces between RB structures and NPP systems/components:
1. Interface between RB structure response and stability of pressure vessel (potential loss of cooling function) 2. Interface between RB structure response and loss of suppression function of the wet-well (potential loss of containment function) 3. Interface between RB roof structure and stability of the RB crane (possible failure and impact on the floor covering the SF pool) 4. Interface between RB structure response and insertion of shutdown rods (potential loss of reactivity control function) 5. Interface between RB structure response and spent fuel pool (loss of cooling function and sub criticality) 6. Interface between RB structure response and reactor containment internal liner at penetrations points (loss of containment function) 7. Interface between RB structure response and other buildings interconnected through piping (Turbine Building and Auxiliary Building) 8. Interface between RB structure response and anchors/ supports stiffness of piping and mechanical components (loss of safety functions) 9. Interface between RB structure response and anchorages of electrical cabinets, local instrumentation, including sensors and associated electronics (loss of safety functions) 10. ………

The assessment of margins requires the identification of the “ultimate” earthquake that the structure can sustain, to be compared with the NCOE earthquake that effectively strikes the NPP.

The IAEA Secretariat requires to express this margins in terms of NCOE.

Several analyses have been performed to develop the Margin Assessment. In general, the approach used consisted in a first pushover analyses to evaluate the Performance Points according to ATC 40 and to identify the parameters of a Single DOF model to be used in a non linear time history analysis for several input motions. Four events have been considered, according to the indication of IAEA Secretariat, identified as NCOE1, NCOE2, NCOE4 and NCOE6, corresponding respectively to NCOE man shock event and to higher events with increasing strong motion, obtained altering the main shock at the bedrock by factors respectively equal to two, four and six.

To evaluate the response of the structure for increasing levels of ground motion, a non linear model of the structure is required.
The global finite element model used for the first phases of the project is very detailed and a non linear time history analysis on that model is not feasible.
Duo to this a simplified approach has been used, based on the use of a simplified non linear model of the structure, that takes into account only the first two modes of vibration.
In particular, push-over analyses have been conducted on the 3D model applying a displacement distribution according to the first and the second eigenvectors, in order to identify an equivalent non linear single degree of freedom representative of the mode.
The aim of the procedure is the identification of a F.E.. model like the one sketched in the following figure.

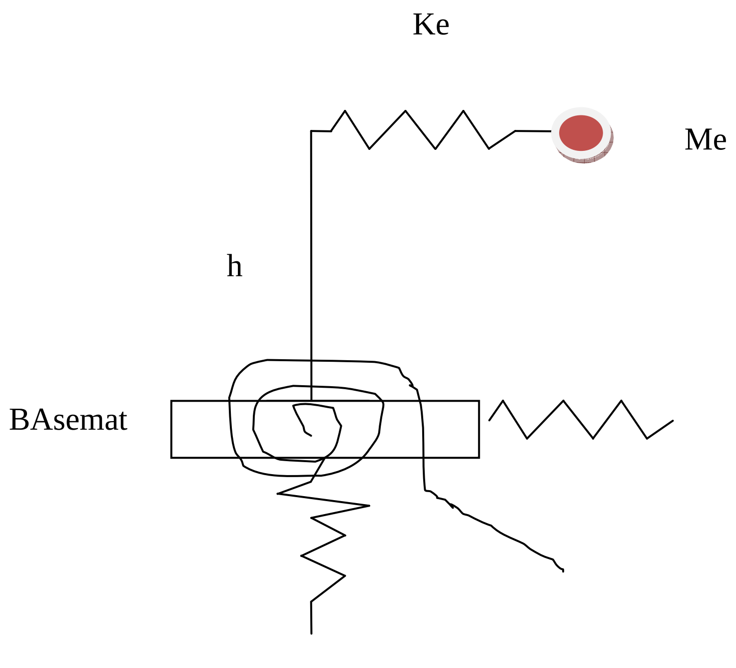

The parameter Ke, Me and h have be identified by means of a push-over analysis using the corresponding eigenvectors, according to the methodology outlined in paragraph 2.2.4

The force-displacement curves obtained in x and y direction are shown in the following figures, where it has been also reported the linear elastic relationship.

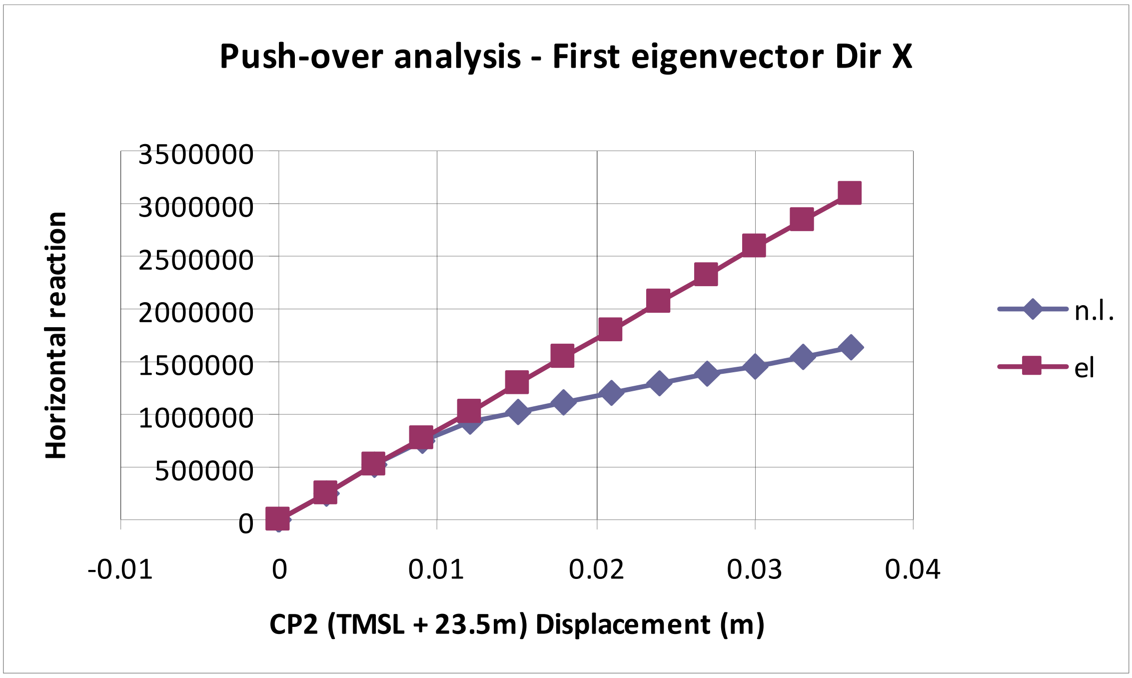

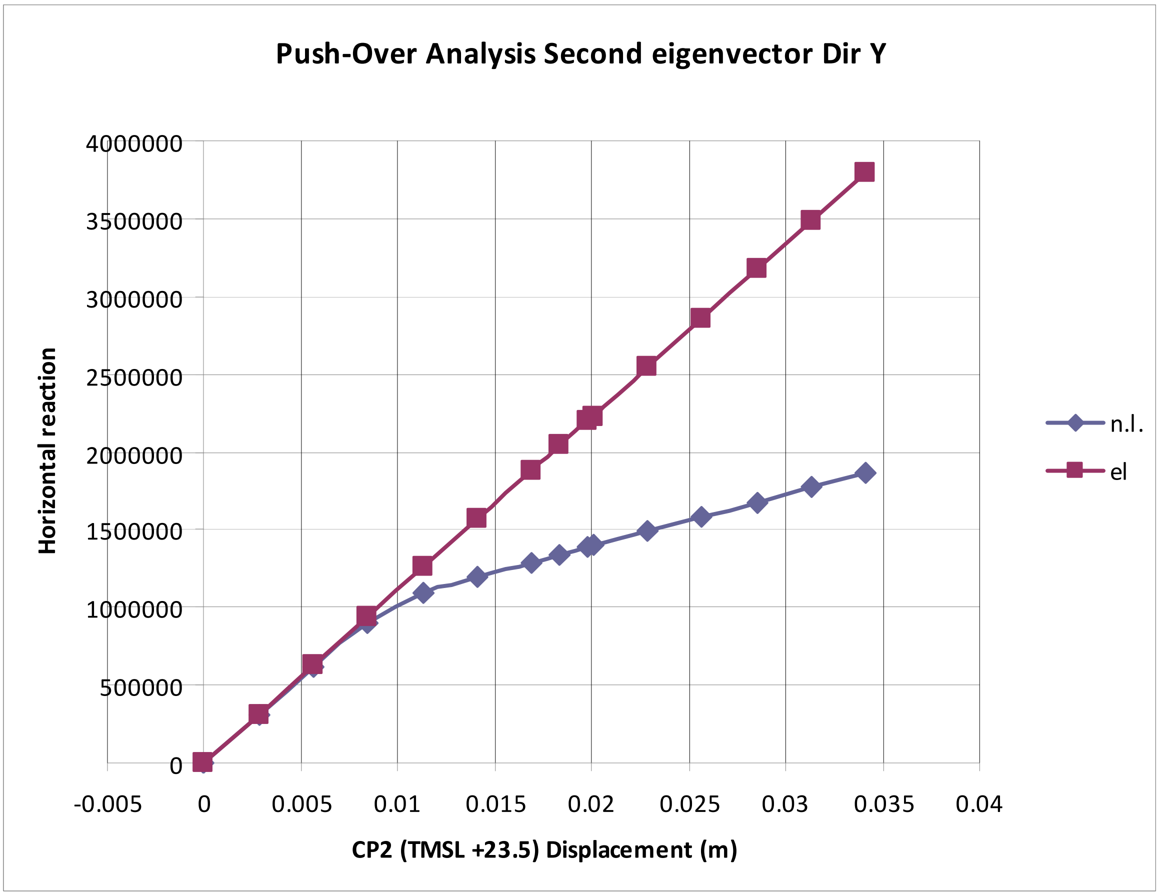

Using these data, a non linear model has been assembled and direct integration analyses have been conducted applying the NCOE_1, NCOE_2 , NCOE_4 and NCOE_6.

A first series of analyses has been conducted using material properties defined separately by each participant. In this series, ITER-Consult analyses have been conducted neglecting the soil around the embedded part of the structure, based on the advice in the Guidance Document that *"Due to the procedure used for construction, it can be considered that there is no backfill around the R/B."* (Chapter3, soil properties).

The finite element model is shown in figure, where underneath the basemat springs and dashpots elements according to the procedure used in the previous phases of the project have been inserted. In this case the springs are elasto-plastic with gaps to simulate the possible uplift of part of the basemat.

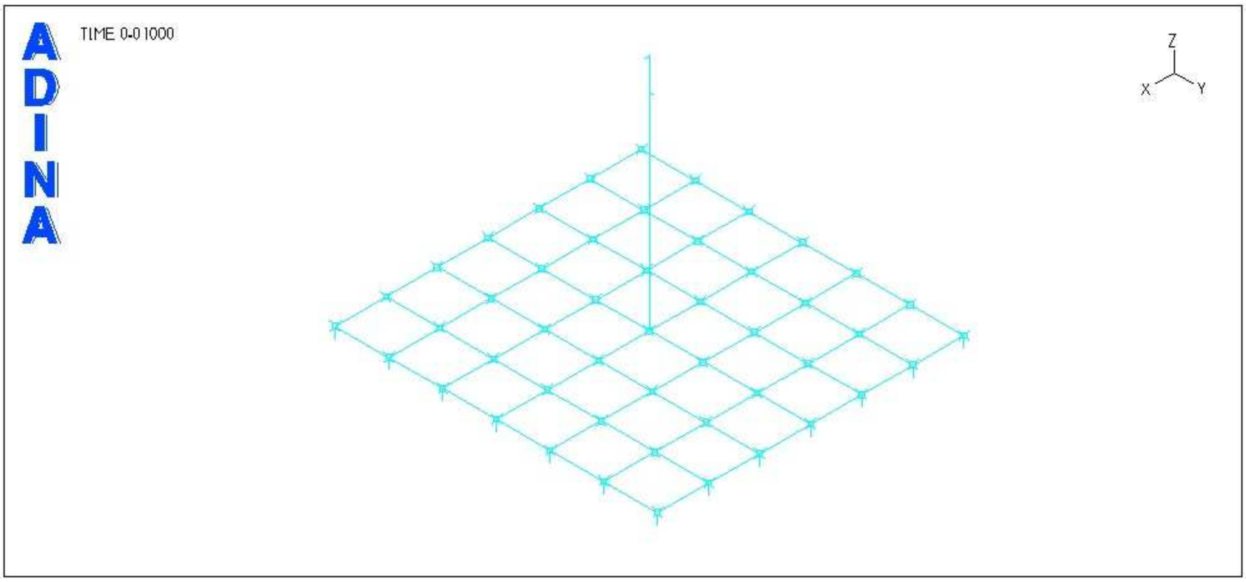

A second series have of analyses has been performed using material properties provided by the Secretariat. In this second series, ITER-Consult analyses take into account the soil backfill and a more detailed representation of the Soil Structure Interaction phenomena has been used as described in paragraph 2.4.1. The first series of analyses yield to the conclusion that the effect of the backfill shall be taken into account to get a realistic estimate of the response. The problem is that very few data are available about this soil.
In the following the results of the two series of analyses have been presented. The first series of analyses have been identified as Reference Analyses, while the second series results have been identified as Best Estimated Analyses.

3.3.1 Pushover Analysis and ATC 40 approach

Push-over analyses of the general 3D Finite Element Model have been conducted applying a uniform distribution of horizontal accelerations. Two set of boundary conditions have been considered. At first a fixed base structure model has been used. Subsequently soil structure Interaction effects have been taken into account. Results obtained in the Reference Analyses are shown in Figure 3.47 and Figure 3.48.
In the figures the force-displacement curves have been shown, for x and y direction and for fixed base and spring-based models.

In the graphs, the response at point CP2, at elevation TMSL +23.5, have been reported. Forces are in KN.

The curves for the SSI model show a limit in the horizontal force that the system can sustain. The force-displacement curves are controlled by the displacement and non linear behaviour of the soil (yielding and uplift).
For the fixed base model, the curve express the non-linear behaviour of the structure, with respect to the top of the basemat.

The analyses, in this case, are more difficult and time consuming. At the maximum displacement values, the structure is cracked is an extensive way. The steel rebars, however, are still in the elastic range.

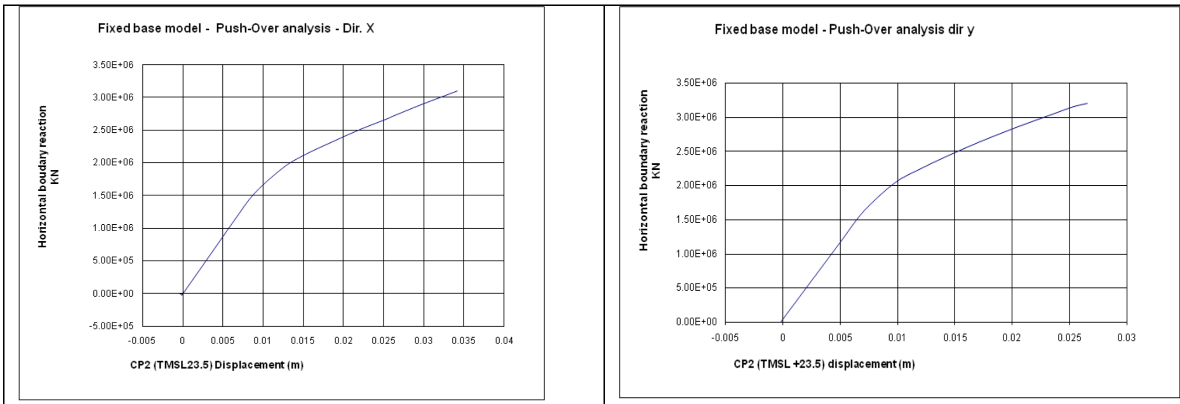

Figure 3.47 – Push Over Analyses results: Fixed base model

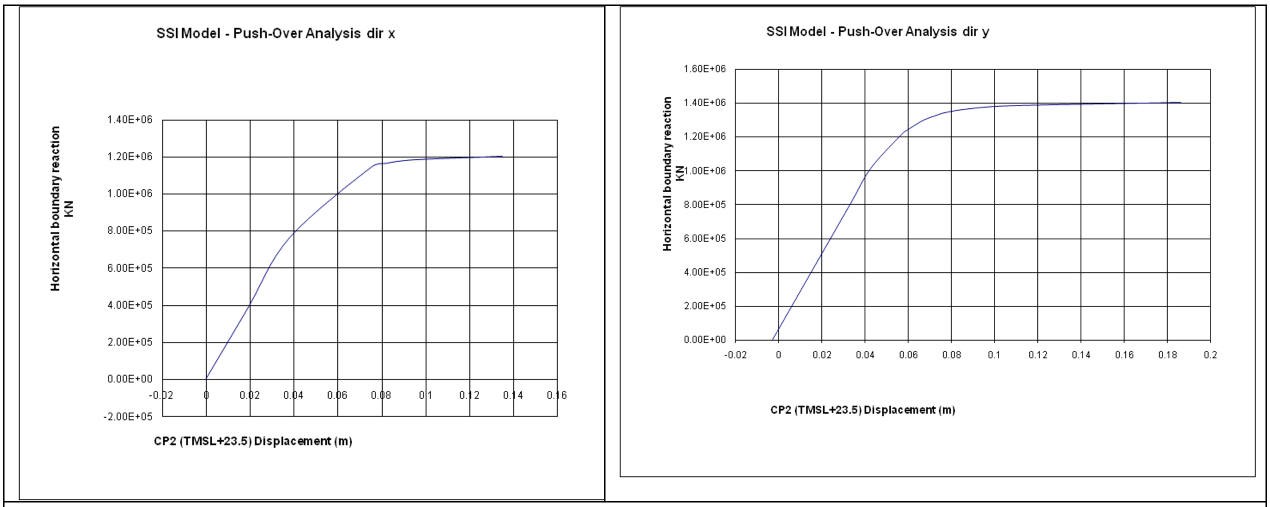

Figure 3.48 – Push Over Analyses results: deformed base model

The evaluation of the performance points requested by the IAEA Secretariat has been developed using the approach of ATC 40.
In this approach, you have to compare the Response Spectrum and the Capacity Spetrum, both of them expressed in terms of Acceleration-Displacement Response Spectra (ADRS).

The evaluation of the performance points is of course approximated, but the methodology can be used to have a first estimate of the response of the structure subject to an earthquake.
In this case, the results obtained with the approximated procedure have been compared to the results obtained by a step-by-step nonlinear calculations.

The figures show the comparison between Capacity and Demand, in terms of ADRS Spectra, for all the examined cases.
In the following tables, the performance points evaluated using the ATC 40 method have been listed. Note that for the strongest earthquakes, it was not possible to identify the performance point, because the demand curve is larger than the capacity curve for the considered displacement range.

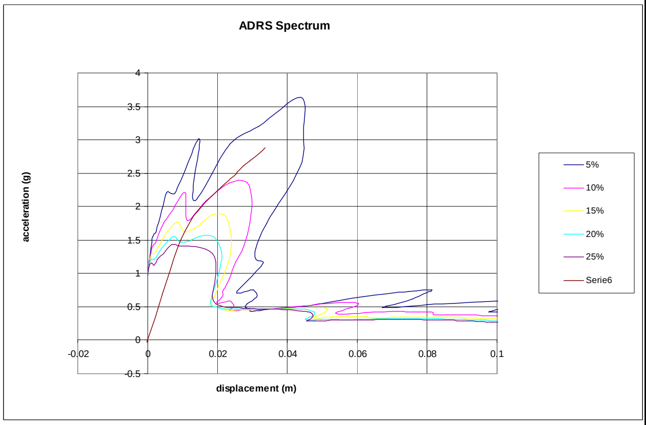	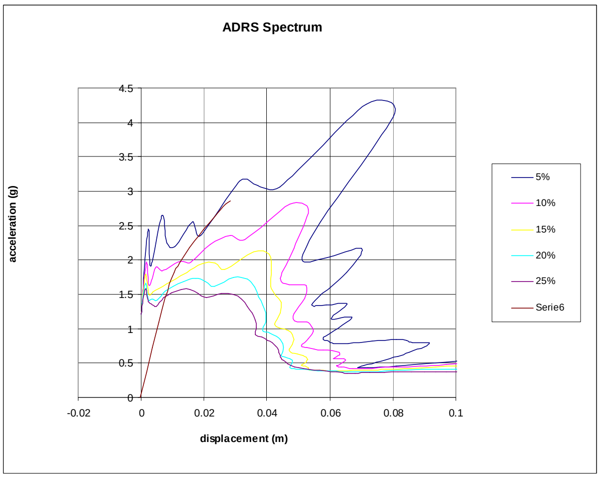
NCOE 1 – DIR. X – FIXED BASE	NCOE 1 – DIR. Y – FIXED BASE
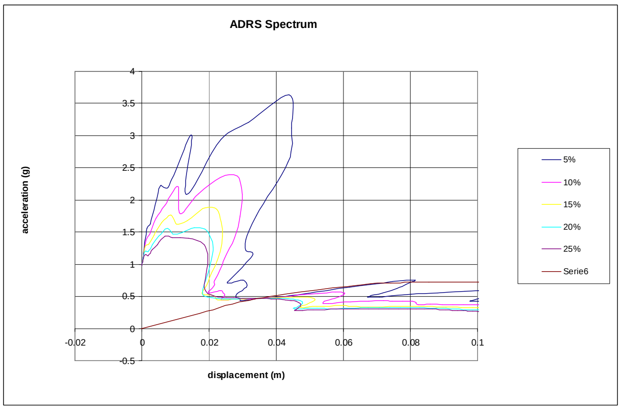	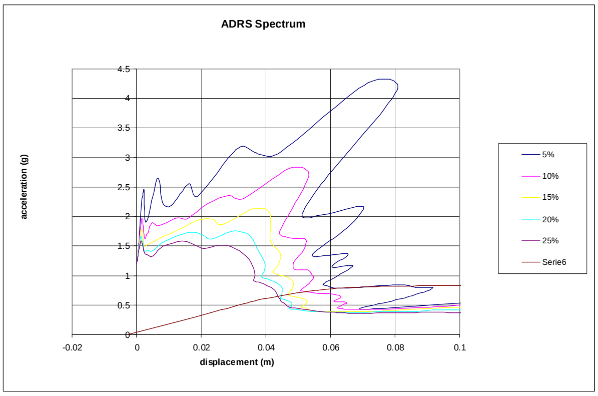
NCOE 1 – DIR. X – DEF. BASE	NCOE 1 – DIR. Y – DEF. BASE

Figure 3.49 – Response Spectrum and the Capacity Spectrum (ADRS): NCOE 1

Table 3.17– Performance points: NCOE 1			
		Displacement m	Force KN
Fixed base	X direction	0.012	1.93e6
Fixed base	Y direction	0.014	2.44e6
Deformed base	X direction	0.038	0.75e6
Deformed base	Y direction	0.056	1.21e6

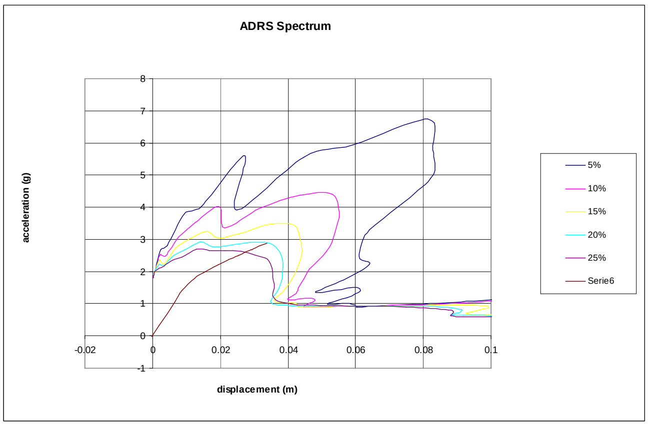

NCOE 2 – DIR. X – FIXED BASE

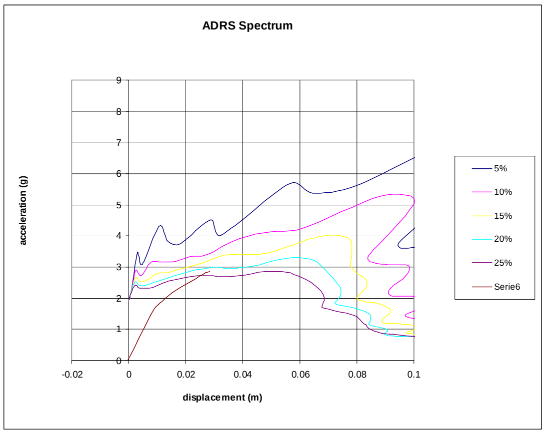

NCOE 2 – DIR. Y – FIXED BASE

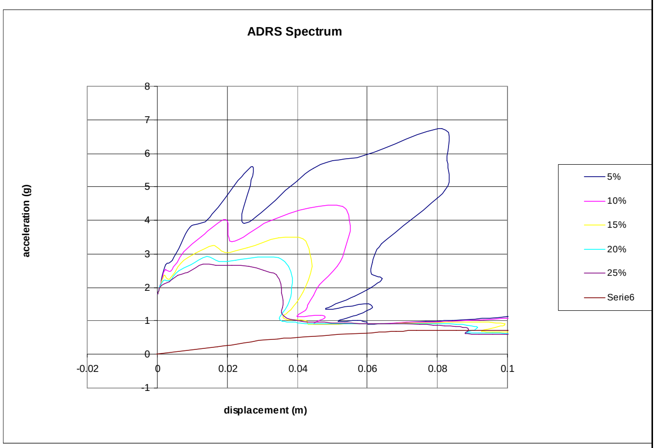

NCOE 2 – DIR. X – DEF. BASE

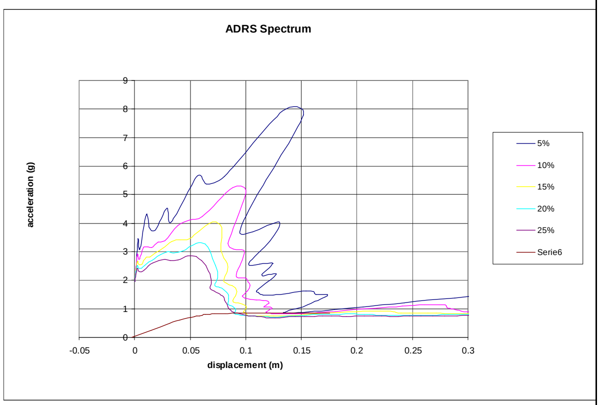

NCOE 2 – DIR. Y – DEF. BASE

Figure 3.50 – Response Spectrum and the Capacity Spectrum (ADRS): NCOE 2

Table 3.18– Performance points: NCOE 2			
		Displacement m	Force KN
Fixed base	X direction	?	?
Fixed base	Y direction	?	?
Deformed base	X direction	0.10	1.19e6
Deformed base	Y direction	0.10	1.39e6

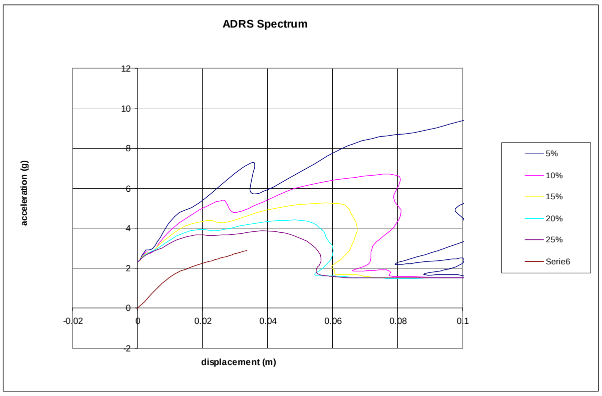

NCOE 4 – DIR. X – FIXED BASE

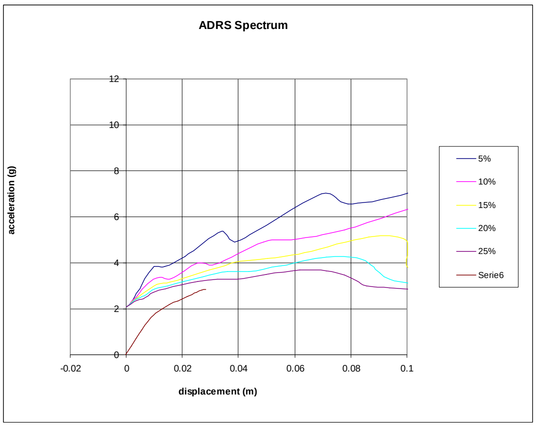

NCOE 4 – DIR. Y – FIXED BASE

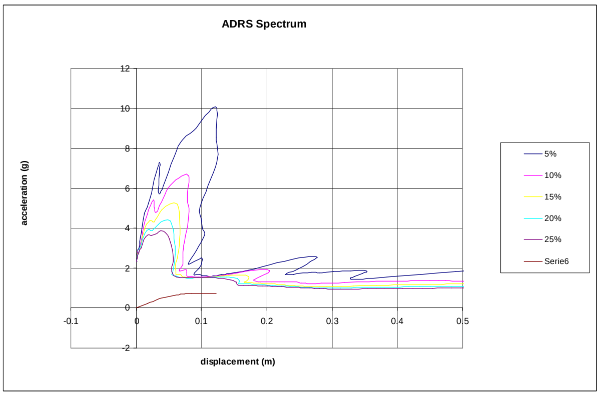

NCOE 4 – DIR. X – DEF. BASE

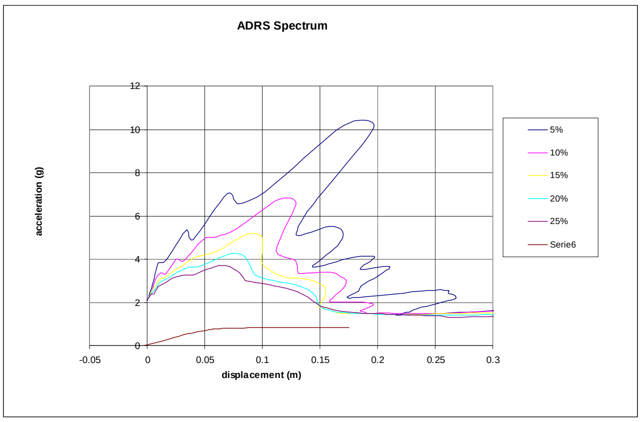

NCOE 4 – DIR. Y – DEF. BASE

Figure 3.51 – Response Spectrum and the Capacity Spectrum (ADRS): NCOE 4

Table 3.19– Performance points: NCOE 4			
		Displacement m	Force KN
Fixed base	X direction	?	?
Fixed base	Y direction	?	?
Deformed base	X direction	?	?
Deformed base	Y direction	?	?

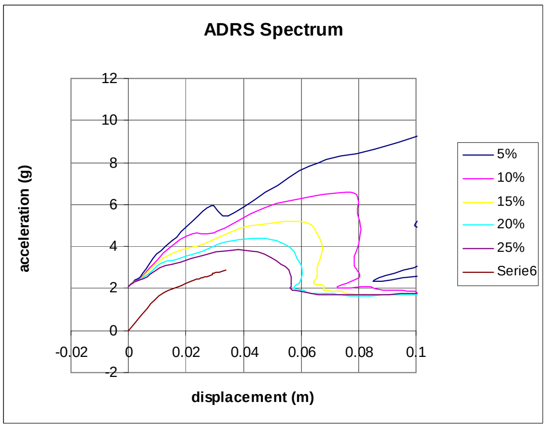

NCOE 6 – DIR. X – FIXED BASE

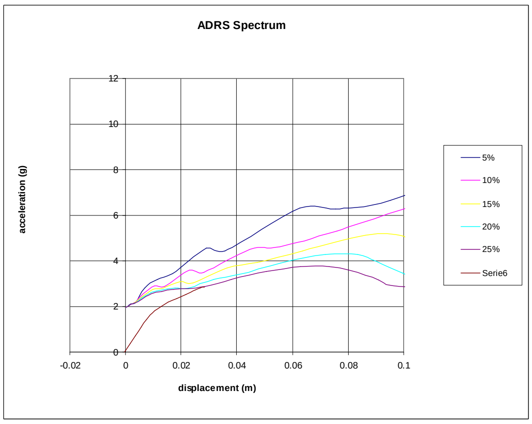

NCOE 6 – DIR. Y – FIXED BASE

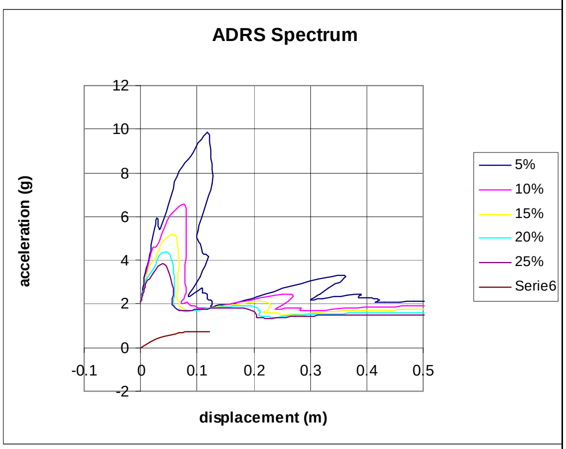

NCOE 6 – DIR. X – DEF. BASE

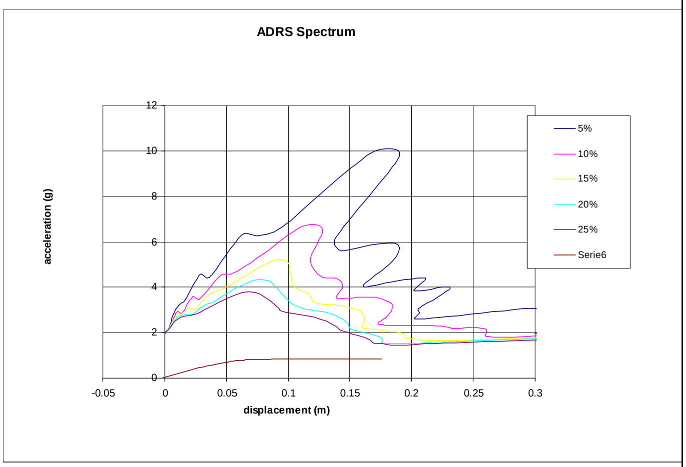

NCOE 6 – DIR. Y – DEF. BASE

Figure 3.52 – Response Spectrum and the Capacity Spectrum (ADRS): NCOE 6

3.20– Performance points: NCOE 6			
		Displacement m	Force KN
Fixed base	X direction	?	?
Fixed base	Y direction	?	?
Deformed base	X direction	?	?
Deformed base	Y direction	?	?

In the second series of analyses, updated materials properties have been used. However, with respect to the values previously used, the new values are very similar so the results obtained in the pushover analyses with fixed base do not change very much with respect to the Reference Analyses. On the contrary, some differences in the push over curve for the deformed base situation have been gathered, taking into account the presence of the backfill stratum of soil and the more refined soil structure interaction model.

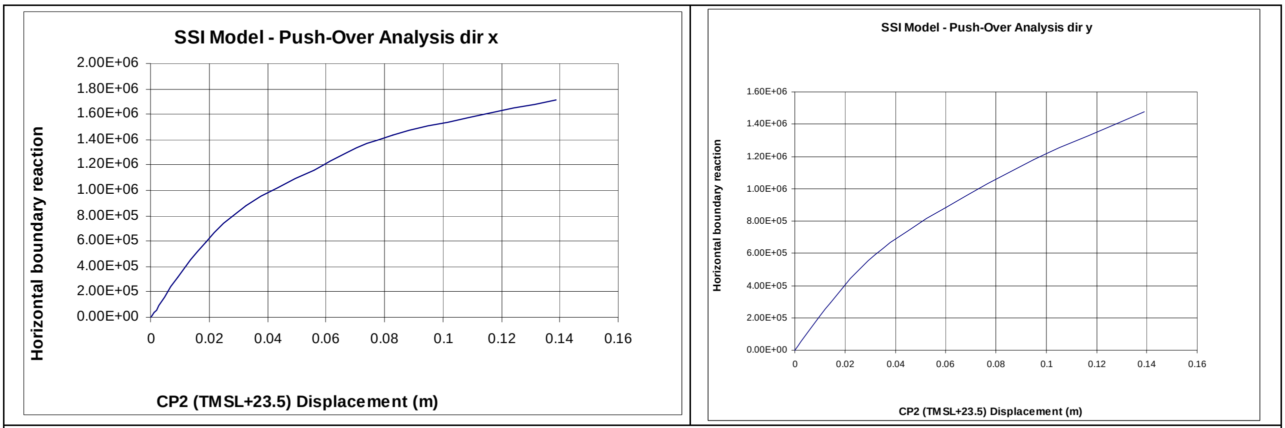

Figure 3.53 – Push Over Analyses results: deformed base model (Best Estimated Analyses)

3.3.2 Dynamic Response Analysis

3.3.2.1. Reference Analysis of the Soil-Structure Model

For the Reference Analyses, the same model introduced at the Phase II of the projects has been used. As input, the Time Histories provided by IAEA at -13.7 have been used in the analyses.

The results are summarised, in terms of Response Spectra for the two reference point BP1(Bottom basemat) and FP2 (third floor), in Figure 3.54 and Figure 3.55.

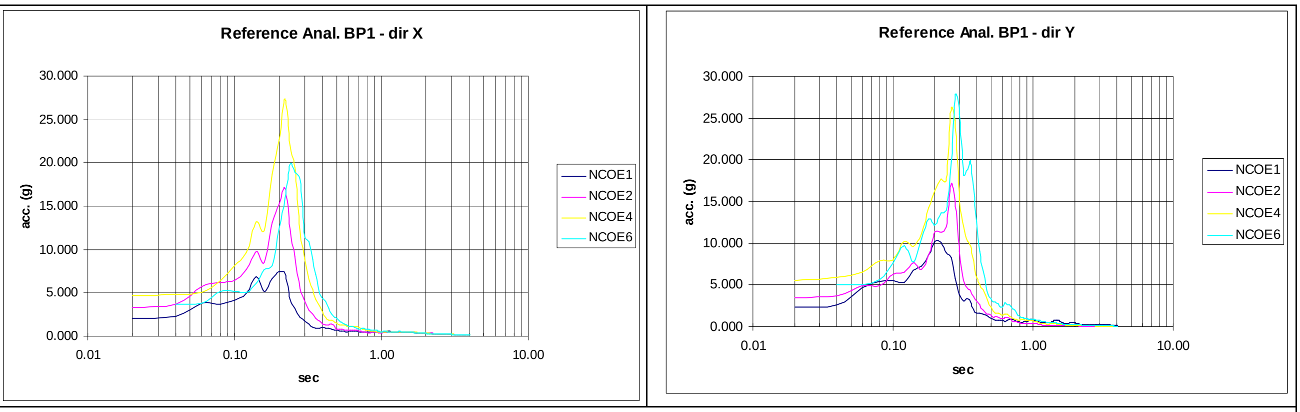

Figure 3.54 – Reference Analyses: BP1 Results

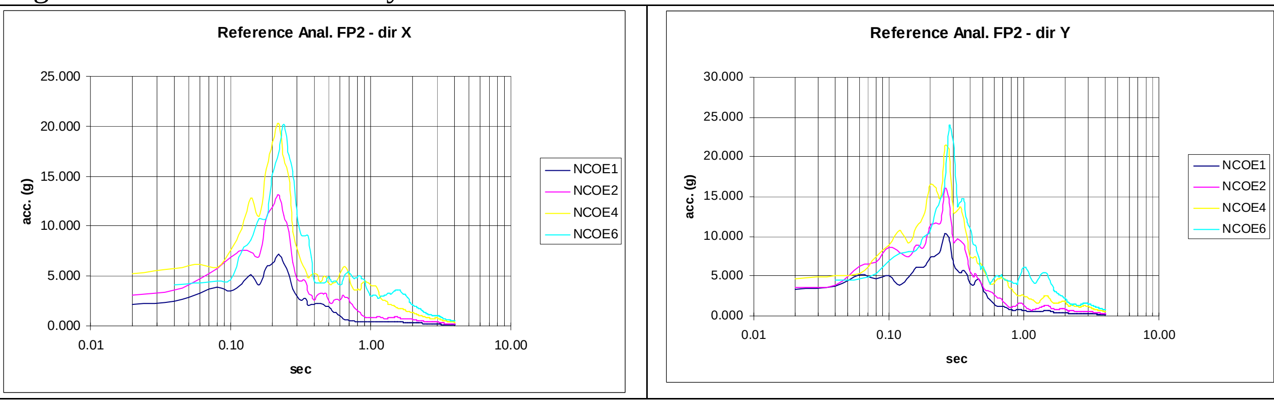

Figure 3.55 – Reference Analyses: FP2 Results

3.3.2.2. Best Estimate Analysis of the Soil-Structure Model

To improve the approximation of the analyses, the Soil Structure Interaction approach has been improved, using the methodology and the models previously outlined.

Using this approach, the spectral acceleration are generally lower. The results are summarised in Figure 3.56 and Figure 3.57, in terms of Response Spectra.

To be noted that the values obtained for NCOE6 are often lower then the corresponding values obtained for NCOE4. There is a saturation of the response for increasing level of earthquake.

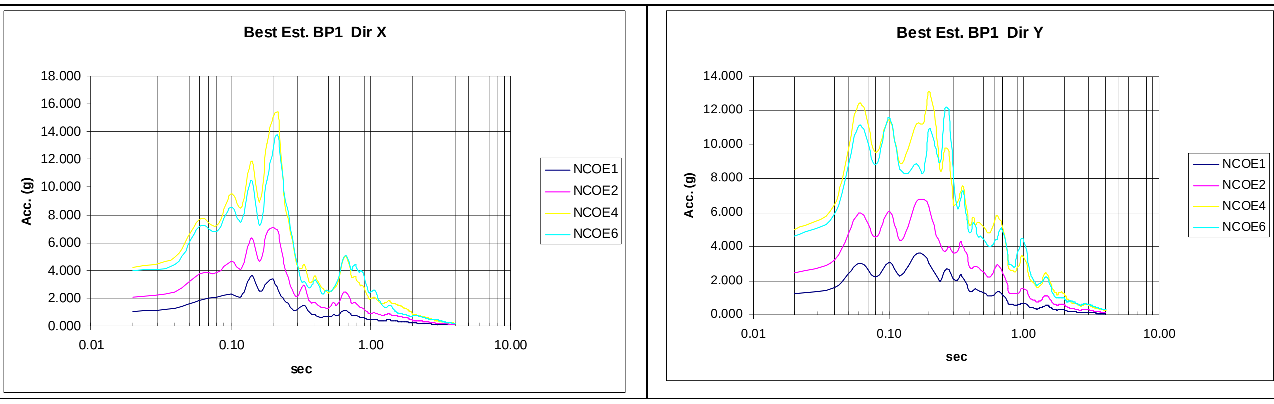

Figure 3.56 – Best Estimated Analyses: BP1 Results

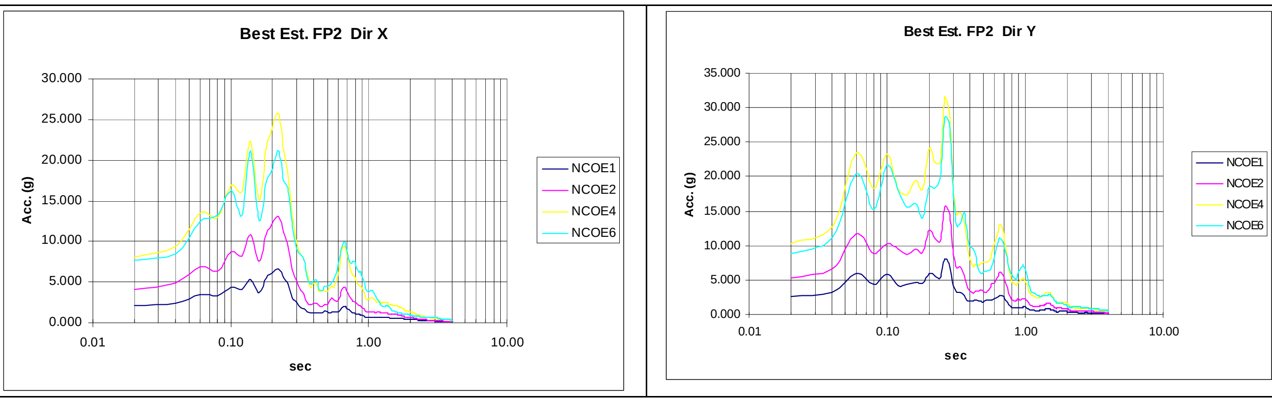

Figure 3.57 – Best Estimated Analyses: FP2 Results

In Figure 3.58 and Figure 3.59 some comparison are reported, for NCOE1 earthquake.

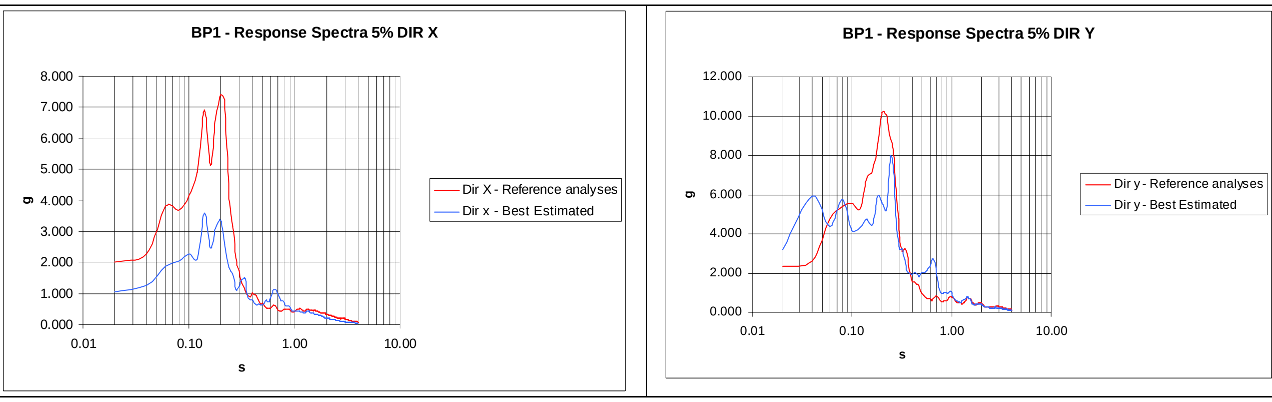

Figure 3.58 – Comparison Reference - Best Estimated Analyses: BP1 Results

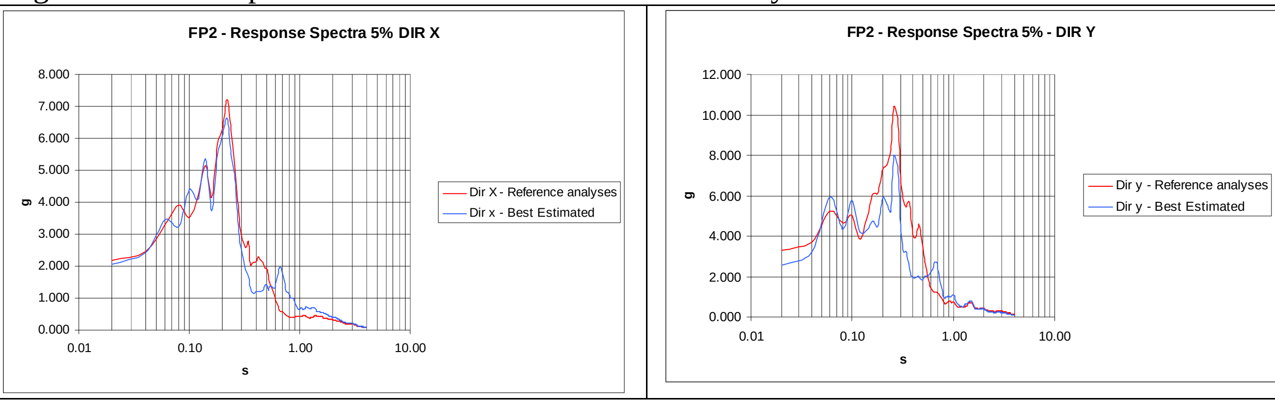

Figure 3.59 – Comparison Reference - Best Estimated Analyses: FP2 Results

It is interesting to make a further comparison among the best estimate results at FP2 point for NCOE1 and the Response Spectra evaluate for the recorded signal at the same point during the main shock(Figure 3.60).

This comparison can be also studied looking at the results obtained in phase II analyses (Figure 3.46).

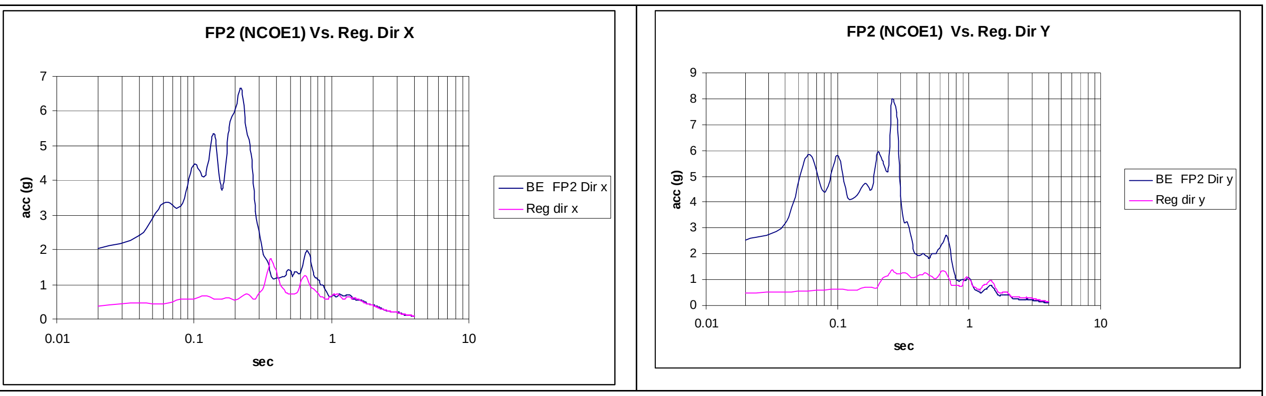

Figure 3.60 – Comparison Best Estimated Analyses and Recorded signal: FP2 Results

Another interesting comparison can be performed among the Response spectra evaluated on the Best Estimated results at BP1 (bottom of the basemat) and the Response Spectra evaluated for the input signal provided by IAEA at the same elevation (-13.7).
It is evident that the frequency content of the input signal is transferred to the bottom of the structure and this can be a justification of the discrepancies founded among recorded and calculated values at high frequency content.

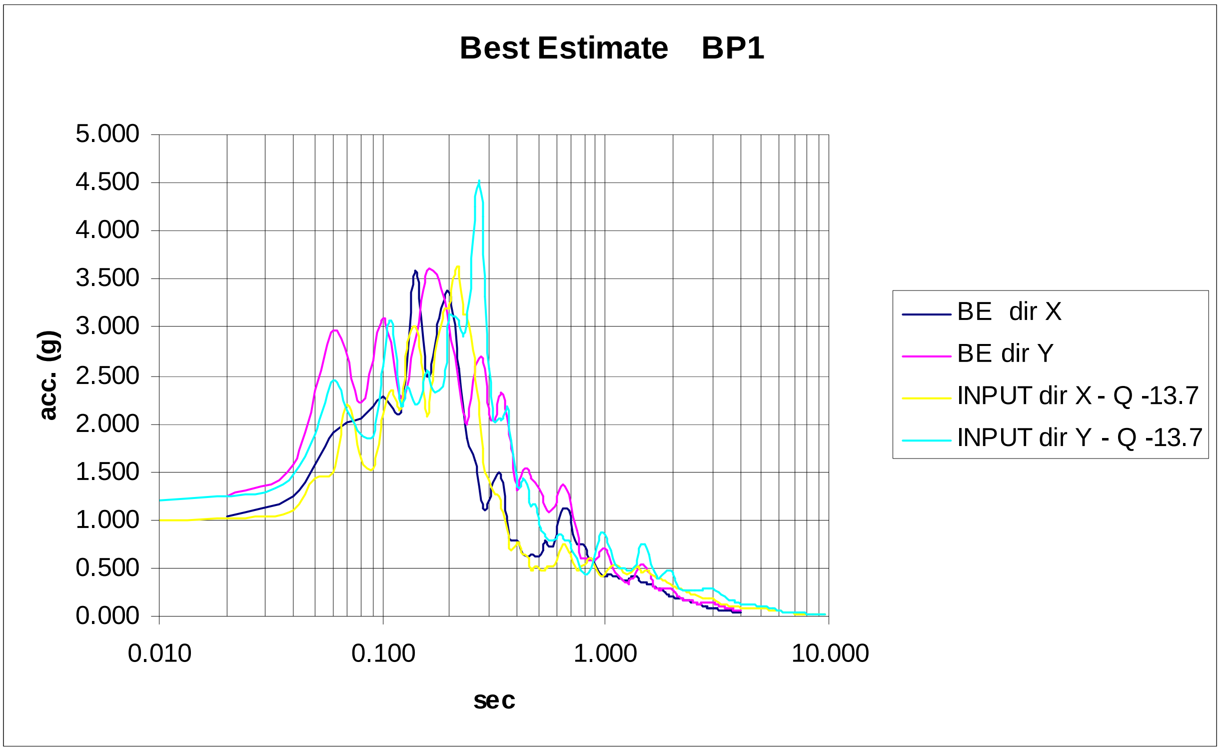

Figure 3.61 – Response spectra at the bottom of the basemat

3.3.2.3. Results of Margin Assessment.

The major problem to solve in margin assessment is the identification of this “ultimate” earthquake, to which correspond a Ultimate Limit State of the structure, taking into account the safety functions of the building and the systems and component present inside.

It is not just a structural problem, but this evaluation implies the study of the response of all the systems and components and how this response affects the functionality and the safety of the plant under the earthquake.

Traditionally, the seismic analysis of nuclear structures have been conducted with respect of two level of earthquake: the OBE and SSE. After the OBE the plant must not loose its functionality. In case of SSE, a safe shutdown process has to be safety conducted to bring the plant in a safety status.

In margin assessment, we have to look for a "ultimate" earthquake that is supposed to be larger than the SSE; in case of this event, what should be the response of the structure (and its systems and components …)?

Considering the need to guarantee a safe shutdown of the plant, the Ultimate Limit State of the structure that can be still considered allowable is a "state" in which the structure does not loose its functions (equipment support, containment,….) and the systems and equipment are still able to assure their safety functions. In this respect, it should be emphasized that after a strong earthquake the integrity of the containment structure can mitigate the internal accident due to a failure of equipment and systems, affecting the temporal evolution of the NPP response. Also this aspect could be significant in Margin Assessment.

However, in a general margins assessment, the performance of SSC's of the plant has to be verified through the respect of specific technical requirements.

Some of these can be summarized as:

- The global structure does not have to collapse;

- The structure has to maintain the containment function. In this respect the cracks in reinforced concrete walls should not reach excessive values that can cause stress/strain concentration in the steel liner and penetrations, with loss of their capacity to avoid releases of fluids in the environment;

- The support systems of equipment have to maintain their function, without collapse, In this respect, the accelerations experienced by the supports have to be lower than specific ultimate values, in dependence of the support and of the supported equipment. Moreover, the relative displacements among support points have to be compatible with the capacity of the structure-equipment complex;

- The accelerations experienced by the equipment important to safety have to be lower than specific ultimate values;

- Local collapse of internal structures that can affects SSC's important to safety have to be excluded

For the KARISMA benchmark, some simplified assumptions have been made.

In particular, only the following aspects have been considered to evaluate the Ultimate Limit State of the Reactor Building:

1. Global collapse of the structure

2. Residual displacements at foundation level and their evolution with increasing earthquake severity. We considered that displacements larger than specific values are not compatible to guarantee the functionality of building coupling with external structures and equipment;

3. Control point (CP2 – TMSL +23.5) relative displacements, with respect to the rigid body configuration. This parameter can be considered an indicator of the general damage distribution in the structure (earthquake demand);.

4. Absolute peak accelerations at reference floor and their evolution with increasing earthquake severity. Peak accelerations larger than specific values are not compatible for equipment functionality;

5. Localized collapses of internal structures that can affects SSC's important to safety.

Taking into account the previously mentioned requirements and the results obtained in Reference Analyses, the following table summarizes the results obtained against the four earthquakes considered:

Table 3.21– Performance factors for increasing earthquake severity

	NCOE1 CAV≈ 2000 m/s	NCOE2 CAV≈ 3500 m/s	NCOE4 CAV≈ 5000 m/s	NCOE6 CAV≈ 5500 m/s
Global collapse of the structure	to be excluded	to be excluded	to be excluded	to be excluded
Residual vertical displacements at foundation level	≈ 1 cm	≈ 4 cm	≈ 19 cm	≈ 42 cm
Relative max displacement of control point	≈ 0.5 cm	≈ 1. cm	≈ 2.8 cm	≈ 4.5 cm
Peak acceleration at reference floor	≈ 2.2 g	≈ 5.4 g	≈ 6.5 g	≈ 6 g
Cracks distribution	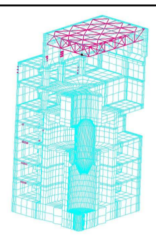	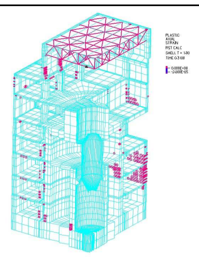	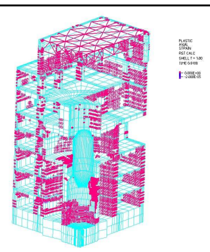	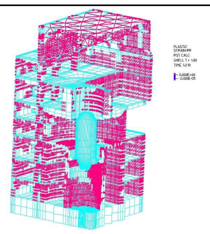
Localized collapses of internal structures	No evidence. Analysis of detailed situations	No evidence. Analysis of detailed situations	No evidence. Analysis of detailed situations	No evidence. Analysis of detailed situations

In Figure 3.62 the evolution of the residual vertical displacement at foundation level is reported versus increasing severity of motion, express by CAV - Cumulative Absolute Velocity evaluated for the four earthquakes, in x and y directions.

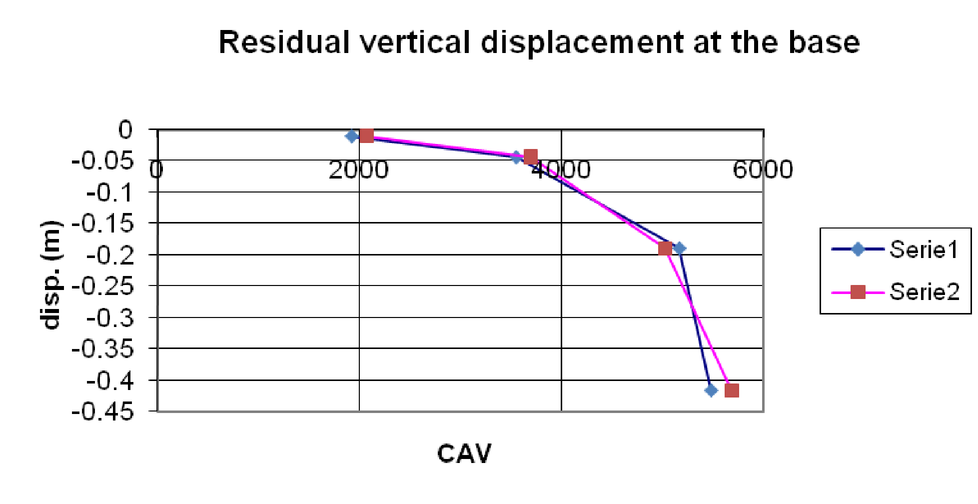

Figure 3.62 – Residual vertical displacement Vs CAV (Reference Analyses)

The analysis of the graphs shows a steep change in the global response of the structure for CAV values higher than 5000 m/s.

It is not easy to say if this changing preclude to an unacceptable situation (the Ultimate Limit State previously mentioned…)

More detailed information are necessary to support a judgment. With the available information and the results obtained in the performed analyses, it is only possible a general discussion of the response of the structure that seems to evidence a critical situation for CAV values higher than 5000 m/s.. At the same time, local collapses of internal structures cannot be excluded also for less severe earthquake.

However, with the aim to contribute to the discussion, we evidence a possible critical situation for earthquakes characterized by CAV values larger than 5000 m/s. Moreover, in correspondence of this, some of the requirements outlined in the previous table seam to reach very high values, as for example the absolute acceleration at reference floor.

In best estimate analysis, some different results are obtained, with displacement and accelerations generally higher than the previous ones. To understand these aspects you have to take into account that previous results have been calculated with different material characteristics (higher tensile stress of concrete) and backfill influence. Results are resumed in the following table.

Table 3.22 – Performance factors for increasing earthquake severity (Best Estimated Analyses)

	NCOE1 CAV≈ 2000 m/s	NCOE2 CAV≈ 3500 m/s	NCOE4 CAV≈ 5000 m/s	NCOE6 CAV≈ 5500 m/s
Global collapse of the structure	to be excluded	to be excluded	to be excluded	to be excluded
Residual vertical displacements at foundation level Max horizontal displacement	≈ 0 cm ≈ 12 cm	≈ 0 cm ≈25cm	≈ 0 cm ≈50 cm	≈0 cm ≈50 cm
Max horizontal displacement Relative max displacement of control point (with respect to rigid body motion)	≈ 10 cm ≈ 0.6 cm	≈ 20 cm ≈ 1.5 cm	≈ 50 cm ≈ 3.6 cm	≈ 57 cm ≈ 2.5 cm
Peak acceleration at reference floor	≈ 2.54 g	≈ 5.12 g	≈ 10.3 g	≈ 8.6 g
Localized collapses of internal structures	No evidence. Analysis of detailed situations	No evidence. Analysis of detailed situations	No evidence. Analysis of detailed situations	No evidence. Analysis of detailed situations

To be noted that residual vertical displacements have not been evidenced during Best Estimate Analyses, because the plastic limit of the soil springs has been calibrated to avoid residual vertical displacements under the event NCOE_1, as a first attempt to back-analyse field evidence.

4. DISCUSSIONS

Discuss the results (including quantification of effect of SSI, matching of borehole acceleration data etc.)

Linear method for the analysis and design were found very robust. The linear part of the benchmark yielded a narrow range of results for the static and modal analyses. Also the comparison between the stick models and the detailed 3d finite element model developed for the benchmark gave good results. The comparison demonstrates that the old design was reliable, in spite of the simplification of the dynamic behaviour of the buildings.
The overall response results seem strongly affected by the soil structure interaction. In general the analysis results were higher than the measured response.
Among the factors that seemed to contribute to this higher response obtained by the numerical simulations, markedly in the high frequency range, we have identified:

- the kinematic interaction between the reactor building and the surrounding soil, given the deep embedment;
- seismic motion incoherency along the foundation not accounted for by the kind of analyses developed
- highly nonlinear behaviour of the backfill, not well captured by equivalent linear approaches, including the separation from the walls and may be a partial uplift.

Anyway all these factors contribute to the confidence we have in the conventional approach to the design procedure used up to date, that seems to overestimate the field response (conservative design).

Progress of the benchmark (what were the main difficulties? Did you need to modify your model during the task and why? etc,)

The margins to be assessed should be defined in a unique way by the steering committee as quantifiable engineering quantities, because the usual structural criteria employed in linear structural analyses (for example stresses or section strength) cannot be easily extended in the nonlinear range and are meaningless for the system and components checks.

What were the main uncertainties and their contribution to results?

Main uncertainties were found in the Soil structure interaction analyses in the nonlinear range, due to the need of take into account soil foundation yielding and uplift.
While the structure’s data were quite completely defined for the benchmark scope of the work, soil properties were only defined by equivalent linear properties. Given the high level of the input to be used for the analyses and the consequent level of strain induced in the soil it seems that this approach cannot give adequate results.
Collapse of soil-foundation system, in the sense of excessive displacements, seems to anticipate extensive structural damage. In these sense the quality of the results is strongly affected by the quality of the soil properties and of the modelling of foundation behaviour in the nonlinear range. In these sense the contribution to result is quite high.

Comments and suggestions for the next phases

Next phases could be focused on the assessment of the seismic margins of the entire facility (NPP) with respect to the loss of the ‘’NPP capacity to bring and maintain the NPP (reactor core and spent fuel) in a safe status". This would require analysis of interfaces between structures an systems in order to determine critical conditions affecting the capability to ensure the required safety functions at NPP level.

5. CONCLUDING REMARKS ON THE BENCHMARK

5.1 Main difficulties encountered and their resolution

The “Margin Assessment” requires a careful definition of the required performance. Limits for the functionality of different SSC shall be defined in terms of quantifiable engineering quantities, in a way similar to Limit States in structural engineering. Because of the inherent oversizing and

conservatism in the structural design it seems that these limits are mainly related to system and components, so the problem cannot be confined in the realm of structures.
This kind of difficulty cannot be resolved within the scope of the structural part of the benchmark.

5.2 Main lessons learned from the benchmark

Soil structure interaction is a key problem in the assessment of margins, at least in cases with soil properties comparable to those at KK site. While the structure's data were quite completely defined for the benchmark scope of the work, soil properties were only defined by equivalent linear properties. Given the high level of the input to be used for the analyses and the consequent level of strain induced in the soil it seems that this approach cannot give adequate result.
Collapse of soil-foundation system, in the sense of excessive displacements, seems to anticipate extensive structural damage.
There is space for a lot of work in defining standard for the evaluation of NPP structures under beyond design base seismic motion. While suitable procedures have been included in codes and standard for ordinary buildings and bridges, there is the need to extend these approaches to NPP structures, which are unique for stiffness, strength, behaviour and required performance.

5.3 Suggestion on improving future benchmarks

The margins to be assessed should be defined in a unique way by the steering committee as quantifiable engineering quantities.
Some directions of the benchmark, mainly those related to the assessment of margins, were defined only during the work. At that moment most of the data were already defined and there was a lack of information to describe the nonlinear behaviour of the soil, which was identified as one of the key factors in the response under high level seismic motions.
Also the nonlinear analysis of NPP structure is not standard in the industry and it seems that an effort in defining standard procedures for this kind of evaluation is needed.
The required results were really a plenty of numbers and it was not completely clear to the participants the intended use of many of them.
A more detailed explanation of these aspects and may be a narrower set of results could improve the level of participation.

REFERENCES

[1] IAEA – Guidance Document. TASK 1:K-K Unit 7 R/B Structure SUBRASK 1.1: Construction and validation of the soil and structure models, Vienna, December 2009.

[2] IAEA-ISSC Database.

[3] COSMOS/M 2.5 – User Guide.

[4] Mylonakis, G.; Gazetas, G.; Nikolaou, S.; Chauncey, A. Development of analysis and design procedures for spread footings MCEER-02-0003 Multidisciplinary Center for Earthquake Engineering Research, Technical report Buffalo, N.Y. :

[5] Werkle H., Steifigkeit und Dämpfung von Fundamenten auf inhomogenem Baugrund, in Steinwachs (Hrsg.): Ausbreitung von Erschütterungen im Boden und Bauwerk, 3. Jtg. DGEB Hannover 1986, Trans Tech Publications, Clausthal, 1988

[6] Stewart, Comartin and Moehle "Implementation of Soil-Structure Interaction Models in Performance Based Design Procedures". Proceedings of Third UJNR Workshop on Soil-Structure Interaction, 2004

[7] ADINA 8.8 - User Manual

[8] SCHNABEL P., SEED H.B., LYSMER J. (1972) – SHAKE - A computer program for earthquake response analysis of horizontally layered sites. Report No. EERC 72-12, University of California, Berkeley.

[9] Chopra A.K., Goel R.K. "A modal pushover analysis procedure for estimating seismic demands for buildings" Earthquake Engineering and Structural Dynamics 2002; 31:561-582;

[10] Chopra A.K., Goel R.K. "A modal pushover analysis procedure to estimate seismic demands for unsymmetric-planbuildings" Earthquake Engineering and Structural Dynamics 2004; 33:903-927;

APPENDIX A

LIST OF TEAM MEMBERS

D. Casertano, Structural Engineer, P.E.

V. Lucarelli, Structural Engineer, Ph.D., P.E

A. Madonna, Electrical - Nuclear Engineer, P.E.

G. Maresca, Mechanical Engineer, P.E.

D. Mazzini, Aerospace Engineer, Ph.D

G. Orsini, Structural Engineer, P.E. (Project Leader)

G. Pino, Structural Engineer, P.E

A. Pugliese, Earthquake Engineer, P.E.

R. W. Romeo, Geologist, Associate Professor Geological Earthquake Engineering

T. Sanò, Structural Engineer, P.E.